Simulation of Cement Degradation Processes by Means of Coupled Water Flow and Reactive Solute Transport Modeling

PhD Thesis submitted by

Juan Manuel Galíndez

Under supervision of

Jorge Molinero Huguet

Departamento de Enxeñaría Agroforestal
Escola Politécnica Superior de Lugo

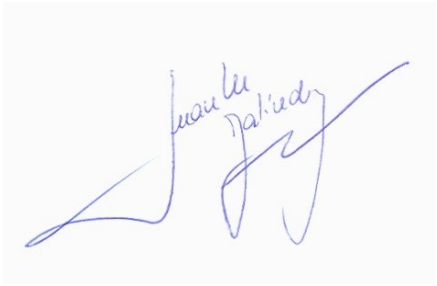

Juan Manuel Galíndez
Doctorando

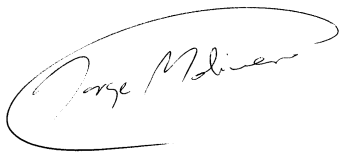

Jorge Molinero Huguet
Director de tesis

Dedicatoria

Si bien el resto de este documento está redactado en inglés, quisiera, con el permiso del lector, expresar estos agradecimientos en castellano: el idioma que siempre he usado para dirigirme a quienes ahora quiero recordar, aquellos sin quienes, como estila decirse, esto no hubiera sido posible.
Entonces, dedico lo poco de bueno (si se me permite el optimismo de creer que efectivamente *hay* algo de bueno) de este trabajo:
Al director de mi tesis, Jorge Molinero, por haber confiado temerariamente en mí;
A mi familia, especialmente a mis padres – sólo ahora que la escribo me doy cuenta de cuánto me gusta esa palabra: 'padres' – y a la memoria querida de mis abuelos;
A Verónica, a quien dedico también el resto de mis días;
A mis amigos, Juan, Fernando, Elizabeth, Eva, Ana, Laura *et al.*, por su infinita generosidad. Por Dios, ¡cuánto les debo!;
A Sergio Liscia, a Cecilia Lucino y a la gente de la Facultad de Ingeniería de La Plata, quienes siempre me recuerdan (han de saber que es recíproco).

Acknowledgments

This work was carried out under the auspices of the Swedish Nuclear Fuel and Waste Management Company (SKB). The author would like to thank its support in the person of Ignasi Puigdomenech, whom has also contributed with several fruitful discussions and pertinent suggestions during the course of this research.
Grateful thanks are also given to the personnel of the University of Santiago de Compostela, and the Escola Politécnica Superior in particular, for providing the ideal environment to develop this work.
Javier Samper, Luis Montenegro, Chanbing Yang, Liange Zheng and Chuanhe Lu are also acknowledged for their help.

Resumen

Pocos problemas hay en el ámbito de la Ingeniería que no tengan carácter multidisciplinario. Menos aún que revistan esa cualidad con tan innegable evidencia como el concerniente al depósito definitivo de los residuos provenientes de la generación de energía de origen nuclear. Y, en efecto, en torno a este dilema se han congregado especialistas de los más diversos campos, desde los de la Geología a la Ciencia de Materiales, hasta los de la Química y la Hidráulica.

Tal es el modo en que ha reaccionado la comunidad científica ante la demanda de la sociedad de la que es su emergente y de cuya responsabilidad para con la resolución de tal problema es su depositaria; una demanda, por otra parte, gestada y catalizada por una sensibilidad crecientemente más agudizada por una noción ecologista en cuya fuerza yacen las esperanzas de preservación de la habitabilidad de este planeta y del bienestar de sus individuos.

Así pues, de entre las varias alternativas factibles, una de las soluciones adoptadas ha sido la de sepultar los residuos a gran profundidad en recintos herméticos. El propósito que se transluce detrás de estas construcciones civiles es el de anular, por todos los medios posibles, los riesgos inherentes a la migración de radionucleidos hacia la biosfera. La consecución de tal objetivo depende, a grandes rasgos de que, por un lado, los eventuales repositorios sean emplazados en macizos rocosos con grado de fracturación leve y poco meteorizados; por el otro, de que cuenten con una envoltura, generalmente de múltiples barreras, efectivamente opaca (y capaz de conservar tal cualidad por miles de años) al paso de sustancias radioactivas, resguardando al entorno de posibles fugas.

Por proveer un medio altamente alcalino para la fijación de radionucleidos, los materiales cementicios se han mostrado potencialmente apropiados para integrar las estructuras multibarreras mencionadas. Sin embargo, las principales bondades de estos materiales descansan en gran medida de sus propiedades hidráulicas, a saber, porosidad y conductividad hidráulica, que los señalan como indicados, además, para el sellado de las fisuras y grietas presentes en los macizos rocosos que, de ser de otro modo, acabarían por comportarse como canales preferenciales de flujo y de transporte, en la eventualidad de fugas.

No ha de sorprender, por tanto, que los años recientes hayan sido testigos de un interés creciente por parte de los investigadores en los procesos involucrados en la degradación del hormigón, por cuanto su peso es decisivo en su durabilidad así como ésta, a su vez, lo es en buena medida en la evaluación de la

seguridad a largo plazo de los repositorios de residuos radioactivos. Este fenómeno se ha desenvuelto paralelamente a una dramática evolución en el desarrollo de las herramientas de modelización por ordenadores que, si bien ha desplegado su poderosa influencia en diversos campos de la ciencia por igual, resulta de particular valía en este del que ahora se trata, con vistas a conseguir los objetivos perseguidos por la presente tesis. En efecto, los ordenadores y su fuerza de cálculo no sólo brindan un medio para modelizar los procesos de transporte tales como la difusión y la advección, sino también, como se verá, para simular la misma composición de la matriz de cemento hidratado, logrando, por consiguiente, mejorar el conocimiento actual del comportamiento de los materiales cementicios.

En torno a esta materia se centrará entonces la presente tesis, que se propone indagar en los fenómenos involucrados en la evolución de la degradación de las propiedades de los materiales cementicios en el largo plazo (entendiendo por tal tiempos geológicos) por medio de simulaciones efectuadas con modelos de transporte reactivo.

A tal fin convergen dos líneas de investigación no enteramente independientes: por un lado, la conceptualización del hormigón tanto como un agregado mineral, y como tal susceptible de deterioro, tanto como un material poroso, en cuyos vacíos han de desarrollarse procesos de transporte de solutos; y por el otro, el empleo de modelos de transporte reactivo de solutos, que ha sido creciente y más ampliamente frecuentado en este campo, pues proporcionan una aproximación mecanística para abordar los complejos fenómenos químicos y de transporte involucrados en los procesos de degradación del cemento.

El concepto abstracto al que alude la enunciación de la primera de tales líneas asume una significación concreta en la generación de representaciones tridimensionales de la microestructura del cemento endurecido sobre la base de imágenes digitales de éste en su estado anhidro. Este proceso se vertebra en una serie de etapas que consisten en: 1) la determinación de la distribución del tamaño de las partículas (i.e., la relación de la fracción correspondiente a cada diámetro de las partículas) tanto del cemento como del humo de sílice (en caso de que éste último contribuya a la composición de la lechada o el hormigón, tal como es el caso de los materiales cementicios de bajo pH); 2) la generación del arreglo inicial (es decir, en estado anhidro) de las partículas; 3) la distribución de las fases del cemento (a saber, silicato dicálcico, silicato tricálcico, aluminato tricálcico y ferroaluminato tetracálcico) en su representación tridimensional, extrapolada por medio de funciones de correlación desarrolladas sobre imágenes reales del cemento; y 4) la simulación de los procesos de hidratación, bajo condiciones de modelización tendientes a representar aquellas correspondientes a las de la inyección de la lechada *in situ*. Asimismo, la conceptualización del hormigón como un material poroso implícitamente

conlleva al desarrollo de los métodos apropiados disponibles para describir la difusión iónica – sobre este punto se hablará más en extenso líneas abajo, en relación con la comparación de las aproximaciones puramente difusivas (fickianas) y las correspondientes a la formulación de Nernst – Planck, que incorpora las interacciones químicas y eléctricas – y la precisión de las leyes constitutivas (por ejemplo, porosidad/permeabilidad, porosidad/difusividad, etcétera) desarrolladas para estos materiales.

En lo que refiere a la segunda línea de investigación, a saber, la aplicación de modelos de transporte reactivo, me limitaré a citar a Steefel *et al.*[1], a quienes traduzco literalmente, al apuntar que '[a]quello a que se refiere con "modelización del transporte reactivo" es entonces una serie de herramientas interpretativas destinadas a esclarecer las complejas interacciones entre los procesos y los efectos ensamblados en múltiples escales espaciales y temporales en la Tierra. Pero la modelización del transporte reactivo también puede verse como una aproximación a la investigación, un modo de organizar y evaluar los efectos de los procesos dinámicos acoplados de índoles geoquímica, microbiológica y física en las ciencias de la Tierra.' Y continúan '[r]ecientemente, ha habido un creciente interés en el uso de la modelización del transporte reactivo como una actividad sintetizadora para la investigación fundamental de las ciencias de la Tierra, que se suma a sus potenciales, y tal vez más obvios, usos predictivos. Desde este punto de vista, la simulación del transporte reactivo brinda medios para aplicar la investigación fundamental de la ciencia de la Tierra a sistemas naturales y un medio objetivo y sistemático de evaluar la importancia relativa y el rol de los procesos fundamentales que normalmente se estudian por separado.'

El campo de los materiales cementicios es uno de aquellos a los que Steefel y sus colegas refieren en los que la aplicación de los modelos de transporte reactivo es relativamente reciente. Más aún, con frecuencia, ésta se ha circunscripto a la consecución de objetivos diversos (por ejemplo, la difusión de cloro, que incide sobre la corrosión de las armaduras de acero del hormigón armado, el ataque de sulfatos, que conduce a reacciones expansivas, etcétera) de los que se propuso esta investigación. Por todo lo cual, se estimó no sólo útil sino también necesario efectuar el trazado de la evolución de tales procedimientos hasta la fecha e identificar cómo han repercutido (y repercuten) sobre ellos las propiedades idiosincrásicas de estos materiales. Habría resultado superficial concebir que la mera descripción de los modelos que han jalonado la transición hacia el actual estado del arte (tal cual se ha acometido en la parte introductoria del presente trabajo) habría bastado para cristalizar la consecución de tales objetivos. En realidad, esa tarea habría sido vacua sin una evaluación crítica de los actuales modelos, máxime por tratarse de un campo de investiga-

[1] Steefel, C.I., DePaolo, D.J., Lichtner, P.C., Reactive transport modeling: An essential tool and a new research approach for the Earth sciences, Earth and Planetary Science Letters 240(3–4) (2005), 539–558

ción en constante evolución. Esta última opción admite indudablemente varios flancos de los que vale citar algunos, siquiera someramente: por ejemplo, la modelización de las intrínsecamente complejas (y aún no del todo comprendidas) características mineralógicas de los productos de hidratación (principalmente los llamados silicatos hidratados de calcio, o C-S-H) y de su consecuencia: su ambiguo comportamiento termodinámico; la descripción de las intrincadas características geométricas de la red intersticial de la pasta endurecida, que gobierna en buena medida las propiedades hidráulicas del material, y exhibe un alto nivel de heterogeneidad a diferentes escalas; etcétera. De entre esos campos abiertos a la investigación, en el presente trabajo, se ha procurado abordar la indagación de los métodos más apropiados para la modelización de la difusión de partículas eléctricamente cargadas. Esta particular faceta es uno de los aportes originales de este trabajo. Para ello se llevó a cabo (véase el Paper III) la simulación del deterioro del hormigón por causa de la exposición a una solución ligeramente enriquecida en sulfatos, empleando para ello dos diferentes formulaciones de la difusión, a saber, las acuñadas por la ley de Fick y por la ecuación de Nernst – Planck. Los resultados obtenidos de esta experiencia mostraron que aquélla (al contrario de esta última) era incapaz de reproducir la precipitación de una fina capa de yeso en el entorno de la cara expuesta del hormigón (lo cual está verificado por medio de ensayos de laboratorio), en razón de que tiende a subestimar la concentraciones de calcio y de sulfatos en la solución intersticial, manteniéndola alejada de su umbral de saturación. En virtud de ello, es dable sugerir que puede que las aproximaciones al transporte por difusión basadas en la ley de Fick sean insuficientes para modelizar la degradación de materiales cementicios y que, en su lugar, la modelización de Nernst – Planck provea un marco fenomenológico más apropiado.

Las dos líneas de investigación bosquejadas líneas arriba confluyen, pues, en el núcleo de esta tesis: la modelización de la degradación en el largo plazo de materiales cementicios por medio de modelos de transporte reactivo.

Son oportunas entonces algunas definiciones, de la degradación de los materiales cementicios, por ejemplo, tal como es estudiada en el presente trabajo, por cuanto conlleva implícita la determinación de los escenarios que se pretenden reproducir por medio de los modelos. Efectivamente, por degradación se entenderá el complejo fenomenológico que se desencadena por efecto de la interacción de los materiales en cuestión con un entorno agresivo y que redunda en el declive gradual de las cualidades de aquél (e.g., sus propiedades hidráulicas), en desmedro de su durabilidad. Es por tal motivo que el escenario típico de los modelos contemplados en este trabajo, y por medio del cual se pretende reproducir las condiciones más probables a las que se hallarán expuestos los materiales cementicios durante su vida en servicio, importa invariablemente el entorno relativamente ácido que provee un agua subterránea. El agua intersticial que satura los poros del hormigón (o de la lechada de ce-

mento) es marcadamente alcalina (su pH es de alrededor de 13,5 para mezclas que contengan cemento Portland ordinario; del rango 9 – 11 para mezclas que involucren cementos especiales y adiciones sustantivas de humo de sílice). El fuerte contraste entre la composición química y la alcalinidad de un agua y otra conduce a una serie de reacciones de precipitación y de disolución de cuyo balance habrá de depender la durabilidad del material. Los principales procesos involucrados en la degradación han sido identificados en previas experiencias y confirmados en los ensayos presentados en este trabajo: por ejemplo, la disolución del hidróxido de calcio (portlandita) y la decalcificación de los silicatos hidratados de calcio por el constante transporte hacia el exterior por difusión de los iones de calcio. Sin embargo, los procedimientos de modelización con frecuencia enfrentan arduos problemas en la práctica que ponen de manifiesto la extrema complejidad de los fenómenos en cuestión. La disolución incongruente de los silicatos hidratados de calcio, tanto como la influencia de la disolución en el incremento de la porosidad se suman a las complejidades inherentes al acoplamiento del transporte reactivo de solutos en un medio poroso y las reacciones químicas que emanan de él. Ésta es una preocupación mayúscula, considerando la relevancia que se espera de las simulaciones numéricas como una herramienta fundamental para complementar los ensayos experimentales para los cuales el tiempo de simulación representa una seria restricción.

De acuerdo con la Epistemología de impronta popperiana, las teorías científicas, abstractas por naturaleza y, en rigor, sólo contrastables en el plano de las implicaciones que de ellas derivan – el de los ensayos experimentales –, son de verificación imposible, independientemente del número de veces que fueran corroboradas (ya que no confirmadas) por la realidad empírica; contrariamente, basta una sola experiencia que contradiga las implicaciones de la teoría para hacerla objeto de *falsación*. La confiabilidad de los modelos de transporte reactivo para el uso que de ellos se hace en este trabajo corre el mismo albur que aquéllas. Y es que en efecto, en virtud de una simple operación de la Lógica, es posible declarar que si bien no ha sido dado afirmar que los modelos de transporte reactivo habrán de reproducir la realidad empírica (esto es, predecir con certeza la evolución del hormigón en el largo plazo), sí es posible afirmar que no serán capaces de ello si no reproducen con algún grado de precisión aquellos de los que hoy en día se tiene constancia.

Siguiendo esa línea de razonamiento, se concibió (del mismo modo que al científico resta darse a la tarea de contribuir a la extensión de la serie finita de ensayos cuyo último término es aquel que prueba la falsedad de la teoría) la iniciativa de contrastar la performance de los modelos presentes, en particular, el construido sobre la base del programa de transporte reactivo CORE^{2D}, específicamente adaptado para evaluar la evolución de las propiedades físicas del hormigón. Concretamente, se llevó a cabo una simulación de un estudio de

caso extraído de la literatura científica que proveía el marco de comparación contra el cual se contrastó la eficiencia del modelo presente, en búsqueda de confiabilidad para efectuar predicciones de largo plazo. A diferencia de otros estudios, el problema en cuestión involucra transporte de solutos difusivo y advectivo (el uno asociado a una desigual distribución de los solutos en el espacio ocupado por una solución; el otro asociado a la velocidad del flujo de agua), lo cual introduce, por consecuencia, la necesidad de definir una relación constitutiva apropiada entre la porosidad y la conductividad hidráulica. Esto podría resultar de relevancia cuando las estructuras de hormigón se hallen sujetas a ligeros gradientes hidráulicos durante su vida en servicio. Por medio del acoplamiento de las propiedades físicas de la pasta de cemento endurecido con las reacciones de disolución y de precipitación, el desarrollo de la porosidad, y su impacto en la evolución de la conductividad hidráulica podría ser tenido en cuenta apropiadamente.

Los resultados obtenidos son comparables a los datos experimentales provenientes de los ensayos publicados (véase el Paper I), lo cual, por lo dicho anteriormente, no agota la discusión en torno de la fiabilidad de los modelos ni excluye la posibilidad de que en algún momento sus resultados (por estas herramientas) sean refutados. Hasta ese entonces, sin embargo, los modelos de transporte reactivo pueden disfrutar del aval logrado por estos medios.

Más aún, en concierto con programas de generación de representaciones de la microestructura del cemento endurecido sobre la base de imágenes digitales, es posible expandir su espectro de aplicación para así constituirse en una herramienta de suma utilidad en el proceso de diseño de mezclas de hormigón y de lechada de cemento. Este último caso (véase Paper II), que puede considerarse crítico por cuanto lleva consigo un compromiso entre dos requerimientos en conflicto (el de trabajabilidad y capacidad de inyección en estadios tempranos, por un lado; el de durabilidad, por el otro), es ilustrativo de los alcances de esta metodología. Este nuevo enfoque metodológico (por cierto, otra de las contribuciones originales de la presente tesis) es, en efecto, un aporte relevante con vistas al estudio racional del diseño óptimo de mezcla de lechada de inyección. Brevemente, consiste en definir (contando apenas con las proporciones de los materiales de la mezcla – la 'receta' de la mezcla –, y mediante el empleo de las simulaciones de la microestructura) puntos de partida razonables para la modelización de la degradación, que habrá de correr a cargo de los modelos de transporte reactivo. Estos, por su parte, habrán de evaluar las respectivas performances en el largo plazo de las mezclas analizadas y guiar la búsqueda en una manera práctica y efectiva.

Por cierto, tal como se puede comprobar en el mencionado artículo, concuerdan con las propiedades características esperables de la lechada de inyección. En efecto, estos muestran un alto grado de hidratación, grandes porosidades,

bajo contenido de compuestos de aluminio y aun bajos contenidos de portlandita. Asimismo, el pH de la solución intersticial en equilibrio con las fases sólidas, obtenidas por medio de especiación geoquímica se halla en el rango de cementos típicos de bajo pH. Restaría, desde luego, disipar las incertidumbres conectadas a cuán ajustadamente es posible simular la evolución real del proceso de hidratación bajo condiciones de campo, lo cual excede los alcances de este estudio.

Para concluir este Resumen, cabe un comentario acerca de la presentación de este trabajo. Apunta Borges, al reseñar *Men of Mathematics*, de E.T. Bell, que '[l]a historia de las matemáticas (…) adolece de un defecto insalvable: el orden cronológico de los hechos no corresponde al orden lógico natural. La buena definición de los elementos es en muchos casos lo último, la práctica precede a la teoría, la impulsiva labor de los precursores es menos comprensible por el profano que la de los modernos[2].' Aun siendo el tópico de este trabajo harto más modesto, supongo que es probable que el lector le infiera una crítica similar, por cuanto aquí también se ha privilegiado el orden cronológico de la publicación de los artículos sobre otros criterios. No la negaré, por supuesto, pues tal no es posible; antes bien, argüiré que el 'orden lógico natural' es, en este trabajo, ciertamente menos discernible – los artículos admiten, sin mayor dificultad, su exposición como piezas independientes de investigación – y que, de cualquier modo, su omisión no es obstáculo para la percepción del mérito (o ausencia de él) de sus hallazgos.

[2] Textos cautivos (1986). En Obras Completas (volumen IV), Emecé Editores (2005)

Abstract

Given the risk inherent to radioactive waste repositories and that cementitious materials have achieved widespread use in recent years in the construction of the multi-barrier systems that protect the environment from potential leakage, the estimation of the durability of such materials is of vital importance for it is tied to the safety of those structures in the long term. The present thesis is aimed towards that goal, intending to provide insight into the phenomena involved in the evolution of the degradation of cementitious materials by means of simulations carried out with reactive transport models.

Two not entirely independent lines of research converge to this end: on the one hand, the conceptualization of concrete as a mineral aggregate (as such liable to deterioration) as well as a porous material, in whose voids transport processes develop, and on the other hand, the use of reactive solute transport models, which has been increasingly and more widely adopted in this field, since they provide a mechanistic approach to address the complex chemical and transport phenomena involved in the processes of cement degradation.

The first of such guidelines acquires a concrete meaning in the digital-image-based generation of three-dimensional representations of hardened cement microstructure, as well as in the appropriate methods available to describe ionic diffusion and the accuracy of the constitutive laws (e.g., porosity/permeability, porosity/diffusivity, etc.) that were developed for these materials.

With respect to the other guideline, the application of reactive transport models to the field of cementitious materials is relatively recent. It is thus important to trace the evolution of such procedures up to this date and identify how they were (and are) affected by the idiosyncratic properties of these materials. These objectives not only crystallized in the description of the milestones of the transition that has led to the current state of the art but also in the critical appraisal of current models, as has been attempted here by examining the most appropriate methods for modeling the diffusion of electrically charged particles. Addressing this particular matter is one of the original contributions of this work and, in that sense, results showed that Fick's law-based approaches to diffusive transport might not be accurate enough to model the degradation of cementitious materials (see Paper III).

At the core of this thesis, results obtained by means of the reactive transport program CORE^{2D}, specifically adapted to evaluate the evolution of the physical properties of concrete, were found to satisfactorily match empirical data from experiments published in the scientific literature (see, e.g., Paper I).

Moreover, in concert with digital-image-based cement hydration programs, reactive transport models can become an extremely useful tool in the design process of concrete and cement-based grout mixes. The latter case (see Paper II), which can be considered critical since it implies a compromise between two conflicting requirements (the workability and injection capacity at early stages, on the one hand, durability, on the other), is illustrative of the scope of this methodology.

Index

1. Introduction

1.1 Background

The work presented here comprises the most significant results of a four-and-a-half-year research carried out at the University of Santiago de Compostela. Most of it was developed within the framework of the Project DECON for the development, testing and calibration of a model of degradation of concrete, funded by the Swedish Nuclear Fuel and Waste Management Company Svensk Kärnbränslehantering AB. It is noteworthy that the company, owned by the four Swedish power companies, is tasked with managing and disposing of radioactive waste from the Swedish nuclear power plants in a manner that complies with extremely stringent standards. In pursuit of the objectives laid by the Project, one of the main focuses of the present research was put on the refinement of modeling techniques, so as to provide a valuable tool for the long-term prediction of the behavior of concrete, in particular when it is exposed to contact with groundwater. The understanding gained should be of valuable help in the context of the safety assessment of nuclear waste disposals.

1.2 Objectives

The subject of this thesis is therefore strongly oriented towards the development and practical application of reactive transport models. For the sake of summarizing, what this work was intended for was to build up a reactive transport model able to make reliable predictions of the degradation of concrete in the long term. That entails the accomplishing of, among others, the following items:

1. Examine critically the modeling techniques available at present;

2. Incorporate the latest innovations into our own reactive transport models;

3. Analyze the peculiar features of concrete in detail and evaluate how they should be contemplated from a modeler's standpoint;

4. Test the reactive transport models against experimental data.

To which extents those aims were achieved will be the matter of the following Sections.

1.3 Outline

For the present work, the amount of material gathered through these years was limited to the most substantial results obtained. Firstly, a brief recapitulation of the evolution of modeling techniques for both the simulation of cement hydration and of reactive transport processes throughout recent years is presented. It is intended to set forth an overview of the trends that have converged in the current state of the art on these matters while, at the same time, bringing the content of this thesis in a proper context. This will be followed by an extended resume of each of the papers into which this research has crystallized, with emphasis on the main contributions that they leave in this field of knowledge. The papers themselves will be presented afterwards, namely, in chronological order, 'Simulating concrete degradation processes by reactive transport models', which was already published in volume 136 of the Journal de Physique IV (2006); 'Assessment of the long-term stability of cementitious barriers of radioactive waste repositories by using digital-image-based microstructure generation and reactive transport modelling', accepted for publication in Cement and Concrete Research[3]; and 'On the relevance of electrochemical diffusion for the modeling of degradation of cementitious materials', also accepted for publication in Cement and Concrete Composites. The publications are all catalogued in the Journal Citation Report.

[3] The paper is in press at the moment and available online since December 2009.

2. State of the art

2.1 About cement and hydration processes

Cement is made up of cement minerals, formed by burning of limestone and clay. The main components are tricalcium silicate ($(CaO)_3SiO_2$, ~58 % by weight), dicalcium silicate ($(CaO)_2SiO_2$, ~13 % by weight), tricalcium aluminate ($(CaO)_3Al_2O_3$, ~8 % by weight) and tetracalcium ferritealuminate ($(CaO)_4Al_2O_3Fe_2O_3$, ~7 % by weight). All the compounds present in Portland cement are anhydrous, but when brought into contact with water they are all attacked or decomposed forming hydrated compounds. The process by which these anhydrous cement clinker minerals react with water to give rise to new hydrated solid compounds is referred to as hydration. During this process, supersaturated and unstable solutions are formed temporarily, but these gradually deposit their excess solids and tend to come into equilibrium with the hydrated compounds produced. The rate of attack and the degree of temporary oversaturation of the solutions are determined by the physical state of the cement compounds as well as by their chemical nature. Since the original anhydrous compounds cannot exist in equilibrium with aqueous solutions, the ultimate result of the action of water must be complete hydration. As a result, hydrate products arise, among which calcium silicate hydrates (C-S-H), calcium hydroxide, calcium aluminate and calcium ferrite are found.

The amount of water added, usually expressed in terms of water-to-cement (w/c) ratio, influences the properties of the hardened paste in a twofold way. On the one hand, w/c ratios below approximately 0.3 are insufficient to fully hydrate the cement clinker minerals and, as a result, to give the mature paste the desired mechanical strength. On the other hand, high w/c ratios allow an excess of water to take place in the mixture which, after the main hydration reactions occur, remains as free water, giving the concrete a characteristic porous structure. In fact, porosity is ruled by two main factors, namely, capillary and gel pores, the former induced by high w/c ratios, the latter arising because of the disordered structure of the calcium silicate hydrates (as will be explained below).

According to Krstulovic and Dabic (2000), hydration can be thought of as three superimposed processes, namely: (1) nucleation and crystal growth, (2) interactions at phase boundaries and, (3) diffusion which, although occurring simultaneously, are governed by the slowest in each stage. Fresh cement paste has a complex structure as it forms in a rapidly changing environment. The exothermic dissolution reactions give rise to a supersaturated solution in which different components nucleate and grow. Some components like C-S-H

precipitate and grow on the surface of the clinker grain, whereas others like calcium hydroxide and ettringite can precipitate in the water phase.

The first stage of the process consists of the dissolution of sulfate and alkali constituents, together with the protonolysis of tricalcium aluminate. Almost simultaneously the major calcium silicate minerals of the cement start to react. The main reaction starts with the protonolysis of silicone oxygen bonds at tricalcium-dicalcium surface. Hydroxil and silicate ions are generated, and the simultaneously calcium ions will precipitate the silicate ions as C-S-H at the surface. The first-stage product has a very low permeability, slowing down the migration of water to the clinker surface and the release of calcium and hydroxil ions to the pore water. A couple of hours later, the first product undergoes changes which turn it more permeable, thus accelerating the hydration process. Prolonged hydration times reduce the amount of free water in the mixture and stabilize the cement structure. As a consequence, concrete becomes denser and stronger.

Regarding the inherent intricacies of the hydration reactions (a reaction system consisting of multi-size, multi-phase particles that evolves from a viscous suspension to a rigid load-bearing solid) researchers have frequently approached this phenomenon from a spatial evolution standpoint. Whether models are continuum (see, for example, the work by Livingston (2000)) or discrete, both attempt to simulate the microstructure of the progressively hardened paste as a set of particles whose attributes change with time.

Conceptually, akin to discrete hydration models, the work developed mainly by Bentz and Garboczi during the 90s certainly stands out, having become one of the most widely accepted and tested. Like many other models, it is focused on the development of the solid phase. Unlike them, however, it features the incorporation of digital image analysis and random 'cellular automaton' growth rules. In the following paragraphs, this method is reviewed on the basis of Bentz (1999) (Figure 1).

Digital-image-based models consider these materials at the sub-particle level and operate on all of the pixels comprising the microstructure using a series of cellular automaton rules, i.e., a computer algorithm that is discrete in space and time and operates on a lattice of sites. Examples of physical processes that can be simulated using cellular-automaton-like rules include dissolution, precipitation, nucleation and diffusion.

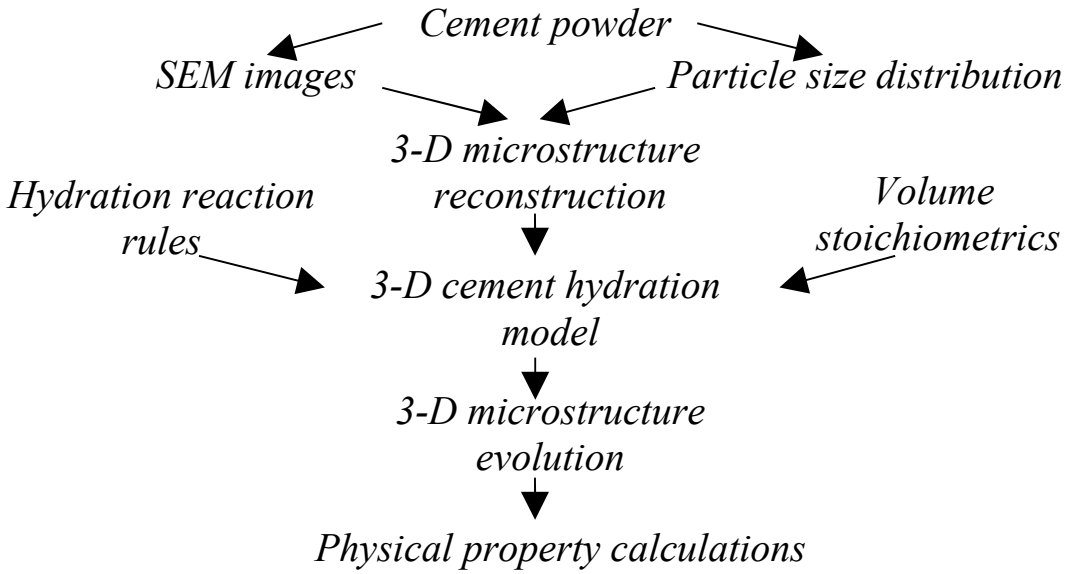

Figure 1. Flow diagram summarizing experimental and modeling program for predicting cement performance (after Bentz, 1999).

A digital image typically consists of a two-dimensional array of pixels, each assigned a grey level value indicative of the strength of the measured signal. Such images can be easily analyzed to determine quantities such as phase volume fractions and surface areas as well as the sizes and other stereological properties of individual particles. Computationally, the concept of digital image can be easily extended to three dimensions. These digital images are easily mapped onto finite difference or finite element grids for the subsequent computation of properties such as electrical conductivity or elastic modulus.

Three-dimensional image reconstruction techniques originally developed for two-phase porous materials can be readily adapted to distribute the most important cement phases amongst a collection of digitized spherical cement particles. The image reconstructions rely on the fact that for an isotropic material, the autocorrelation function of a phase is the same in two and in three dimensions. In the reconstructed three-dimensional image, the particle size distribution, phase volume fractions and phase surface area fractions of the real cement powder can all be preserved. Indeed, the autocorrelation functions for various different phase combinations are calculated by means of a two-dimensional digital image (usually obtained by Scanning Electron Microscopy and X-ray techniques) of cement powder.

Once a digital image is obtained and autocorrelation functions are derived, the next step is to place digitized spherical particles at random locations in the three-dimensional computational volume following the measured particle size distribution, for the cement of interest such that the desired water-to-cement ratio is reached.

In a later stage, clinker phases are distributed amongst the particles assigned to be cement during particle placement. The measured autocorrelation functions are used to create a three-dimensional filter that is applied to an image of Gaussian random noise overlaid on the 3-D cement particle image. After the filtering process, the correlated random noise image is thresholded to obtain the requested volume fraction of a specific phase. A curvature assessment algorithm is then employed to match the surface area fraction of the phase to that measured in the real 2-D image. This procedure is first executed to separate the cement into silicates and aluminates and later to split silicates into C_3S and C_2S and aluminates into C_3A and C_4AF.

The hydration model implements a series of cellular automata rules to simulate the reactions that occur between the starting cement phases and water, taking into account the densities, molar volumes and heats of formation of the individual phases, as schematized in Figure 2. An analogous procedure will be discussed later when commenting upon random models of degradation of cement.

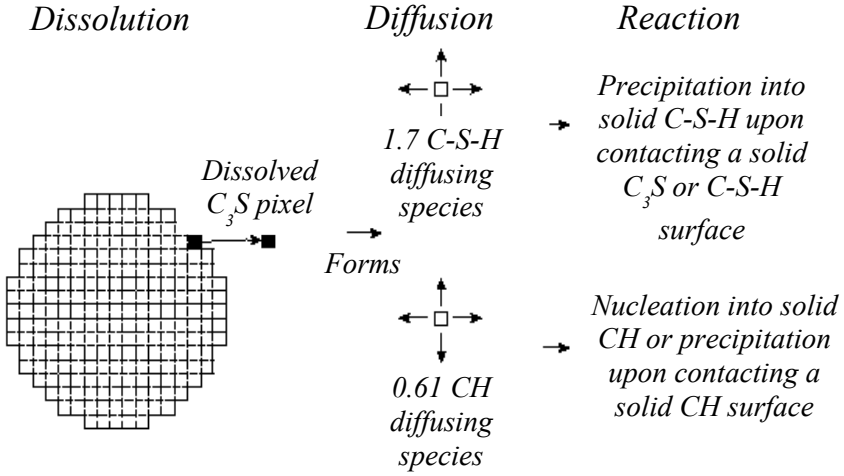

Figure 2. Schematic diagram of the cement paste microstructural development algorithm (after Garboczi and Bentz, 1992).

Figure 3 shows the resulting intermediate phases of the simulation of hydration, beginning with the original digital image of cement powder.

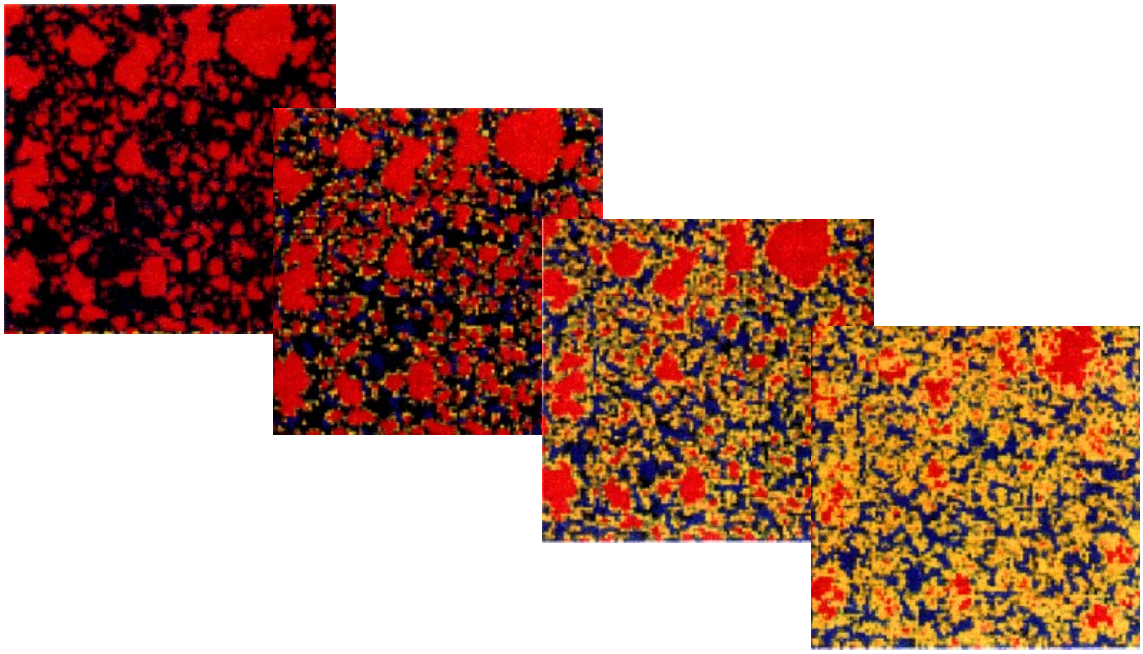

Figure 3. Four stages of hydration in a microstructural model of C_3S hydration. The degrees of hydration are, from left to right, 0 %; 20 %; 50 %; and 87 %. Colour assignments are: red – unreacted cement; blue – calcium hydroxide; yellow – C-S-H; and black – porosity (after Garboczi and Bentz, 1996).

A practical application of these procedures is discussed in Paper II, where they are put into use to help in the process of selection of the optimum mixture recipe for a cement-based grout. This material, usually designed to seal the fractures of the surroundings of nuclear waste disposals, to reduce its hydraulic conductivity, is characterized for high water-to-binder ratios, which are required to meet the desired workability and injection ability at an early stage. As a consequence, once being hardened, grout is left with a large volume of pores, which may affect its durability and undermine its long-term geochemical performance.

Paper II then presents a methodology that involves the combined use of the computer programs CEMHYD3D (for the generation of digital-image-based microstructures) and CrunchFlow (Steefel, 2008) (for the reactive transport calculations affecting the materials so simulated), and that is applied to two grout types, namely, the so-called Standard mix 5/5 and the "low-pH" P308B.

Interested readers can confirm that the results of the digital reconstruction of the mineralogical composition of the hardened paste are entirely congruent, as the microstructures display high degrees of hydration, large porosities and low or nil contents of aluminum compounds.

2.2 About reactive transport models

Hardened cement paste is a porous material filled with a solution in thermodynamic equilibrium with solid hydrates. Attack on cement pastes by water with a low mineral content and approximately neutral pH is one of the worst possible scenarios which can be envisaged, because the hydrates, which are stable at approximately pH 13, are no longer in thermodynamic equilibrium and risk of being dissolved.

During the last decades, researchers have faced various alternatives to describe the diffusion properties of the porous material at the macroscopic scale. Numerous authors have chosen to model the pore structure of cement systems on the basis of microstructural information such as that provided by mercury intrusion porosimetry. More recently, the reconstruction of the microstructure by means of random models has become an equally valuable choice. Given the intrinsic complexity of the pore structure of most cement-based systems, the effective application of these data constitutes a formidable task. In most cases, though, these models rely on "material" parameters (determined on the basis of simplified assumptions that are meant to represent the physical characteristics of the system, however loosely) to fully describe the intricate nature of the microporous solid.

Another solution consists in simply averaging the variables of interest over a representative elementary volume (REV). The main advantage of this approach (called the homogenization technique) is that it does not require any detailed knowledge of the material inner structure. Another significant advantage is that the new averaged variables appearing in the equations can easily be measured in practice.

Three main methodological approaches can be distinguished for the modeling of leaching of concrete, namely, empirical models, random models and phenomenological models.

Several models can be found in the scientific literature that fit into the first category. For the sake of this overview, however, only the work published by Kamali *et al.*, (2003) will be looked at since it is among the most recent ones and is archetypical of this kind of models. This one is a simplified one-dimensional model based on a laboratory database built with published experimental data dealing with the effect of material parameters and environmental conditions on the kinetics of leaching. The model assumes that the rate of leaching exhibits a square-root-of-time dependence, as does the theoretical solution of the Fick's law (Eq. 1).

$$L_d = at^{0.50} \quad (1)$$

where L_d represents the leached depth; t is time; and a is a constant parameter. The constant a is taken to be the product of five weight functions, each denoting the isolated influence of one of a set of given material and environmental conditions which, allegedly, fully defines the problem in question. These are, namely: 1) water-to-cement (w/c) ratio; 2) percentage of silica fume content (SF); 3) pH of the aggressive water; 4) temperature (T) of the system; and 5) test protocol (Pr).

Therefore:

$$a = e \times f(w/c) \times g(SF) \times h(pH) \times i(T) \times j(\mathrm{Pr}) \quad (2)$$

The constant parameter e and the analytical expressions of functions, f, g, h, i and j are then evaluated by least squares procedures after the available data have been normalized with respect to the given reference material and test protocol.

Even though this model highlights the qualitative influence of the some selected parameters its applicability is restricted to a very narrow range of practical conditions. Obviously, the main advantage of this method lies on its simplicity but the superimposed effect of five independent variables is hardly enough to cope with the complexity of concrete degradation, which demands many more, often interrelated, variables to be taken into account. In any case, perhaps the most arguable feature of the model (which is shared with any other of this category) is that, apart from the relative unreliability for making long-term predictions, its inability to give insight into the very nature of leaching, thus remaining as a mere mathematical artifact.

Random models, on the other hand, are of an entirely distinct nature, of which the digital-image-based model developed by Garboczi and Bentz (1992) is illustrative. Degradation is herein modeled as a cyclic random dissolution process for which one digital image of the hydrated cement paste sets the starting point. As long as the resolution of the digital image allows it, every pixel (approximately one μm in size in real scale) is distinguished to be made up either of calcium hydroxide, C-S-H (calcium silicate hydrate) or capillary water. Calcium hydroxide being the most soluble product of hydration, for each leaching cycle, the 3-D microstructure is scanned to identify all elements of occupied by it, one or more of whose nearest neighboring pixels belong to the pore space. All such elements are then applied an impulse to execute a one-step random walk to one of their adjacent sites. If the step is such that the selected particle lands in a pore space pixel, the element of calcium hy-

droxide is removed from the image, which stands for its dissolution. Otherwise, the element remains in its place, undissolved.

Since the calcium hydroxide elements that dissolve increase the capillary porosity, the dissolution process is likely to affect the percolation and diffusion properties of the pore space of the material.

One dramatic effect that leaching can have on cement paste is that a material in which the capillary pore space was initially discontinuous may be transformed into a material with a continuous capillary pore structure. This latter system will be much more susceptible to degradation, as the transport of ions which was originally dominated by "slow" transport through the C-S-H gel phase will now be dominated by "fast" transport through the percolated capillary pore structure. This effect becomes more and more relevant with decreasing water-to-cement ratios, as was corroborated by Marchand *et al.* (2001).

Although a very valuable tool to evaluate the qualitative response of the cement paste to leaching, the applicability of random models could be open to question as it fails to properly observe the physicochemical laws underlying the process of deterioration. The reliability of the model when applied to the simulation of hydration lies also on the large amount of available experimental data. When leaching is concerned, the absence of data precludes the model to provide good predictions. Nevertheless, its predictive ability could be much improved if the random mechanisms involved were coupled to statistical laws derived from analytical models, as pointed out by Marchand *et al.*, (2001).

To close this enumeration, a more detailed review of the broad spectrum of phenomenological models is done. Reactive transport models (as will often be referred to in the following) involve the numerical resolution of the coupling between solute transport and the chemical processes arising from it.

A significant number of reactive transport models performed for simulating concrete leaching rely on the assumption of local equilibrium. According to it, the rate of the chemical reactions of the various species in solution is intrinsically much faster than the rate of transport. The validity of this assumption rests on the observations that, in most degradation cases involving construction materials, chemical reactions usually progress as fronts originating from the external surfaces of the solid. Barbarulo *et al.*, (2000) subjected the hypothesis of local equilibrium to a dimensional analysis, which essentially consists of reducing the governing transport equation to a dimensionless equation through the use of scaling variables. This approach then proceeds in four different steps:

1. Identification of the characteristic values (scaling parameters) of the problem;

2. Identification of the dimensional quantities and fundamental units of the problem;

3. Reduction of the governing equations to a dimensionless expression;

4. Identification of the dimensionless numbers.

Neglecting activity effects, the following dimensionless numbers were then obtained:

$$\left(\frac{\tau D_i}{L_0^2}\right), \left(\frac{D_i}{D_j}\right), \left(\frac{c_0 L_0^2 F}{\varepsilon \Gamma \Psi_0}\right), \left(\frac{F\Psi_0}{RT}\right), \left(\frac{K_\Phi^{sp}}{\overline{c_0^L}^{\nu_a+\nu_b}}\right), \left(\kappa_\Phi \tau \overline{c_0^L}^{\nu_a+\nu_b-1}\right)$$

where c_0, L_0, τ and Ψ_0 stand for characteristic values of concentration, length, time and diffusion potential dependent of the problem under analysis; $\overline{c_0^L}$ is the normalized dimensionless concentration; R is the ideal gas constant; F is the Faraday constant; T is the temperature; Γ is the tortuosity of the aqueous phase; $K_\Phi^{sp} = (\gamma_a c_a)^{\nu_a} (\gamma_b c_b)^{\nu_b}$ is the equilibrium solubility constant of a given phase Φ and κ_Φ is its reaction rate coefficient of dissolution/precipitation; γ_i is the chemical activity coefficient of the i-th chemical species and D_i is its diffusion coefficient in the liquid phase.

The first dimensionless number provides information on the characteristic time required by a given species to diffuse through the system. The second one compares the diffusion coefficient of one species to the other. The third number characterizes the linearity of the diffusion potential Ψ_D distribution across the system. The fourth number denotes the relative importance of the diffusion potential term on the overall transport process. The fifth number can be used to verify whether the system is anywhere close to its equilibrium condition. Finally, the sixth number determines the scale of the kinetics of a given reaction.

It was demonstrated that for most cases, $\left(\kappa_\Phi \tau \overline{c_0^L}^{\nu_a+\nu_b-1}\right)$ is much greater than $\left(\frac{\tau D_i}{L_0^2}\right)$, which leads to the conclusion that the global behavior of the system will be dominated by the rate of the transport process, i.e., the kinetic rates of the reactions are much higher and, for practical purposes can be regarded as

instantaneous with respect to diffusion, in agreement with the local equilibrium hypothesis.

The most significant issues concerning the coupling of transport phenomena and chemical reactions arising in the water/cement system could be tackled by reactive transport modeling techniques (Saaltink, 1999; Samper *et al.*, 2000). The mathematical handling of the problem depends on whether the latter are either homogeneous (i.e., those reactions which involve a single phase, such as complexation reactions) or heterogeneous (i.e., involving both the solid and the aqueous phase). In turn, heterogeneous reactions could be further divided into surface chemical reactions (e.g., ion exchange) and dissolution/precipitation reactions. The following paragraphs are intended to summarize the usual procedures made in order to describe the problem from a rigorously mathematical standpoint, based upon a global overview afforded by Samson *et al.*, (2000):

a) Treatment of homogeneous chemical reactions.

A mixed set of nonlinear equations arises as a result of simultaneously assuming that:

a.1) transport of each species and complexes obeys certain well-established diffusion laws (e.g., Fick's law, Nernst-Planck equation);

a.2) local equilibrium relationships hold;

a.3) chemical activity coefficients can be accurately defined by some appropriate expression (e.g., Debye-Hückel or Davies equation);

a.4) mass conservation laws apply for each species considered, regardless of whether they are present as free ions or chemically bound to aqueous complexes.

The resolution of the set of equations requires the discretization into a finite-difference or finite-element framework, and leads to the determination of the local concentration of every ionic species and complexes at each node of the meshed liquid-phase space, along with their respective chemical activity coefficients. In this manner, usually very large sets of equations are obtained, all the more so as more ionic species are included in the calculations. This is an extremely challenging task for "traditional" methods of resolution. More modern techniques, such as neural networks, are expected to enhance the efficiency of current codes available.

b) Treatment of surface chemical reactions.

This kind of chemical reactions involves the presence of ionic species competing for sites available on the solid surface. Since all species are interchangeable, the ion-exchange capacity, $c_T^{(s)}$, denoting the total amount of sites available could be defined as follows:

$$c_T^{(s)} \sum_{i=1}^{n} c_i^{(s)} \tag{3}$$

where n is the number of exchanging ions and $c_i^{(s)}$, the concentration of the i-th species adsorbed by the solid surface.

The foregoing expression is then coupled with the local equilibrium relationship and the transport equations, expressed in such a fashion that concentration of the exchanging ionic species are explicitly taken into account.

c) Treatment of dissolution/precipitation reactions.

Even though formally similar to the previous cases, the methodology applied to solve dissolution/precipitation reactions should observe that local equilibrium laws hold as long as a precipitate is present in the system. Otherwise, the following inequality is valid instead:

$$K_{\Phi}^{sp} > \left(\gamma_a \overline{c_a^L}\right)^{\nu_a} \left(\gamma_b \overline{c_b^L}\right)^{\nu_b} \tag{4}$$

where all variables have already been defined.

This inequality allows the precipitate concentration to be discontinuous in the material (Kirkner and Reeves, 1988). Thus, the solid concentration behaves like a moving boundary in the direction opposite to the leaching of ions.

Three techniques were developed in order to cope with this type of problem. The first separates the porous material into k zones of constant mineralogical properties and solves the transport equations in each zone with the proper conservation equations at the moving boundary interfaces. The second technique combines the algebraic equations for chemical equilibrium with the partial differential transport equations to form a global system of equations (Kirkner *et al.*, 1984) so that chemical equilibrium relationship is presumed not to be in effect initially but it is checked at every node after each iteration. The other technique consists in uncoupling the transport and the chemical reactions (Xu *et al.*, 1999). Concentration profiles of the various species are calculated with a transport model without taking into account chemical reactions and later checked at every node whether chemical equilibrium relationships of

the various reactions considered are violated or not. In case they do, they are brought back to equilibrium with a separate chemical code and the solid phases are modified appropriately if dissolution or precipitation occurs.

Diffusion-controlled ionic transport is sensitive to the porosity changes undergone by the concrete microstructure because of either dissolution of calcium compounds or precipitation of carbonates and magnesium and aluminum compounds on the outer surface of the degraded region. A relevant contribution on the former was provided by Carde and François (1999), who modeled the variation of the porosity based on the experimental results of accelerated leaching tests. According to it, two zones could be identified in the degraded region, the first associated to the dissolution of calcium hydroxide, and the other to both the dissolution of calcium hydroxide and the decalcification of the C-S-H gel. The loss of calcium present in the solid phase, mainly as massive crystals of calcium hydroxide, is directly related to the increase of the porosity. As a corollary, the addition of pozzolanas is suggested to have a beneficial effect on durability, as it hydrates at expense of the formation of calcium hydroxide.

Mainguy *et al.*, (1999) introduced a model, for both pure cement and mortar, which solves the following governing equation, accounting for the mass balance of calcium in a two-phase system:

$$\frac{\partial \phi\, Ca_{(aq)}}{\partial t} = \nabla \bullet \left[D \nabla\, Ca_{(aq)} \right] - \frac{\partial\, Ca_{(s)}}{\partial t} \qquad (5)$$

where $Ca_{(aq)}$ represents the calcium concentration in the aqueous phase, $Ca_{(s)}$ denotes the calcium concentration in the solid phase and D is the diffusivity of calcium and ϕ is the porosity of the hardened paste.

The model relies on the assumption that capillary porosity is univocally related to the fraction of calcium hydroxide dissolved (i.e., the decalcification of the calcium silicate hydrates is ignored in the calculations). The calcium concentration in the solid phase is then chosen as the main state variable, as dissolution of calcium hydroxide occurs at a constant concentration of calcium ions in the pore solution. The following equation is therefore given rise:

$$\frac{\partial \phi \left(Ca_{(s)} \right) Ca_{(aq)} \left(Ca_{(s)} \right)}{\partial t} = \nabla \bullet \left[D\left(Ca_{(s)} \right) \nabla\, Ca_{(aq)} \left(Ca_{(s)} \right) \right] - \frac{\partial\, Ca_{(s)}}{\partial t} \qquad (6)$$

where all the variables are explicitly expressed as functions of $Ca_{(s)}$. Those functions are defined in terms of the mathematical expression of the regres-

sion curves derived from the empirical relation between each of them and the first one.

Sensitivity analyses demonstrated that model results are very sensitive to the variation of concrete porosity, which underlines the relevance of a reliable prediction of its evolution.

A more sophisticated model was developed by Yokozeki *et al.*, (2004). Yet, in spite of dismissing the data fitting procedures in favor of more proper thermodynamical considerations, the main assumptions remain but hardly changed. As in the previous models, transport processes are accounted for by means of a purely diffusive approach, where the diffusion coefficient exhibits a dependence of the changes of porosity and, in turn, the evolution of porosity is governed by calcium hydroxide dissolution. Indeed, the authors distinguish three kinds of porosity, namely gel porosity, θ_{gel}, capillary porosity, θ_{cap}, and the porosity induced by leaching, θ_{leach}, such that, according to the expressions proposed by Powers (1960):

$$\theta_{gel} = \frac{0.19 F_{avg}}{w/c + 0.32} \tag{7}$$

$$\theta_{cap} = \frac{w/c - 0.36 F_{avg}}{w/c + 0.32} \tag{8}$$

where F_{avg} is the degree of hydration (1.0 for hydrates after a long period, usually greater than 35 years). On the other hand, porosity induced by leaching is expressed as:

$$\theta_{leach} = \frac{M_{CH}}{d_{CH}} \left(C_{P0} - C_P \right) \tag{9}$$

where $M_{CH} = 74$ g/mol and $d_{CH} = 2230$ g/L are the molecular weight and the density of calcium hydroxide, respectively; C_P and C_{P0} are the general and initial calcium concentration in the solid phase, respectively.

Furthermore, the effective diffusion coefficient is given by:

$$D_{eff} = \frac{1 - cG_{vol}}{1 - dS_{vol}} P_{vol} f\left(\theta - \theta_{gel}\right) D_0 \tag{10}$$

where G_{vol} and S_{vol} are the volumetric ratio of coarse and fine aggregates in concrete, respectively; $P_{vol} = 1.0 - G_{vol} - S_{vol}$ is the volumetric ratio of paste in

concrete; D_0 is the diffusion coefficient in water; and $f\left(\theta - \theta_{gel}\right)$ is a reduction factor applied to the diffusion coefficient to reflect micropore tortuosity.

Calcium hydroxide dissolution is ruled by the following equilibrium law:

$$K_{sp} = \log\left[Ca^{2+}\right]\left[OH^{-}\right]^2 = 556\frac{1}{T} - 6.28 \qquad (11)$$

where T, expressed in ºK, is the absolute temperature of the system.

The model just reviewed was proven to roughly match experimental data drawn from natural analogues with ages ranging from 34 to 104 years. However, considering calcium ions as the only diffusive species in the model is certainly a liability, since then the influence of other reactions on the evolution of the leaching process is unjustifiably neglected.

This latter point was addressed by Moranville *et al.*, (2004). Apart from calcium, a number of ionic species were identified as significant for the progress of degradation: silica, aluminum, sulfate, sodium and potassium. The first four species are involved in dissolution or precipitation of the main solid constituents present in a Portland cement paste: C-S-H, calcium hydroxide, ettringite, and calcium monosulfoaluminate. Alkaline ions (Na^+, K^+) were also taken into account because of their presence during the cement hydration process.

The reactive-transport system of equations was numerically solved in three stages: (i) diffusion transport; (ii) chemical reaction calculations; and (iii) calculation of transport parameters, from the volume balance of dissolved or precipitated solid species.

A purely diffusive approach, based on the use of the Fick's law (Eq. 12), was taken in order to evaluate the transport processes.

$$\frac{\partial c}{\partial t} = D_{eff}\frac{\partial^2 c}{\partial x^2} \qquad (12)$$

As for the second stage, additional equations were included, accounting for the mass conservation for all species, the mass action laws that determine for each solid an equilibrium relationship with the ions involved and the electroneutrality of the pore solution.

The arising nonlinear set of equation was then evaluated by means of the Newton–Raphson algorithm in such a manner that ionic activities were computed at each iteration with the Debye–Hückel model. This reactive calculation scheme was done with the PHREEQC geochemical code (Parkhurst and

Appelo, 1999) and a modified thermodynamical database based on PHREEQC default one. The C-S-H chemical behavior was simplified by using two calcium silicate hydrates: the first one with a calcium-to-silica ratio C/S = 1.65, i.e., $C_{1.65}SH_{2.45}$, and the second one with a C/S equal to 1.10, i.e., $C_{1.10}SH_{1.90}$. The decalcification of C-S-H is then ruled by a linear combination of both compounds.

An interesting feature of the model consists in the simulation of the study domain by means of the digital-image-based microstructure analyses, as described in the "random models". The mass of each solid that dissolves or precipitates until a new thermodynamical equilibrium is reached, as calculated by PHREEQC, is then used to calculate in each cell the new capillary porosity which, in turn, rules the magnitude of the new apparent diffusion coefficient. This is the last instance in the numerical resolution of the reactive-transport equation previous to the following time step.

The relative solid species profiles obtained by the model were found to resemble those obtained by relative EDS X-ray analysis, all the more closely after calcium hydroxide has totally dissolved. Nevertheless, the model is unable to reproduce the sharp dissolution fronts observed in experiments, which can be attributed in part to the fact that different solid minerals are allowed to precipitate and dissolve simultaneously.

Although diffusion is calculated for each species, no mention is made by Moranville *et al.*, (2004) as to the different diffusion coefficients considered nor how were they derived. This point has serious implications on the evolution of dissolution/precipitation reactions, which might be magnified by the particular resolution strategy adopted, i.e., the decoupling of transport and chemical calculations. It is worth noting that once the transport calculations are performed, chemical equilibrium is reached at expense of the amount of solids dissolved. On the other hand, on the basis of their own leaching tests, Moranville *et al.*, (2004) observed that the leaching rate of concrete exposed to mineralized water is less than that exposed to pure water due to the positive effect of carbonation. The formation of calcite microcrystals decreases the porosity of the external zone and, consequently, the diffusivity of ions from the aggressive water. Such a likely scenario was not modeled, suggesting that a greater number of ionic species are required to properly evaluate the evolution of the deterioration.

Despite these shortcomings, the inclusion of ionic species other than calcium into the process and the use of 'synthetically-generated' microstructure, sets the model closer to the actual concrete behavior than the previous ones. This is essentially the same approach employed in Paper I, where a reactive transport models built with the help of the computer program $CORE^{2D}$ (Samper *et*

al., 2000), was tested against an experiment reported in the scientific literature, involving both diffusive and advective transport. Paper I was also intended to evaluate the accuracy of the constitutive laws (e.g., porosity/permeability, porosity/diffusivity, etc.) developed for cement-based materials.

A further step forward was made by the Laval University (Canada) research group, mainly through the papers published by Marchand *et al.*, (2001), Marchand *et al.*, (2002) and Maltais *et al.*, (2004). Diffusion transport and electroneutrality are taken into account simultaneously by solving the Nernst – Planck equation at each time step:

$$j_i = -D_i \mathrm{grad}(c_i) - \frac{D_i z_i F}{RT} c_i \mathrm{grad}(\psi) - D_i c_i \mathrm{grad}(\ln \gamma_i) \tag{13}$$

where j_i is the flux of the species of concentration c_i in the aqueous phase and z_i is the valence of the ionic species; the remaining variables were defined above.

The diffusion potential ψ set up by the drifting ions is defined according to the Poisson equation:

$$\nabla^2 \psi - \frac{\rho}{\varepsilon} = 0 \tag{14}$$

where ε is the permittivity of the medium and ρ represents the electrical charge density, which is defined as:

$$\rho = F \sum_{i=1}^{N} z_i m_i \tag{15}$$

m_i being the molality of the i-*th* (out of a total of *N*) ionic species.

In this case, eight ionic species were deemed relevant for the description of leaching, namely, K^+, Na^+, Mg^{2+}, Ca^{2+}, SO_4^{2-}, OH^-, $Al(OH)_4^-$ and Cl^-. Diffusion coefficients were reported for K^+, Na^+, Ca^{2+}, SO_4^{2-}, OH^- and $Al(OH)_4^-$, for the different cement types and water-to-cement ratios studied.

The numerical model set forth by Maltais *et al.*, (2004) reproduces accurately the shape of the calcium profile for the samples constantly immersed in deionized water. Microprobe analyses, SEM observations and the output of the model confirm that calcium hydroxide is the first calcium-bearing phase to be influenced by the exposure to deionized water. Microprobe analyses also demonstrate that C-S-H is not stable in presence of deionized water, i.e., C-S-H decalcification begins when the amount of available calcium hydroxide is no longer sufficient to restore the pore solution equilibrium. When all the cal-

cium hydroxide has been dissolved, the equilibrium of the system is controlled by the C-S-H, which undergoes partial decalcification. The decalcification of C-S-H leaves a residual skeleton of "silica gel" with almost no residual mechanical strength (Maltais *et al.*, 2004).

So far, the recent history of the evolution of reactive transport models has been traced through the description of some of its milestones. Paper III is intended to contribute to it with a discussion of the performance of the two different formulations for the ionic transport which have just been introduced, namely the Fick's law and Nernst – Planck equation, judged by their ability to reproduce the results of a simulation of the deterioration of concrete exposed to a weak sulfate solution. Results tend to confirm that for the particular case analyzed, the Nernst – Planck model provides more accurate predictions of the behavior of cement in the long-term, which is immediately apparent from the calculated evolution of gypsum, in good agreement with actual measurements.

3. Main contributions of this work

3.1 Paper I: Simulating concrete degradation processes by reactive transport models (Galíndez *et al.*, 2006)

The increase of porosity of the hardened cement paste is a well-known consequence of concrete degradation, on account of the dissolution of calcium hydroxide and the decalcification of calcium silicate hydrates (C-S-H). The evolution of porosity with time can then be taken as an index of the degree of deterioration undergone by concrete, when exposed to a slightly acidic environment. It is also a widely known property of porous materials that their porosity is related to the transport properties of the aqueous medium that they harbor. However, hardened cement being a very idiosyncratic material, it was not until relatively recently that proper mathematical expressions were developed to characterize the actual constitutive relationships that connect its porosity with both the diffusivity and the hydraulic conductivity. In fact, the function diffusivity versus porosity was first published in 1992 (Garboczi and Bentz, 1992) and, to our knowledge (that is to say, as far as our bibliographical review could reveal), was not used extensively in practical cases after 2001 (Marchand *et al.*, 2001).

In spite of their intrinsic heterogeneity, cement-based materials can be regarded as homogeneous at a much smaller scale than natural granular materials. In practice, two different types of porosity are generally distinguished, namely, gel porosity and capillary porosity. When capillary porosity falls below 18 %, even though there might be some capillary pore space left in the form of isolated clusters, solute transport is mainly controlled by diffusion through C-S-H gel pores (Bentz and Garboczi, 1991) which obeys a law of the Archie's type, but modified by adding a cutoff value R_{min}. For the higher side of the spectrum of porosity values, diffusion rate should increase due to the contribution of capillary pores. On the basis of numerical tests performed on a quantitative representation of the microstructure of the cement paste, generated by means of a digital-image-based random growth model (Garboczi and Bentz, 1992), the following equation was developed:

$$D_{eff} = \left[0.001 + 0.07\phi_f^{\,2} + 1.8H\left(\phi_f - \phi_c\right)\left(\phi_f - \phi_c\right)^2 \right] D_0 \qquad (16)$$

where D_{eff} denotes the effective diffusion coefficient; D_0, the diffusion coefficient in pure water; $\phi_c = 0.18$ represents the critical capillary porosity of the material; and $H\left(\phi_f - \phi_c\right)$ is the Heavyside function.

On the other hand, an expression of hydraulic conductivity in terms of the variation of porosity originally devised for concrete does not exist, but has been borrowed from the field of groundwater hydraulics and adapted to that aim in (Pfingsten and Shiotsuki, 1998). The reasons may probably lie in the fact that few practical problems involving cement-based materials exist where the influence of advection is relevant with respect to diffusion, given the extremely low permeability of the medium. Hydraulic conductivity actually depends on both porosity and the degree of connectivity of the porous network, but the latter is an abstract entity, difficult to grasp in mathematical terms. As a consequence, it was deemed acceptable to follow that previous work and adopt the Kozeny-Carman equation for simplicity's sake, even though it is mainly applicable to granular materials. Recent studies (Huang, 2001) have provided more data concerning this issue, although further research might be needed.

According to its general expression, the Kozeny-Carman equation states that hydraulic conductivity and porosity are linked to each other in the following terms:

$$K = c\frac{\phi^3}{(1-\phi)^2} \tag{17}$$

where K [m/sec.] denotes hydraulic conductivity and c is an empirical constant.

At the start of this research, the numerical code for water flow and reactive solute transport CORE^{2D} (Samper *et al.*, 2000) did not feature any definition for the diffusion coefficient that was valid for concrete nor any constitutive relationship that connected hydraulic conductivity to porosity and thus it was unable to cope with problems involving cementitious materials – it was simply not originally thought for that purpose but rather to groundwater flow in subsurface environments.

With the objective of enhancing the code and its capabilities, new lines of code were programmed, in order to incorporate the formulation of Garboczi and Bentz for the definition of diffusivity and the one of Kozeny-Carman for hydraulic conductivity. Furthermore, a study was carried out under the title *On the methods to evaluate the effective diffusion coefficient in a porous medium* in order to assess the performance of Eq. 16 with respect to other approaches for the description of diffusivity already contemplated in the code. It can be found in Appendix IV of the *Trabajo de Investigación Tutelado* (Galíndez, 2006).

The mentioned improvements made in CORE^{2D} were tested and calibrated in Paper I, Simulating concrete degradation processes by reactive transport models, against the empirical results of a flow-through experiment reported in the scientific literature (Pfingsten and Shiotsuki, 1998).

The experimental setup of the problem in question is shown in Figure 4.

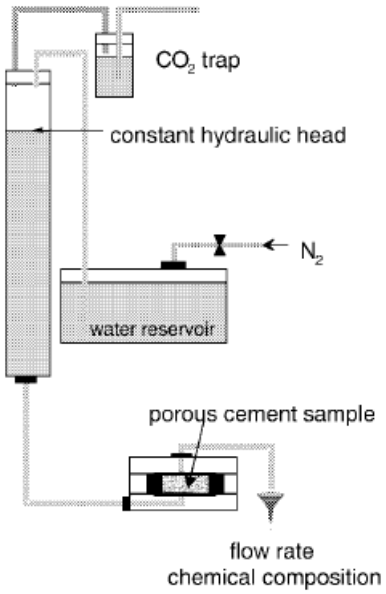

Figure 4. Experimental setup for the degradation of a porous cement disc by pure water (after Pfingsten and Shiotsuki, 1998).

Water flow was driven by a constant hydraulic head through a cylindrical cement specimen. Under CO_2-free conditions, porosity increased indefinitely as a consequence of dissolution of calcium compounds. In turn, discharge rates through the specimen increased with time.

The term hydraulic conductivity will be employed in this context in reference to the entity defined in Eq. 18.

$$K = \frac{q\, d}{\Delta h} \tag{18}$$

where q [m/sec.] is the specific discharge through the cement specimen; d [m] represents its thickness; and Δh [m] is the hydraulic head difference between the inlet and outlet surfaces of the hardened cement specimen.

Paper I also takes a distinct approach from the one used in (Pfingsten, 2001) regarding the thermodynamical behavior of the C-S-H complex. In fact, whereas the model developed in Berner (1988) was used for the description of to that effect, the mineralogical composition of the cement paste was con-

sidered therein to comprise amorphous silica, calcium hydroxide and two minerals, namely, $C_{1.65}$-S-$H_{2.45}$ and $C_{1.10}$-S-$H_{1.90}$, which would account for the calcium silicate hydrates.

Given that no details were reported about the cement composition apart from the weight percentages of cement clinker, a search was made into the Virtual Cement and Concrete Testing Laboratory (VCCTL; http://ciks.cbt.nist.gov) database in order to find a type of cement that could approximately match the known mineralogical composition and series of simulations of the hydration process were performed by means of CEMHYD3D (Bentz, 2000) (a modeling package one of whose main capabilities is the depiction of the resulting synthetic three-dimensional microstructure of the hardened cement paste), in order to obtain the targeted porosity of 0.65 for the hardened cement paste, as reported in Pfingsten and Shiotsuki, (1998). This was done by assigning different volumes (or more precisely, a variable number of pixels in a three-dimensional image) to each compound of the mixture, accounting for the amount of water added, and preserving the relative proportion to one another.

A reactive transport model simulation was carried out once the amount of minerals that constitute the hardened paste was quantified. It was found that the hydrochemical evolution of the system, in terms of the total amount discharged of characteristic aqueous species, such as calcium (Figure 5), are in fairly good agreement with experimental data.

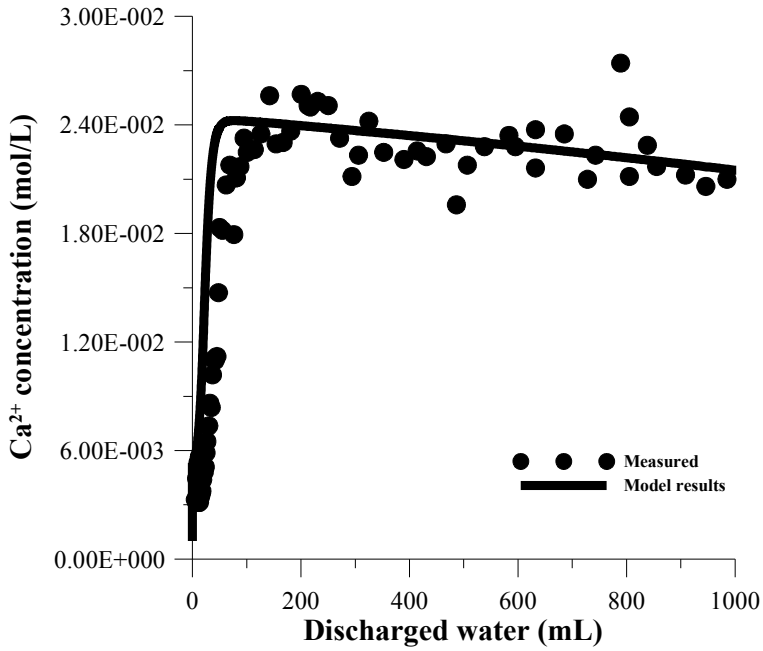

Figure 5. Calcium concentration in discharged water as simulated by the model, compared to experimental data.

Furthermore, the development of the hydraulic properties (e.g., hydraulic conductivity) of the hardened cement paste (Figure 6) was excellently reproduced by the model.

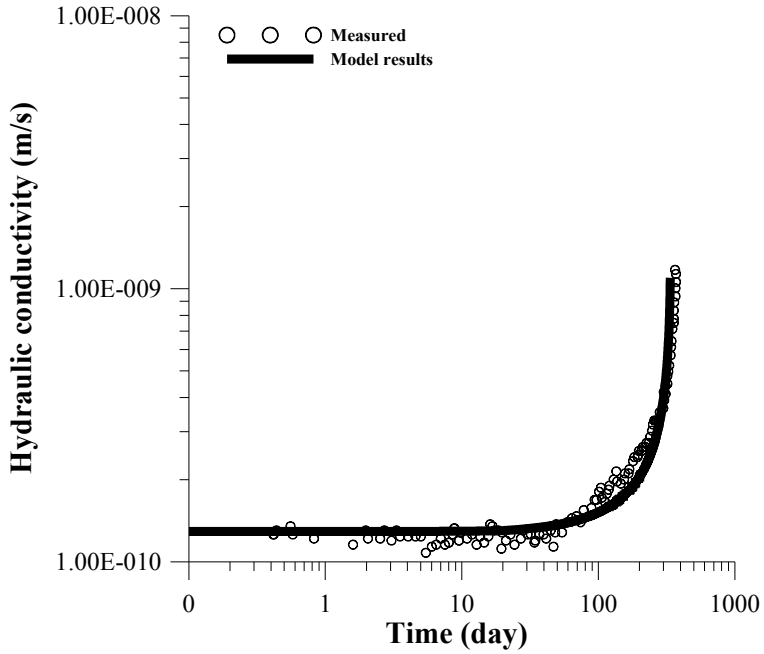

Figure 6. Evolution of hydraulic conductivity as computed by the reactive transport model, compared to empirical data.

On the basis of the results obtained, it was then concluded that the reactive transport model was, above all, sound. Therefore, it should provide a reliable theoretical framework for further study of the long-term degradation of concrete.

3.2 Paper II: Assessment of the long-term stability of cementitious barriers of radioactive waste repositories by using digital-image-based microstructure generation and reactive transport modelling (Galíndez and Molinero, 2009)

The process of selection and testing of the mixture design of cement-based grouts is an arduous task, usually characterized by continual trials and errors. For the sake of illustration, an excerpt of a recent Report on the subject (Bodén and Sievänen, 2005) reads:

'The development of low-pH cementitious grout consisted of several tasks. First the potential systems were selected, based on the outcome of the earlier studies and on expert judgement, and the technical properties of some ***two hundred recipes*** (emphasis added) *were tested. The most promising recipes were then selected for pH and leaching tests. Based on these results, the most promising recipes were tested in two small pilot field-tests in Finland.'*

Indeed, several elements should be contemplated in the process, one of the most relevant ones consisting in the compromise between the two conflicting requirements of workability and injection ability at an early stage, on the one hand, and the long-term durability, on the other hand. (These two factors should eventually converge in the optimum combination of quality and proportions of materials, the latter also including the water-to-cement ratio.) Furthermore, the difficulties to reproduce actual field conditions by means of laboratory add to the complexity of the problem.

In view of this, in Paper II (Assessment of the long-term stability of cementitious barriers of radioactive waste repositories by using digital-image-based microstructure generation and reactive transport modeling), an original and substantially more economical methodology was devised for the optimization of the procedure. It involves the digital-image-based generation of grout microstructure and, on the basis of its output, long-term reactive transport simulations, which would account for the hydration of cement-based grout and the gradual degradation which would occur thereafter, respectively.

As a brand new methodology that is just introduced in this paper, circumspection should be in order. In this respect, it is worth stressing that this method in not intended to replace field experiments –simulating the actual evolution of the process of hydration under field conditions might be an overambitious if not an altogether unrealistic goal– but, rather, to provide a rational method to obtain the likely constitution of grout, in order to define reasonable starting points for subsequent modeling of degradation. Its recognizable potential should, nevertheless, not be ignored for, in absence of more reliable empirical

data, it constitutes a powerful tool to assess the durability of cement-based structures.

Two different types of cement were tested, namely, the mix design labeled as Standard grout mix 5/5 (Holt, 2006) (for use in the upper sections of a tunnel under construction at Olkiluoto, Finland) and P308B grout (one of the most promising ones of the low-pH type (Kronlöf, 2004), which was developed to be injected at higher depths).

The process of numerical generation of the final microstructure of the hardened grout proceeds in a series of steps consisting of the creation of the particle size distribution for both cement clinker and silica fume, the generation of the initial microstructure, the distribution of cement phases and the simulation of hydration. A three-dimensional cement-based grout mixture microstructure is then generated, consisting of the sum of the selected compounds in water, namely cement clinker and, when available, silica fume, with their respective particle size distribution. Once the initial arrangement of generic anhydrous particles in water has been created, the four major phases of cement clinker (i.e., C_3S, C_2S, C_3A and C_4AF) should be distributed amongst the cement particles by filtering based on two-point correlation functions measured, in absence of SEM images of the actual cement employed (Ultrafin 16), through one SEM image of a cement clinker of similar composition, on the assumption that alike results would be obtained in this manner.

The process of hydration, simulated by means of CEMHYD3D (Bentz *et al.*, 1994), was based on the assumption that the microstructural characteristics of the hydrated paste would be roughly the same regardless of the conditions of curing if the degree of hydration was high enough, although further research might certainly be needed on this topic. Its results, however, were entirely congruent, as the microstructures displayed high degrees of hydration (of nearly 100 % for all cases considered), large porosities (i.e., between 40 % and 60 %) and low or nil contents of aluminum compounds, to which sulfate-resistant cement and the addition of silica fume have contributed. These characteristics can be seen in the two-dimensional slices of the generated microstructure of the hardened cement pastes that are shown in Figure 7, where it is apparent that the addition of silica fume derives in a large decrease of the volume fraction of calcium hydroxide, almost absent for mix P308B. All these effects are supported by a huge amount of empirical evidence.

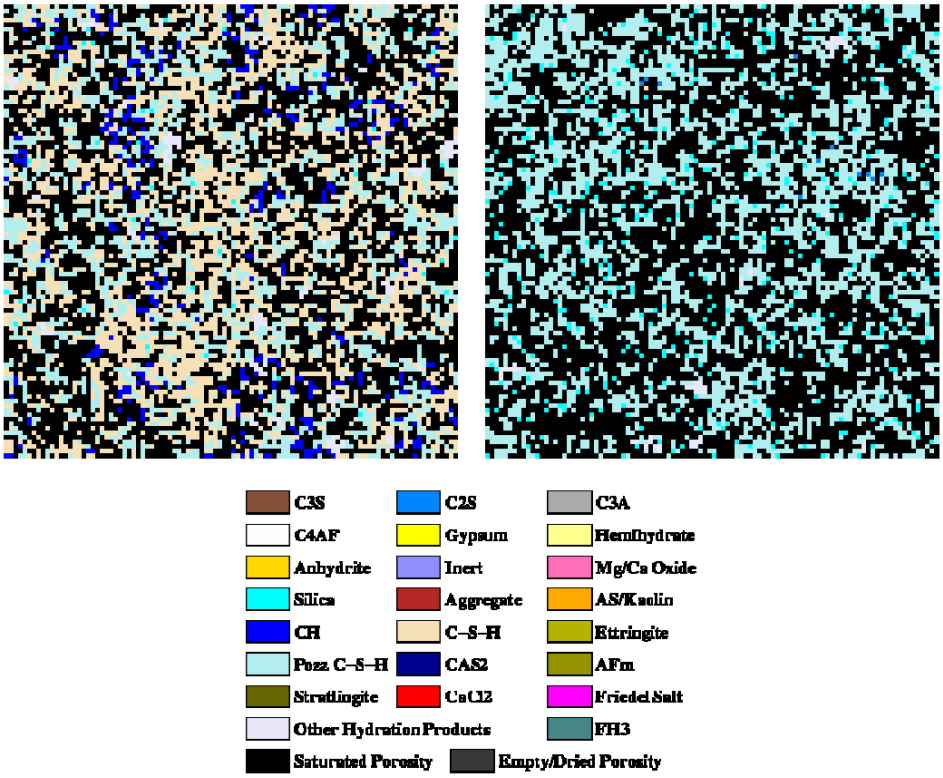

Figure 7. Slices of the three-dimensional microstructures of the hydrated cement paste of the two mix designs analyzed, namely, Standard grout mix 5/5 (left) and P308B (right).

Results of the simulation of the microstructure of hardened cement paste (its estimated mineralogical and physical properties) were then linked to the evaluation of its long-term degradation under aggressive conditions. In this case, a model was developed in an attempt to reproduce the degree of alteration undergone by a cylindrical grout specimen, intended to simulate a long drill hole for grout injection in fractured granite. The chemical composition of the boundary water was assumed to match a water sample of the Laxemar area (Sweden) at a depth of 500 m, a characteristic depth often considered for a nuclear waste repository.

Calcium silicate hydrates were considered to be an assemblage of different mineral phases, characterized by diverse calcium-to-silica ratios and solubility products, as in previous investigations (Guillon, 2004; Moranville *et al.*, 2004) and diffusion of solutes in the pore solution was considered to be the dominant transport process. It was found that the evolution of the deterioration process is sensitive to the chemical composition of groundwater.

Results obtained by the reactive transport model for Standard grout mix 5/5 were in strong agreement with previous reported experiments: calcium hydroxide was found to be the first solid species to totally dissolve and is followed by the decalcification of C-S-H (reproduced by the increase of the relative proportion of $C_{1.1}$-S-H in detriment of $C_{1.8}$-S-H) (Figure 8).

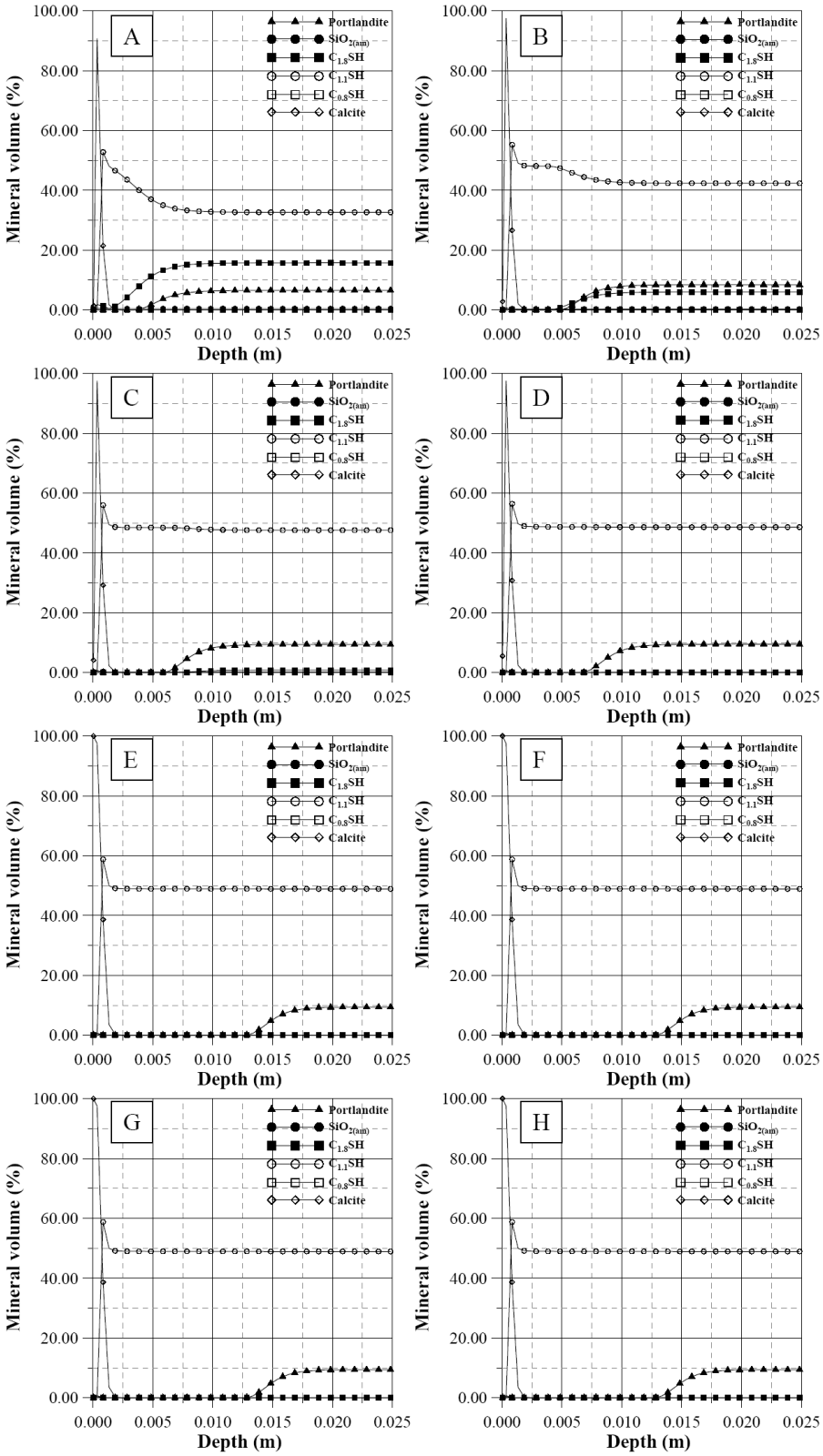

Figure 8. Mineral constitution of Standard 5/5 injection grout after (A) 0.25 year, (B) 0.50 year, (C) 0.75 year, (D) 1 year, (E) 50 years, (F) 100 years, (G) 500 years and (H) 1000 years.

Furthermore, the evolution of the concentration of the aqueous species and of pH was also seen to match known patterns for ordinary Portland cements until the precipitation of calcite is such that it seals the pore network on the surface of the specimen, thus isolating the pore solution from its environment (Figure 9).

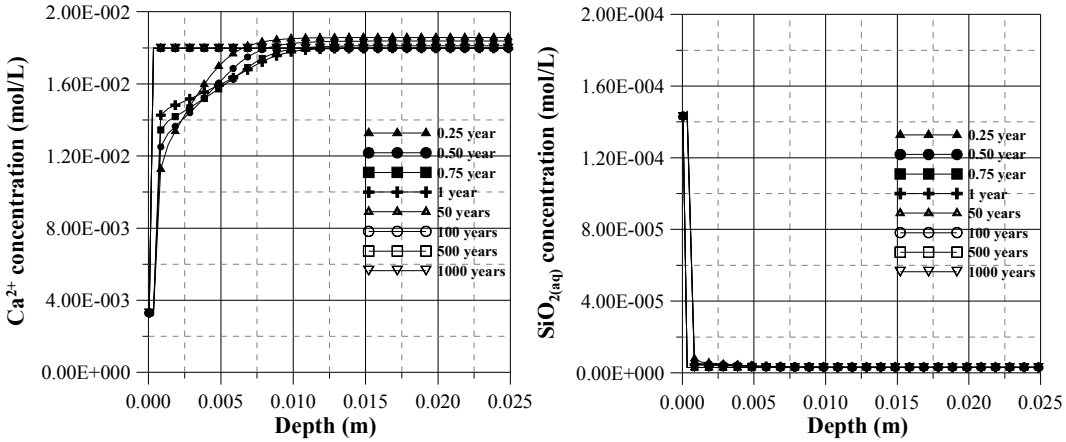

Figure 9. Concentration of aqueous species in the pore water of the Standard 5/5 injection grout specimen (left: calcium; right: silica).

The evolution of porosity (Figure 10) is related to a great extent to the dissolution of calcium hydroxide and the precipitation of a large amount of calcite on the exposed surface.

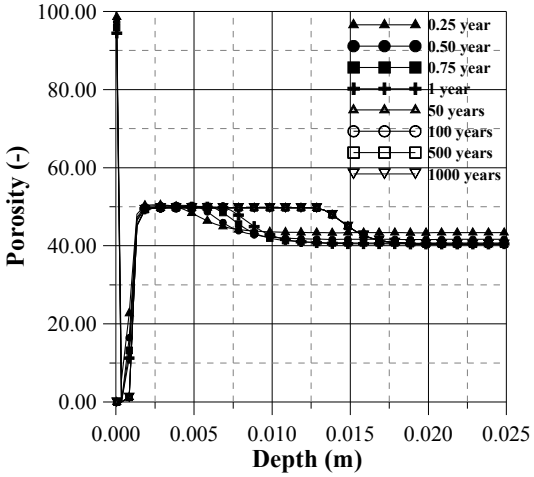

Figure 10. Evolution of porosity with time for the Standard 5/5 injection grout specimen.

On the other hand, the process of deterioration of the P308B grout mix is reflected mainly on the decalcification of C-S-H, which has two-fold consequences: it leads to the evolution of the C-S-H from calcium-richer, more soluble phases towards more stable compounds under low-pH conditions (Figure 11), but at the expense of almost the complete disintegration of the material in the vicinity of the exposed surface (Figure 12).

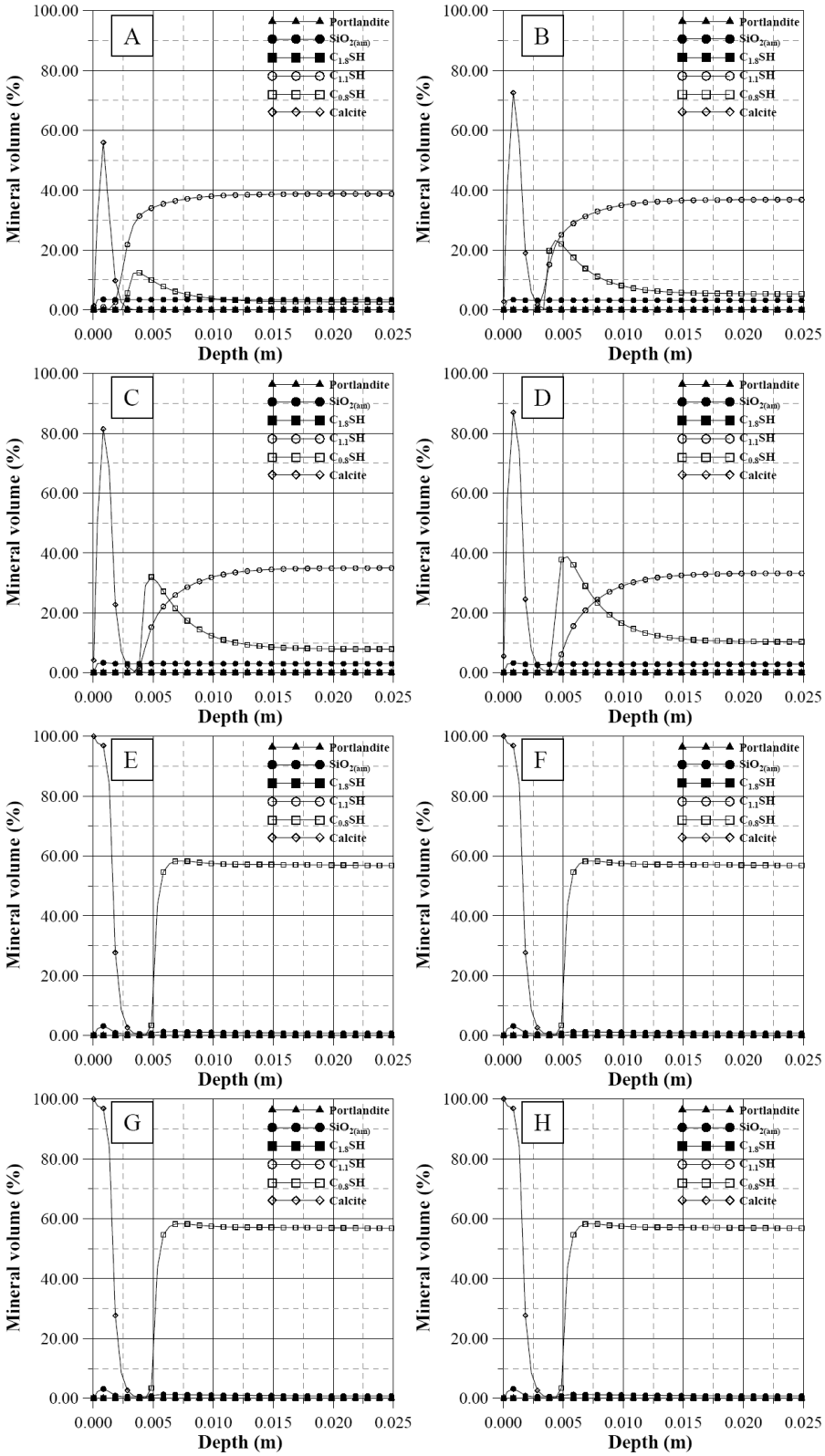

Figure 11. Mineral constitution of P308B injection grout after (A) 0.25 year, (B) 0.50 year, (C) 0.75 year, (D) 1 year, (E) 50 years, (F) 100 years, (G) 500 years and (H) 1000 years.

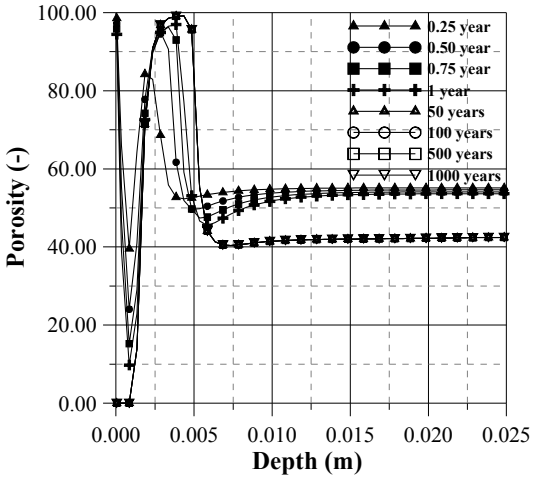

Figure 12. Evolution of porosity with time for the P308B injection grout specimen.

The most dramatic effects of degradation are then confined to a shallow depth from the exposed surface, whereas in inner regions, the higher amount of $C_{0.8}$-S-H precipitated induces the decrease of the porosity, thus further hindering the progress of deterioration.

The pore solution in contact with such grout is characterized by lower contents of calcium and higher concentrations of silica with respect to Ordinary Portland cements (Figure 13), as well as a significantly lower value of pH.

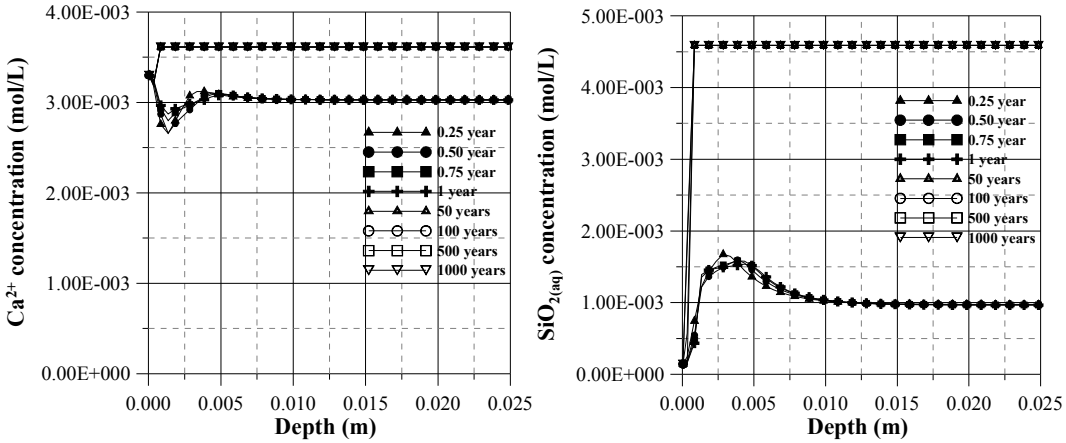

Figure 13. Concentration of aqueous species in the pore water of the P308B injection grout specimen (left: calcium; right: silica).

An original conclusion also drawn from this paper was derived by additional simulations carried out for both cases, wherein very diluted groundwater, with low bicarbonate concentrations was considered as boundary water. Indeed, it was observed that, because of the precipitation of calcite is being prevented under such conditions, the rate of degradation was steeply accelerated. In this manner, it can be concluded that the service life of grout is intimately linked to the precipitation of calcite on the surface. For further details, the reader is referred to Appendix II of this work.

3.3 Paper III: On the relevance of electrochemical diffusion for the modeling of degradation of cementitious materials (Galíndez and Molinero, 2009)

In latest years, reactive transport models have been intensively used in addressing the evolution of very disparate hydrogeochemical systems, ranging from, e.g., groundwater characterization to biodegradation or (as is the case) concrete degradation. Sound solute transport modeling is one of the cornerstones on which rests the conceptualization of the physical problems that this category of models is intended to tackle. In this respect, the second Fick's law, which describes molecular diffusion of solutes, has been used for many years and until our days. Only recently has the work of several researchers attracted the attention towards the use of the more sophisticated Nernst – Planck equation, which incorporates the influence of forces arising from the generation of an electrical potential associated to the movement of charged particles. However, somewhat perplexingly, this transition is being witnessed without, to our knowledge, a proper discussion on the merits and handicaps of either formulation. Through the countless papers that were reviewed in the course of this research, a recurrent pattern emerges wherein diffusion transport fundamentals (either the Fick's law or the Nernst – Planck equation) are but briefly sketched and their use lacks due grounds. In a way, the present situation resembles, however vaguely, that of the scientific communities with respect to their paradigms (the conceptual frameworks on which scientific theories rest), as described by Thomas Kuhn in *The Structure of Scientific Revolutions*. Though capable to deal with increasingly complex hydrogeochemical problems under either the Fick or the Nernst – Planck paradigm, researchers have proven unable to question the extent of paradigms themselves, to see from beyond them and then evaluate their qualities on one and the same plane.

Paper III is an attempt to set out to fill this gap. It deals with a problem extracted from one of those stereotyped papers which have just been referred to (Marchand *et al.*, 2002). Indeed, what was originally oriented towards the verification of a reactive transport model developed by the authors, by means of the numerical simulation of the degradation of concrete under such aggressive conditions, will serve in this context to analyze the divergence of two conflicting models of transport of electrically charged particles in aqueous solutions, especially in connection to dissolution/precipitation processes evolving in the solid matrix.

The Fick's law (Eq. 12) provides the exact solution of a molecular diffusion problem. Yet, molecular diffusion is but one of the sources of movement of electrically charged particles. Different ionic species tend to drift at divergent speeds (in response to their respective concentration gradients and diffusion

coefficients in the medium where the movement takes place) thus inducing electrical unbalances which conspire against the local electroneutrality of the system. Nevertheless, any local excess charge transferred by the ions movement generates an electrical field (referred to as diffusion potential) which tends to restore the electroneutrality by harmonically altering the diffusion rate of all the species involved.

Diffusion transport of ionic species is therefore constrained by the electroneutrality requirement, which should hold at any point of the liquid phase. Electroneutrality is evaluated by lumping the electric contribution of all the species present in solution. This requirement is taken into account by the Nernst – Planck equation (Eq. 13).

Both formulations were applied to the simulation of the hydrogeochemical evolution of a 15-cm-thick completely saturated concrete slab whose bottom edge is directly in contact with sulfate contaminated soil. Concrete was assumed to be made of CSA Type 50 cement with a water-to-cement ratio of 0.65 and the concentration of sodium sulfate in the boundary water was fixed at 10 mmol/L.

The numerical model developed with CrunchFlow (Steefel, 2008) was successfully verified against the performance of STADIUM (the code used in Marchand *et al.*, 2002) for the simulation of a 20-year period and then numerical simulations were carried out over a period of 2500 days. The conditions of the problem were in all cases designed to properly reproduce those of the original model, in relation to the chemical composition of both the interstitial solution and the boundary water as well as the mineralogical composition of concrete.

When diffusion transport is assumed to obey the Nernst – Planck equation, the reactive transport model predicts, along with the dissolution of portlandite, the decalcification of C-S-H and the formation of ettringite (which is the most well known and worrisome consequence of the sulfate attack), also the precipitation of gypsum near the exposed surface (Figure 14). As noted in Marchand *et al.* (2002), these results are in good correlation with most investigations on this subject. Additional evidence can be found in Maltais *et al.* (2004).

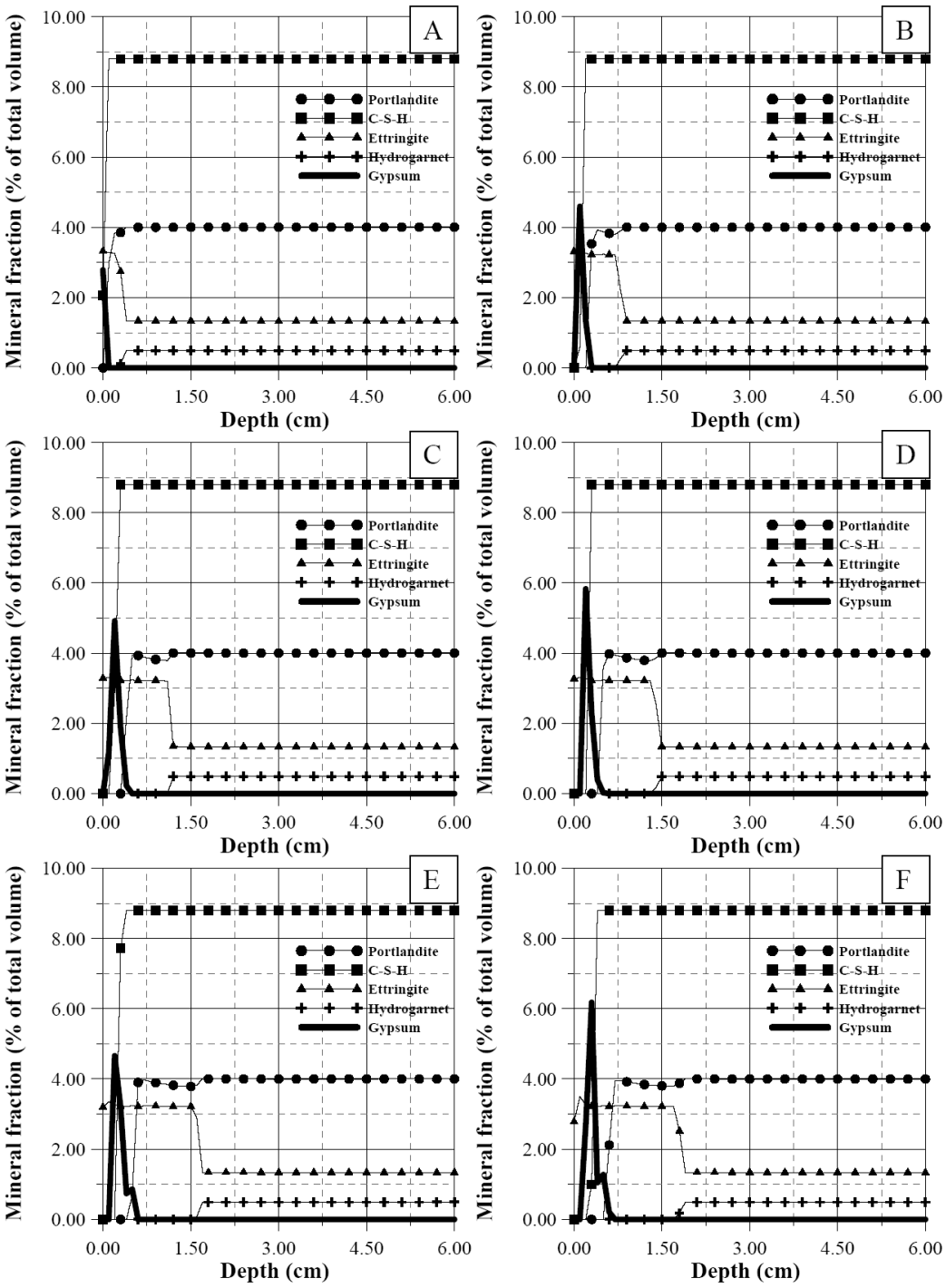

Figure 14. Distribution of the solid phases after (A) 100, (B) 500, (C) 1000, (D) 1500, (E) 2000 and (F) 2500 days, assuming diffusion is ruled by the Nernst-Planck's equation (gypsum precipitation was highlighted with a thick solid line).

On the other hand, when the Fick's law is employed to describe diffusion phenomena (with a diffusion coefficient assumed to be unique for all species and equal to the average of the specific diffusion coefficients of each of them), the model fails to reproduce the precipitation of gypsum, while all oth-

er mineral components evolve in roughly the same manner as in the previous case: two main fronts advance from the surface towards the centre of the slab – the first one denoted by the dissolution of hydrogarnet and precipitation of ettringite, and the second one by dissolution of portlandite and C-S-H (Figure 15).

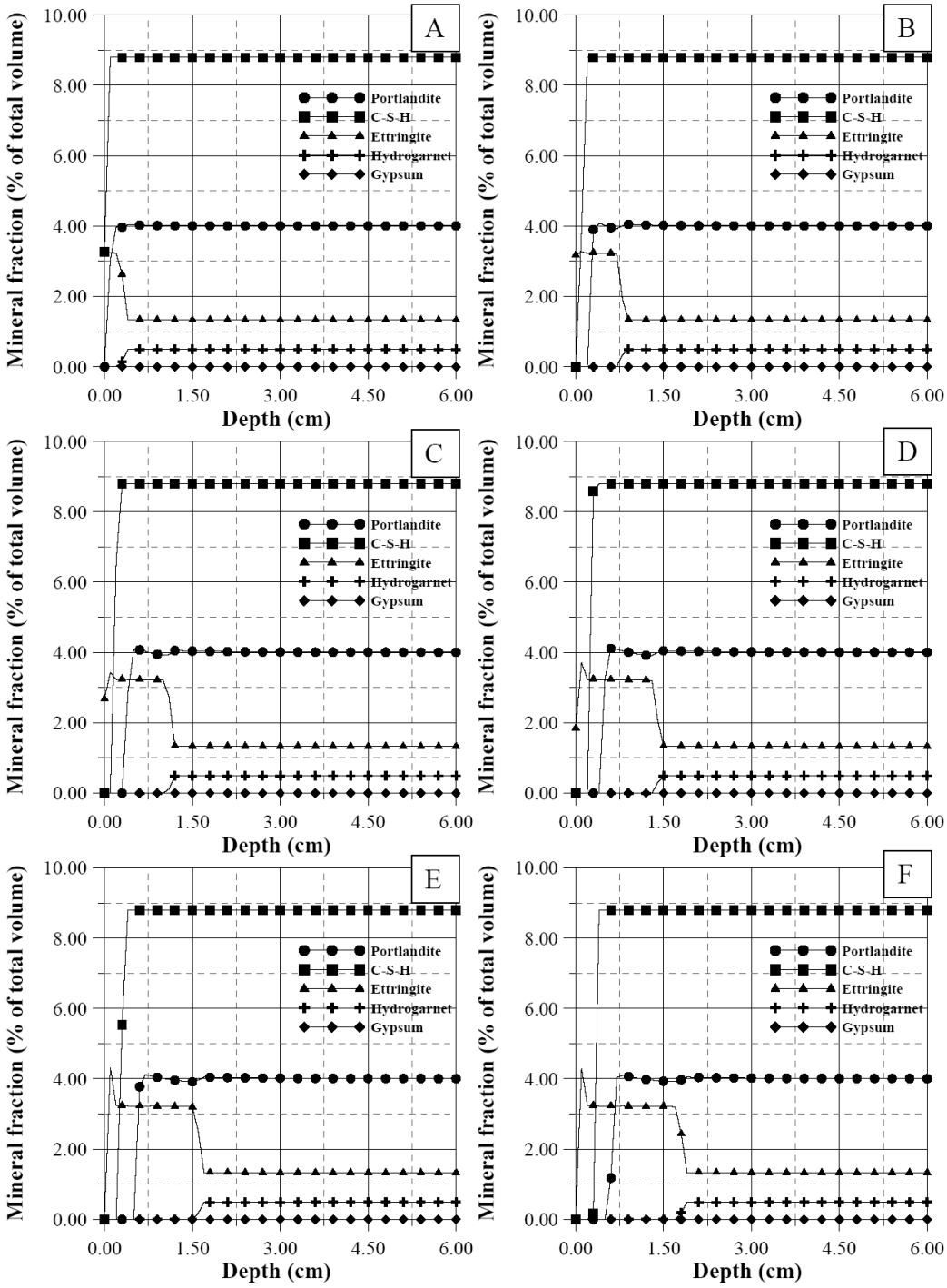

Figure 15. Distribution of the solid phases after (A) 100, (B) 500, (C) 1000, (D) 1500, (E) 2000 and (F) 2500 days, assuming diffusion is ruled by the Fick's law.

This anomaly is rooted into the divergent spatial distribution of concentration of the aqueous species projected by either formulation, in particular that of calcium and sulfate. Whereas the concentration of calcium increases at the expense of the dissolution of portlandite and the decalcification of C-S-H, boundary water is the main source of sulfate ions. Under the Nernst – Planck paradigm, the concentration of sulfate describes profiles which depart from the gently sloped gradient which is predicted by a purely Fickian approach. Furthermore, the latter predicts substantially lower concentrations of sulfate at any time of the simulation. This is translated into a slightly but consistently undersaturated state of the system with respect to gypsum. On the other hand, simulations made contemplating the Nernst – Planck equation result in a global shift towards saturation (Figure 16).

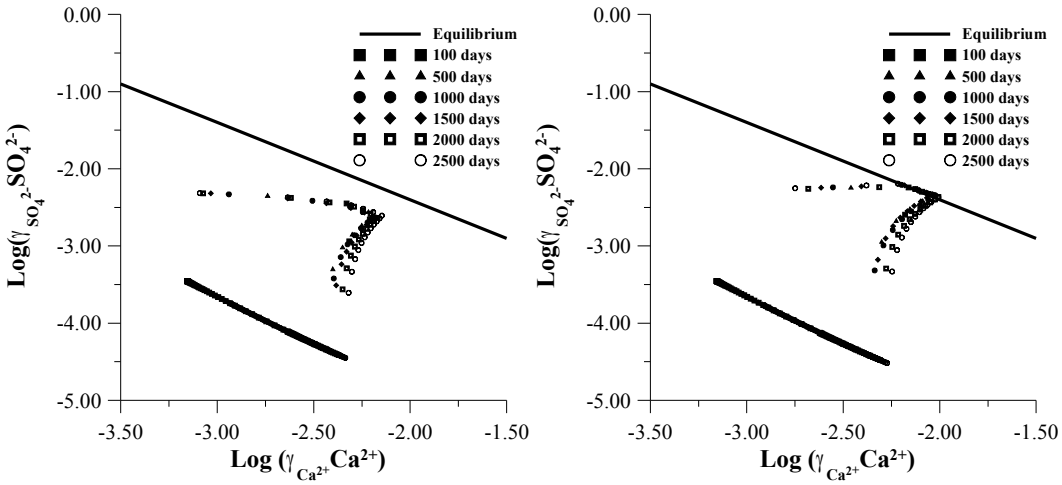

Figure 16. Saturation state of the pore solution with respect to gypsum. Left: Simulation results obtained using the Fick's law; Right: Simulation results obtained using the Nernst-Planck equation.

In light of the results obtained, it can be concluded that purely diffusive approaches based on Fick's law may not be accurate enough for modeling the degradation of cementitious materials. To that aim, in spite of its cumbersomeness, the Nernst – Planck equation may provide a more suitable alternative framework.

The extent of the conclusions just derived should serve modelers as a reminder that, as Einstein once put it: 'Everything should be made as simple as possible, but not simpler'.

4. Conclusions

When commenting on the contribution of the papers derived from this work, some of the main conclusions were anticipated. They are recapitulated here for the sake of clarity.

Reactive transport models provide a reliable theoretical framework for the study of the long-term degradation of concrete, as was corroborated by the results obtained in Paper I, where a case study taken from scientific literature was the reference against which the performance of modeling procedures was tested. It was then observed that both the hydrochemical evolution of the system and the development of the hydraulic properties of the hardened cement paste were simulated with reasonable accuracy.

In combination with modeling tools for the simulation of cement microstructure, reactive transport models constitute a robust methodological approach to a rational pursuit of the optimum mixture design for injection grouts, as was shown in Paper II. Firstly, the microstructure of the hardened paste was simulated by digital-image-based algorithms, on the basis of typical mixture designs. It is worth pointing out that, for the cases studied, results of the microstructure simulations matched the characteristic properties expected from injection grout. Afterwards, reactive transport simulations are carried out for the mixture designs considered and for a boundary water with a chemical composition of a typical granitic environment (that of the Laxemar area, Sweden, at the projected depth of a repository for nuclear spent fuel). Results obtained showed that the process of deterioration is related to the decalcification of calcium-containing mineral phases (which involves the depletion of portlandite, when available) and the precipitation of calcite. It was seen that, under the exposure of such groundwater, the durability of both grout recipes will be guaranteed for thousands of years.

Finally, in Paper III, a numerical simulation of a testing case involving the deterioration of concrete exposed to a weak sulfate solution was performed and analyzed under two different formulations for the diffusive ionic transport in the aqueous phase, namely the Fick's law and the Nernst – Planck equation. Results showed that the former fails to reproduce the precipitation of a thin layer of gypsum close to the exposed surface of concrete, as it tends to underestimate the actual concentration of calcium and sulfate in the pore solution (which, on the other hand, is predicted by the Nernst – Planck equation), thus preventing it from reaching the saturation threshold with respect to gypsum. Given that the precipitation of gypsum was corroborated by experimental studies, the preceding analysis raises the question as to which extent purely diffusive approaches are appropriate in modeling transport processes of elec-

trically charged species in porous media in general and in cement-based materials in particular. To that aim, in light of the results obtained, the Nernst – Planck equation may provide a more suitable alternative framework.

5. Conclusiones

Los modelos de transporte reactivo proporcionan un marco teórico confiable para el estudio de la degradación del hormigón a largo plazo, tal como fue corroborado por los resultados obtenidos en el Paper I, en el que se usó un estudio de caso extraído de la literatura científica como referencia respecto de la cual se evaluó el desempeño de los procedimientos de modelización. Entonces se observó que tanto la evolución hidroquímica del sistema y el desarrollo de las propiedades hidráulicas de la pasta de cemento endurecida fueron simuladas con una precisión razonable.

En combinación con las herramientas de modelización de la simulación de la microestructura del cemento, los modelos de transporte reactivo constituyen un sólido enfoque metodológico para la búsqueda racional del óptimo diseño de mezcla para lechadas para inyección, tal como se mostró en el Paper II. En primer lugar, se simuló la microestructura de la pasta endurecida por medio de algoritmos basados en imágenes digitales, sobre la base de diseños típicos de mezcla. Cabe señalar que, para los casos estudiados, los resultados de las simulaciones de la microestructura alcanzaron las propiedades características esperables de la lechada de inyección. Posteriormente, se llevaron a cabo simulaciones de transporte reactivo para los diseños de mezcla considerados y para el agua de contorno con una composición química de un entorno granítico típico (la de la zona Laxemar, Suecia, a la profundidad prevista de un depósito de residuos nucleares). Los resultados obtenidos mostraron que el proceso de deterioro se halla relacionado con la descalcificación de las fases minerales que contienen calcio (que involucra también la completa disolución de la portlandita, en tanto se encuentre disponible) y la precipitación de calcita. Se observó que, en virtud de la exposición de las aguas subterráneas como, la durabilidad de las dos recetas de lechada está garantizada por miles de años.

Por último, en el Paper III, se llevó a cabo una simulación numérica de un caso de ensayo del deterioro del hormigón expuesto a una solución débil de sulfato, y fue analizada bajo dos formulaciones diferentes del transporte iónico difusivo a través de la fase acuosa, a saber, la ley de Fick y la ecuación de Nernst – Planck.

Los resultados mostraron que el primero es incapaz de reproducir la precipitación de una delgada capa de yeso cerca de la superficie expuesta del hormigón, ya que tiende a subestimar las concentraciones reales de calcio y sulfato en la solución intersticial (que, por otra parte, se prevé por la ecuación de Nernst – Planck), lo cual impide alcanzar el umbral de saturación con respecto al yeso. Teniendo en cuenta que la precipitación de yeso fue

corroborada experimentalmente por medio de estudios publicados, el análisis anterior plantea la cuestión de en qué medida los enfoques puramente difusivos son apropiados para la modelización de procesos de transporte de especies cargadas eléctricamente en medios porosos en general y en materiales cementicios en particular. Con ese objetivo, a la luz de los resultados obtenidos, es posible que la ecuación de Nernst – Planck proporcione un marco alternativo más adecuado.

References

Barbarulo, R., Marchand, J., Snyder, K.A., Prené, S., Dimensional analysis of ionic transport problems in hydrated cement systems Part 1. Theoretical considerations, Cement and Concrete Research 30 (2000), 1955–1960

Bentz, D.P., Modelling cement microstructure: Pixels, particles, and property prediction, Materials and Structures 32 (1999), 187–195

Bentz, D.P., CEMHYD3D: a three-dimensional cement hydration and microstructure development modelling package. Version 2.0, NISTIR 6485, U.S. Department of Commerce (2000)

Bentz, D.P., Garboczi, E.J., Percolation of phases in a three-dimensional cement paste microstructural model, Cement and Concrete Research 21(2) (1991), 325–344

Bentz, D.P., Coveney, P.V., Garboczi, E.J., Kleyn, M.F., Stutzman, P.E., Cellular automaton simulations of cement hydration and microstructure development, Modeling and Simulation in Materials Science and Engineering 2 (1994), 783–808

Berner, U.R., Modelling the incongruent dissolution of hydrated cement minerals, Radiochimica Acta 44/45 (1988), 387–393

Bodén, A., Sievänen, U., Low-pH injection grout for deep repositories. Summary report from a co-operation project between NUMO (Japan), Posiva (Finland) and SKB (Sweden), R-05-40 (2005)

Carde, C., François, R., Torrenti, J.M., Leaching of both calcium hydroxide and C-S-H from the cement paste: modeling the mechanical behavior, Cement and Concrete Research 26 (1996), 1257–1268

Galíndez, J.M., Coupled water flow and reactive transport modeling and its application to the simulation of cement degradation processes, Trabajo de Investigación Tutelado, Universidade de Santiago de Compostela, Spain (2006)

Garboczi, E.J., Bentz, D.P., Computer simulation of the diffusivity of cement-based materials, Journal of Materials Science 27 (1992), 2083–2092

Garboczi, E.J., Bentz, D.P., Multi-scale picture of concrete and its transport properties: introduction for non-cement researchers, NISTIR 5900, Building and Fire Research Laboratory, National Institute of Standards and Technology (1996)

Guillon, E., Durabilité des matériaux cimentaires. Modélisation de l'influence des équilibres physico-chimiques sur la microstructure et les propriétés mécaniques résiduelles, PhD Thesis, École Normale Supériere de Cachan, France (2004)

Holt, E., Durability of low-pH injection grout – A literature survey, Posiva Oy working report 2006-XX (2006)

Huang, W.-H., Improving the properties of cement–fly ash grout using fiber and superplasticizer, Cement and Concrete Research 31 (2001), 1033–1041

Kamali, S., Gérard, B., Moranville, M., Modelling the leaching kinetics of cement-based materials—influence of materials and environment, Cement and Concrete Composites 25 (2003), 451–458

Kirkner, D.J., Reeves, H., Multicomponent mass transport with homogeneous and heterogeneous chemical reactions: Effect of the chemistry on the choice of numerical algorithm Ð 1. Theory, Water Resources Research 24 (10) (1988), 1719–1729

Kirkner, D.J., Reeves, H.W., Jennings, A.A., Finite element analysis of multicomponent contaminant transport including precipitation/dissolution reactions, in: J.L. Laible, et al. (Eds.), Finite Elements in Water Resources, Springer-Verlag, USA (1984), 309–318

Kronlöf, A., Injection grout for deep repositories – low-pH cementitious grout for large fractures: Testing technical performance of materials. VTT Building and Transport, Posiva working report 2004–45 (2004)

Krstulovic, R., Dabic, P., A conceptual model of the cement hydration process, Cement and Concrete Research 30 (2000), 693–698

Livingston, R.A., Fractal nucleation and growth model for the hydration of tricalcium silicate, Cement and Concrete Research 30 (2000), 1853–1860

Marchand, J., Bentz, D.P., Samson E., Maltais, Y., Influence of calcium hydroxide dissolution on the transport properties of hydrated cement systems, Reactions of Calcium Hydroxide in Concrete, American Ceramic Society, Westerville, OH (2001)

Mainguy, M., Tognazzi, C., Torrenti, J.M., Adenot, F., Modelling of leaching in pure cement paste and mortar, Cement and Concrete Research 30 (2000), 83–90

Maltais, Y., Samson, E., Marchand, J., Predicting the durability of Portland cement systems in aggressive environments—laboratory validation, Cement and Concrete Research 34 (2004), 1579–1589

Marchand, J., Samson, E., Maltais, Y., Beaudoin, J.J., Theoretical analysis of the effect of weak sodium sulfate solutions on the durability of concrete, Cement and Concrete Composites 24 (2002), 317–329

Parkhurst, D.L., Appelo, C.A.J., User's guide to PHREEQC (version 2) – A computer program for speciation, batch-reaction, one-dimensional transport, and inverse geochemical calculations, U.S. Geological Survey Report USGS/WRI 99–4259 (1999)

Pfingsten, W., Shiotsuki, M., Modeling a cement degradation experiment by a hydraulic transport and chemical equilibrium coupled code, 21st International Symposium on the Scientific Basis for Nuclear Waste Management, Davos, Switzerland, 1997, (I.G. McKinley and C. McCombie Eds., 1998) Materials Research Society Symposium Proceedings 506 pp. 805–812

Pfingsten, W., Indications for self-sealing of a cementitious L&ILW repository, PSI 01–09 (2001)

Powers, T.C., Physical properties of cement paste, in Proceedings of the Fourth International Conference on the Chemistry of Cement. U.S. National Bureau of Standards Monograph 43 (2), U.S. Department of Commerce, Washington, DC (1960) 577–613

Moranville, M., Kamali, S., Guillon, E., Physicochemical equilibria of cement-based materials in aggressive environments—experiment and modeling, Cement and Concrete Research 34 (2004), 1569–1578

Saaltink, M., On the approaches for incorporating equilibrium and kinetic chemical reactions in transport model, PhD thesis, Universitat Politècnica de Catalunya (1999)

Samper, J., Juncosa, R., Delgado, J., Montenegro, L., CORE^{2D}. A code for non-sothermal water flow and reactive solute transport. Users manual version 2, ENRESA, Technical report 6 (2000)

Samson, E., Marchand, J., Beaudoin, J.J., Modeling the influence of chemical reactions on the mechanisms of ionic transport in porous materials - An overview, Cement and Concrete Research 30 (2000), 1895–1902

Steefel, C.I., CrunchFlow – Software for Modeling multicomponent reactive flow and transport, Lawrence Berkeley National Laboratory (2008). Available online at http://www.csteefel.com/CrunchPublic/CrunchFlowManual.pdf

Xu, T., Samper, J., Ayora, C., Manzano, M., Custodio, E., Modeling of non-isothermal multicomponent reactive transport in field scale porous media flow systems, Journal Hydrology 214 (1999), 144–164

Yokozeki, K., Watanabe, K., Sakata, N., Otsuki, N., Modeling of leaching from cementitious materials used in underground environment, Applied Clay Science 26 (2004), 293–308

Appendix I

Paper I

Simulating concrete degradation processes by reactive transport models

Galíndez, Juan Manuel; Molinero, Jorge; Samper, Javier; Yang, Chambing

Published in Journal de Physique IV 136, 177 – 200 (2006)

J. Phys. IV France **136** (2006) 177–188

DOI: 10.1051/jp4:2006136019

Simulating concrete degradation processes by reactive transport models

J.M. Galíndez[1], J. Molinero[1], J. Samper[2] and C.B. Yang[2]

[1] *University of Santiago de Compostela, Dept. of Agroforestal Engineering, Campus Universitario, 27002 Lugo, Spain*
[2] *University of La Coruña, Civil Engineering School, Campus de Elviña s/n, 15071 La Coruña, Spain*

Abstract. Cement-based materials are commonly used in the multibarrier systems of radioactive waste repositories. Under the sub-surface environmental conditions they are exposed to during service-life, the chemical composition of the initially highly alkaline cement pore fluid may be altered by the influence of external ions and the leaching of dissolved species present in the cement interstitial solution, both of which processes are mainly ruled by ionic diffusion. Furthermore, the perturbation induced in the local thermodynamic equilibrium of the system yields to a series of dissolution/precipitation reactions which may result in a significant reorganization of the microstructure of concrete, in terms of both the distribution of mineral phases and the physical morphology of the capillary pore network, thus causing the concrete properties to undergo a gradual decline. Therefore, the long-term performance of concrete structures is a relevant issue in relation to the safety assessment of radioactive waste disposals. The analysis of the evolution of concrete degradation is a challenging task. It is also one that stresses the relevance of the development of reliable modeling techniques aimed at the prediction of long-term concrete behavior. The present work deals with the conceptualization of concrete both as a mineral aggregate, thus susceptible to deterioration, and as a porous material, where transport processes are expected to take place. Coupled reactive transport models are required to cope with the highly complex cyclic interactions arising between the chemical reactions which take place in the water-concrete interface and diffusive and advective transport in the aqueous phase. The approach taken herein aims at formulating and testing reactive transport numerical models by reproducing recent experiments reported in the scientific literature. Such procedure is intended to provide insight into the very nature of the phenomena involved, particularly those related to the appropriate methods available to describe ionic diffusion and the accuracy of the constitutive laws (e.g., porosity/permeability, porosity/diffusivity, etc.) developed for cement-based materials.

1. INTRODUCTION

The durability of concrete is one of the main concerns involved in the safety assessment of radioactive waste repositories and a considerably large amount of effort has been devoted in recent years to understand the thermodynamic behavior of cementitious compounds when subjected to the aggressive conditions under which they are expected to be during service-life [1, 2, 3, 4]. In fact, the intrusion of slightly acidic lowly mineralized water in the porous structure of concrete disrupts the thermodynamic equilibrium between the pore solution and the hydrated cement minerals. As a consequence, dissolution/precipitation reactions arise which result in the reorganization of the microstructure of concrete, thus altering its original physical properties (e.g., porosity and hydraulic conductivity).

The time of simulation of current experimental tests and the absence of a standardized test protocol [5] constitute a major restriction to the conclusions which can be derived from empirical evidence. Therefore, numerical modeling has emerged as one of the main – if not the only – viable ways to understand the long-term degradation of concrete. In this respect, reactive transport models, which were developed in order to deal with the complex interactions between the transport of solutes in the aqueous phase and the chemical reactions arising as a consequence of it, have provided a solid framework to further study. However, a critical analysis of the performance of such numerical models

should be carried out in order to enhance the robustness and reliability of their predictions in the long term. This task was addressed in this work by contrasting the performance of the model with empirical evidence reported in the scientific literature.

The present paper is intended to offer the fundamentals of the modeling techniques of reactive transport and the particular features required when applied to concrete deterioration. Results of the testing of numerical models available will be presented as well.

2. CONCEPTUAL AND MATHEMATICAL MODEL

2.1 Physical processes

Flow in saturated media is described by the so-called flow equation (Eq. 1), that is derived by combining the mass conservation principle with the well-known Darcy's law to an elementary control volume.

$$\nabla \cdot (K \nabla h) + w = S_s \frac{\partial h}{\partial t} \tag{1}$$

where w represents fluid sink/sources per unit volume of medium and S_s is specific storage coefficient defined as the volume of water delivered per unit time and unit volume of medium in response to a unit change of hydraulic head.

Dissolved species in saturated media are subjected to various physical and chemical transport and accumulation processes. Solute transport through porous media is governed by the Eq. 2:

$$\nabla \cdot (\theta D \nabla c) - q \cdot \nabla c + r\left(c^* - c\right) + \theta R = \theta \frac{\partial c}{\partial t} \tag{2}$$

where q represents the specific discharge (volumetric water flux); c is the solute concentration, usually expressed as solute mass (g or mol in reactive solute transport) per unit fluid volume; and θ is the volumetric water content (which equals the porosity, ϕ, for saturated media). The first term on the left-hand side stands for the contribution of both diffusive and dispersive transport; the second term refers to the amount of solutes transported by advection (solute migration associated to water flow) and the third term to the contribution of possible solute water sinks and/or sources r having a concentration c^* and a solute sink/source term, R (solute mass added per unit time and unit fluid volume).

2.2 Chemical processes

Aqueous complexation reactions can be described as equilibrium reactions. The equilibrium constant relates the average number of ions pairs or complexes that are being formed. Applying the Mass-Action Law to the dissociation of the j-th secondary species, one has:

$$K_j = a_j^{-1} \prod_{i=1}^{N_c} a_i^{\nu_{ji}} \tag{3}$$

where a_i anb a_j are the activities of the species j and i, respectively, and ν_{ji} is the stoichiometric coefficient of i-th primary species in j-th species. The concentration of secondary species or aqueous complexes x_j can thus be expressed in terms of primary species concentrations c_i according to:

$$x_j = K_j^{-1} \gamma_j^{-1} \prod_{i=1}^{N_c} c_i^{\nu_{ji}} \gamma_i^{\nu_{ji}} \tag{4}$$

where x_j and c_i are molar concentrations and γ_j and γ_i are activity coefficients which could be calculated according to the extended Debye-Hückel formula for diluted solutions (less than 1 mol/kg).

Accordingly, the total dissolved concentration of a given component C_k can be written in an explicit form as a function of the concentration of the N_c dissolved primary species:

$$C_k = c_k + \sum_{j=1}^{N_x} \nu_{jk} x_j = c_k + \sum_{j=1}^{N_x} \nu_{jk} K_j^{-1} \gamma_j^{-1} \prod_{i=1}^{N_c} c_i^{\nu_{ji}} \gamma_i^{\nu_{ji}} \tag{5}$$

where N_x is the number of secondary species. Notice the difference between the concentration of primary species c_k and the total dissolved concentration C_k.

Proton concentration in the solution can be obtained by defining a new variable, the so-called total proton concentration C_H, as:

$$C_H = c_H^+ + \sum_{j=1}^{N_x} \nu_{jH} x_j \tag{6}$$

where c_H^+ is the concentration of free protons and ν_{jH} are the stoichiometric coefficients of protons in the acid-base reactions of formation of secondary aqueous species. The total concentration, C_H, represents the net proton balance or "proton excess" of all acid-base reactions taking place in the solution. In this manner, acid-base reactions can be analyzed in the same fashion as the rest of homogeneous reactions.

Under equilibrium conditions, dissolution-precipitation reactions can be described by the Law of Mass Action (Eq. 7), which states that:

$$X_m \lambda_m K_m = \prod_{i=1}^{N_c} c_i^{\nu_{mi}^p} \gamma_i^{\nu_{mi}^p} \tag{7}$$

where X_m represents the molar fraction of the m-th solid phase; λ_m, its thermodynamic activity coefficient (X_m and λ_m are taken equal to unity for pure phases); c_i and γ_i are the concentration and activity coefficient of the i-th species; ν_{mi}^p its stoichiometric coefficient in the dissolution reaction of the m-th solid phase; and K_m is the corresponding equilibrium constant. This assumption was proved to be acceptable for reactive transport problems involving cement-based materials [6].

Chemical processes which involve mass transfer from solid to liquid phases can induce changes in physical and hydrodynamic properties of a porous medium. For instance, mineral dissolution or precipitation can increase or decrease the porosity, respectively. Such a change in porosity may, in turn, affect flow and transport properties (e.g., diffusion coefficient and permeability). Changes in porosity, $\Delta\phi$, can be evaluated from computed dissolution/precipitation rates according to the following equation:

$$\Delta\phi = -\sum_{k=1}^{N_k} \frac{V_k \left(C_k^t V_w^t - C_k^{t-1} V_w^{t-1} \right)}{V_t} \tag{8}$$

where V_k is the molar volume (dm^3/mol) of the k-th mineral phase, C_k^t and C_k^{t-1} are concentrations (mol/L) of the k-th mineral phase at times t and $(t-1)$, respectively, V_w^t and V_w^{t-1} are water contents at times t and $(t-1)$, respectively and V_t is the volume of porous medium. The minus sign in this equation accounts for the fact that an increase in mineral concentration induces a decrease in porosity.

3. REACTIVE TRANSPORT MODELS APPLIED TO THE CONCRETE DEGRADATION ISSUE

The hardened cement paste is made up of the minerals formed by hydration of cement clinker particles. The main products of hydration are calcium silicate hydrates (C-S-H), calcium hydroxide, calcium

aluminate and calcium ferrite. However, owing to their predominant presence in the mineralogical composition of concrete and their influence on such relevant properties as strength and permeability, calcium silicate hydrates are the most important binding phases in all Portland cement-based systems and, in words of Richardson [7], "their exact nature is central to the science of cement and concrete".

Calcium silicate hydrates possess a remarkable level of structural complexity. More than 30 calcium silicate hydrate phases are known, spanning from semicrystalline to nearly amorphous, over a wide range of calcium-to-silicon ratios [8]. Typically, calcium silicate hydrates bear some resemblance to crystalline minerals such as tobermorite and jennite, but are characterized by extensive atomic imperfections and structural variations at the nanometer scale.

There is general agreement as to the close relationship which ties the thermodynamic behavior of calcium silicate hydrates to the underlying structure of the solid. However, such relationship is most frequently blurred by thermodynamic and kinetic ambiguities which abound in any data associated with C-S-H. In fact, the attainment of equilibrium between C-S-H and one liquid phase has yet to be conclusively confirmed by experimental measurements; rather, C-S-H is thought to evolve by successive shifts from one to another metastable state of thermodynamic equilibrium, accompanied by changes in the structure of C-S-H caused by aging [9]. As a consequence, in spite of the development of some sophisticated models of the microstructure of calcium silicate hydrates in recent years [10], the pursuit of such a link still remains at an embryonic stage. Instead, current thermodynamic models rely upon such simple parameters as the calcium-to-silicon ratio [11], or on further spectroscopic and microscopic data [12] provided by recent techniques.

The incongruent dissolution of C-S-H could also be modeled as a process involving a series of different minerals, each with its own characteristic thermodynamic properties, in order of decreasing solubility. Since degradation is mainly ruled by the leaching of calcium ions out of the solid phase, such minerals should account for the higher calcium-to-silicon ratios found at the earliest stages [13].

Although heterogeneous in nature, concrete exhibits homogeneity at a much smaller scale than natural granular materials, which is relevant in relation to the evolution of transport processes. From a practical standpoint, two different types of porosity can be distinguished, namely, gel porosity and capillary porosity, the latter having significantly greater influence on transport processes. Both porosity and the degree of connectivity of the porous network are crucial to hydraulic conductivity. Both factors, however, are closely related to the water-to-cement ratio of concrete which, in turn, is proportionally linked to the rate of degradation.

Even though there might still be some capillary pore space left in the form of isolated clusters, when capillary porosity falls below 18%, then the diffusivity is mainly controlled by transport through C-S-H gel pores [14] obeying a law of the Archie's type, but modified by adding a cutoff value R_{min} which, in this case, equals 0.001. Such law (Eq. 9) was developed based upon numerical tests performed on a quantitative representation of the microstructure of the cement paste, generated by means of a digital-image-based random growth model [15].

$$D_{eff} = \left[0.001 + 0.07\phi_f^2 + 1.8H\left(\phi_f - \phi_c\right)\left(\phi_f - \phi_c\right)^2\right] D_0 \tag{9}$$

where D_{eff} denotes the effective diffusion coefficient; D_0, the diffusion coefficient in pure water; $\phi_c = 0.18$ represents the critical capillary porosity of the material; and $H\left(\phi_f - \phi_c\right)$ is the Heavyside function. This equation has proved appropriate when dealing with cementitious materials [15].

A constitutive law is also required to account for the relationship between hydraulic conductivity of concrete and its porosity. In this respect, it was deemed acceptable to follow a previous work [11] and adopt the Kozeny-Carman equation as such law, even though it is mainly applicable to granular materials. Recent studies [17] have provided more data concerning this issue, although further research might be needed.

According to its general expression, the Kozeny-Carman equation states that hydraulic conductivity and porosity are linked to each other in the following terms:

$$K = c\frac{\phi^3}{(1-\phi)^2} \tag{10}$$

where c is an empirical constant.

4. CASE STUDY

The exposure to an aggressive environment induces changes on the porosity of cement. Since porosity is related to a certain extent to the hydraulic conductivity of the material, one reasonable way to tackle the problem is to consider the latter as the index of the degree of degradation undergone by the hardened cement paste. In fact, this is the approach taken by Pfingsten and Shiotsuki [16]. The present work, in turn, makes use of that experience in order to calibrate the model and test the validity of the constitutive laws which link the hydraulic properties of concrete to one another.

4.1 Numerical resolution

The reactive transport problem may be formulated in terms of a mixed set of equations, comprising both algebraic and partial differential equations. In view of the intrinsic microstructural complexity of the hardened cement paste, the scale over which the integration of differential equations is performed becomes a matter of concern. In this respect, paths have diverged. On the one hand, the problem might indeed be solved at a microscopic scale, which implies the digital simulation of the pore structure of cement systems based, for instance, on microstructural information obtained by means of experimental procedures (e.g., mercury intrusion porosimetry). On the other hand, a Representative Elementary Volume (REV) might be defined, such that its properties can properly describe the heterogeneous material which is composed of. Indeed, the most relevant variables are averaged over such volume, thus slackening the need for detailed knowledge of the microstructure of the material. Such average properties can easily be measured in practice. The validity of this approach, often referred to as the homogenization technique, lies on the adequacy of the definition of the REV for the problem of interest. This is attained when, regardless of its location within the domain, the REV always contains persistent volumes of solid and voids [18]. This latter approach was the one taken in this work for the resolution of the reactive transport problem.

The numerical modeling tool applied herein, CORE^{2D} [19], is a multi-purpose code for the solution of non-isothermal reactive transport problems, and has been successfully employed in subsurface systems [20, 21, 22, 23, 24, 25].

The reactive transport problem is addressed in a hybrid resolution framework where spatial numerical integration is made by means of a finite element discretization and time calculations are solved in a finite-difference scheme. For every time step, calculations are then solved thanks to the Sequential Iterative Approach [19, 26]. This technique consists in uncoupling the transport and the chemical reactions. In the first step of calculation, mass transport is solved in terms of total dissolved concentrations of components accounting for respective geochemical source/sink terms. Total concentrations of components and immobile species, minerals, gases, adsorbed and exchanged species, are then calculated for every nodal point. Once transport calculations are finished, total nodal concentrations are evaluated in order to check whether they violate the chemical equilibrium (or kinetically-driven) relationships of the various reactions considered. If this is the case, they are brought back to equilibrium and duly updated, providing the modified concentration profiles which will serve as a starting point for the calculation of the next time step. Newton Raphson procedures are invoked to deal with the iterative resolution of the set of non linear equations.

4.2 Description of the experience

The experimental setup of the experience experiment can be found in Pfingsten and Shiotsuki [16]. A simple scheme of the problem in question is shown in Fig. 1.

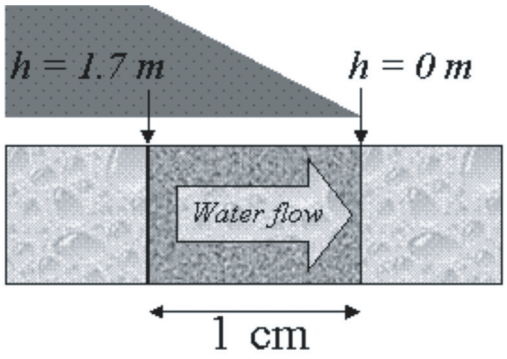

Figure 1. Basic scheme for the degradation of a porous cement disc by pure water.

Water flow was established at a constant hydraulic head of 1.7 m through a cylindrical cement specimen with a transversal area of 13.2 cm^2 and a thickness of 1.02 cm. As expected, under CO_2-free conditions, porosity increased indefinitely as a consequence of dissolution of calcium compounds. In turn, discharge rates through the specimen increased with time.

The term hydraulic conductivity will be employed in this context in reference to the entity defined in Eq. 11.

$$K = \frac{qd}{\Delta h} \tag{11}$$

where K [m/sec.] denotes hydraulic conductivity; q [m/sec.] is the specific discharge through the cement specimen; d [m] represents its thickness; and Δh [m] is the hydraulic head difference between the inlet and outlet surfaces of the hardened cement specimen.

A one-dimensional flow field was induced through the cement specimen by applying boundary conditions of the Dirichlet type on the left and right edges of the solid, where hydraulic head was set equal to 1.7 m and 0.0 m, respectively.

A total of 21 homogeneous hydrogeochemical reactions and 4 mineral processes were considered and are listed in Table 1.

The mineralogical composition of the cement used for the specimen studied is given in Table 2 [27], where all components are expressed in weight percentages.

No further details about the type of cement employed were available, so a search was made into the Virtual Cement and Concrete Testing Laboratory (VCCTL; http://ciks.cbt.nist.gov) database in order to find a type of cement that could approximately match the known mineralogical composition just given. Such cement, numbered 115, is a Type I ordinary Portland cement with a Blaine fineness of 363 m^2/kg. The remaining calculations were made assuming the characteristics of the cement (e.g., the distribution of the size of clinker particles) used in the experiment were those of Cement 115.

Once the anhydrous mixture was defined, the simulation of the hydration process was performed by means of CEMHYD3D [28], a modeling package one of whose main capabilities is the depiction of the resulting synthetic three-dimensional microstructure of the hardened cement paste. The performance of this approach has been intensively tested in numerous applications [29, 30, 31, 32, 33, 34]. The mixture was simulated to be under saturated conditions for a prolonged period at a constant temperature of 25 °C.

Table 1. Hydrogeochemical processes considered in the reactive transport model.

Homogeneous hydrogeochemical reactions	LogK
$H_3SiO_4^- + H^+ \leftrightarrow SiO_{2(aq)} + 2H_2O$	+9.8120
$H_2SiO_4^{2-} + 2H^+ \leftrightarrow SiO_{2(aq)} + 2H_2O$	+22.9116
$NaHCO_{3(aq)} \leftrightarrow HCO_3^- + Na^+$	–0.1541
$NaCO_3^- \leftrightarrow CO_3^{2-} + Na^+$	–0.5144
$NaOH_{(aq)} + H^+ \leftrightarrow H_2O + Na^+$	+14.1800
$NaHSiO_{3(aq)} + H^+ \leftrightarrow H_2O + Na^+ + SiO_{2(aq)}$	+8.3040
$NaSO_4^- \leftrightarrow Na^+ + SO_4^{2-}$	–0.8200
$KOH_{(aq)} + H^+ \leftrightarrow H_2O + K^+$	+14.4600
$KSO_4^- \leftrightarrow K^+ + SO_4^{2-}$	–0.8796
$CaH_2SiO_{4(aq)} + 2H^+ \leftrightarrow Ca^{2+} + SiO_{2(aq)} + 2H_2O$	+18.5616
$CaH_3SiO_4^+ + H^+ \leftrightarrow Ca^{2+} + SiO_{2(aq)} + 2H_2O$	+8.7916
$Ca(H_3SiO_4)_{2(aq)} + 2H^+ \leftrightarrow Ca^{2+} + 2SiO_{2(aq)} + 4H_2O$	+15.0532
$CaHCO_3^+ \leftrightarrow Ca^{2+} + HCO_3^-$	–1.0467
$CaCO_{3(aq)} + H^+ \leftrightarrow Ca^{2+} + HCO_3^-$	+7.0017
$CaOH^+ + H^+ \leftrightarrow Ca^{2+} + H_2O$	+12.8500
$CaSO_{4(aq)} \leftrightarrow Ca^{2+} + SO4^{2-}$	–2.1111
$CO_3^{2-} + H^+ \leftrightarrow HCO_3^-$	+10.3288
$CO_{2(aq)} + H_2O \leftrightarrow H^+ + HCO_3^-$	–6.3447
$H^+ + OH^- \leftrightarrow H_2O$	+13.9951
$H_2SO_{4(aq)} \leftrightarrow SO_4^{2-} + 2H^+$	+1.0200
$HSO_4^- \leftrightarrow H^+ + SO_4^{2-}$	–1.9791

Mineral processes	LogK	Molar volume (cm^3/mol)
$Ca(OH)_2 + 2H^+ \leftrightarrow Ca^{2+} + 2H_2O$	+22.8000	33.056
$SiO_{2(s)} \leftrightarrow SiO_{2(aq)}$	–3.9993	22.688
$C_{1.65}$-S-$H_{2.45} + 3.3H^+ \leftrightarrow 4H_2O + SiO_{2(aq)} + 1.65Ca^{2+}$	+29.2854	108.000
$C_{1.10}$-S-$H_{1.90} + 2.2H^+ \leftrightarrow 3H_2O + SiO_{2(aq)} + 1.10Ca^{2+}$	+17.0974	101.800

Table 2. Mineralogical composition of anhydrous cement.

Component	Weight percentage
CaO	66.40
SiO_2	23.80
Al_2O_3	2.70
Fe_2O_3	2.80
SO_3	1.80
MgO	0.88

Several simulations were carried out in order to obtain the targeted porosity of 0.65 for the hardened cement paste, as reported in Pfingsten and Shiotsuki [16]. This is done by assigning different volumes (or more precisely, a variable number of pixels in a three-dimensional image) to each compound of the mixture, accounting for the amount of water added, and preserving the relative proportion to one another. It was found that such porosity is achieved with a water-to-cement ratio equal to 1.55.

Given all those considerations, the obtained mineralogical composition after cement hydration is presented in Table 3.

As can be observed, a certain amount of anhydrous minerals remains, mainly as nuclei immersed into the larger particles made of the products of hydration. For most practical purposes, however, the hardened paste might well be regarded as completely hydrated.

Table 3. Phase statistics of the hydrated cement paste.

Phase	Volume percentage
Portlandite	7.73
C-S-H	23.62
Katoite	3.00
C_3S	0.07
C_2S	0.45
C_3A	0.00
C_4AF	0.02
Porosity	64.18

4.3 Results

A proper analysis of the results should reflect the twofold nature of reactive transport models. In other words, the performance of these modeling procedures should be judged by their ability to reproduce not only the evolution of the hydrochemical system but also – and in this case, even more relevant – that of the hydraulic properties of the cementitious porous medium.

Even though experimental data on the evolution of pH with time have not been reported in the aforementioned Pfingsten and Shiotsuki's paper [16], evidence is found elsewhere [13] as to that the initial stage of deterioration (that lasts for a few days) is signed by an abrupt drop from 13.5 to 12.5, approximately, induced by the depletion of alkali ions from the interstitial solution. As can be observed from Figs. 2 and 3, such correlation is confirmed by model results. Furthermore, the alkali concentration computed by the model is in fairly good agreement with experimental data (Fig. 3).

Once alkalis had been completely leached out, calcium concentration rises above 0.02 mol/L, whereabouts a dynamic chemical equilibrium is reached (Fig. 4), characterized by a pH of approximately 12.5 (Fig. 2). At this stage, aqueous species removed by transport processes from the porous solution (namely diffusion, induced by the gradient concentration between inner water and the environment; and advection, associated to water flow through the cement specimen) are replaced by others released from the hardened cement paste at expenses of the dissolution of portlandite and C-S-H.

The volume evolution of the mineral phases constituting the hardened paste is shown in Fig. 5, in terms of the amount dissolved or precipitated. As can be observed, the rate of dissolution of portlandite is remarkably higher than that of C-S-H, which points towards the widely accepted observation that portlandite is the first solid species to totally dissolve [1, 13, 35].

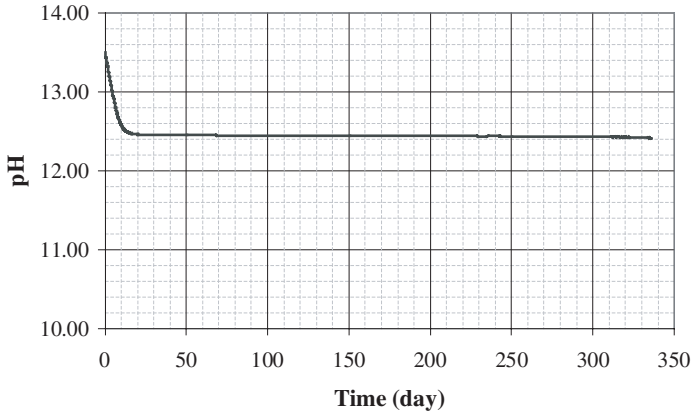

Figure 2. pH of the interstitial solution, as simulated by the model.

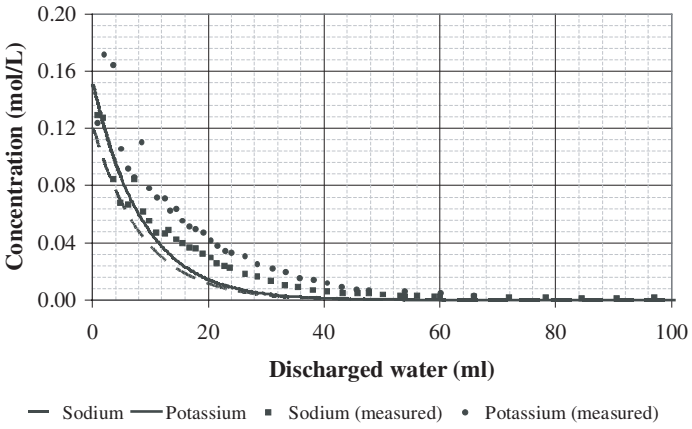

Figure 3. Alkali concentration in discharged water as simulated by the model, compared to experimental data.

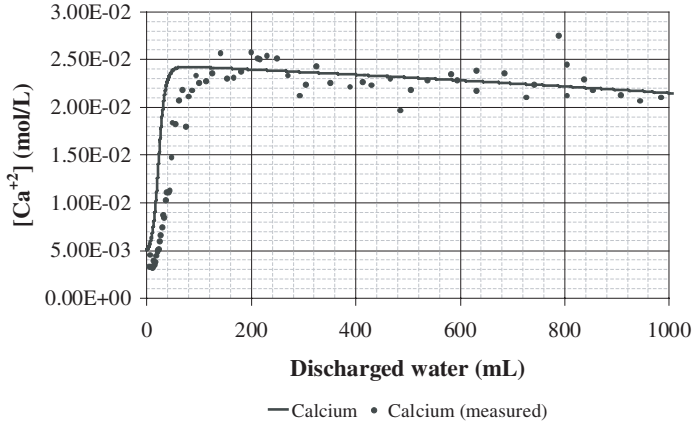

Figure 4. Calcium concentration in discharged water as simulated by the model, compared to experimental data.

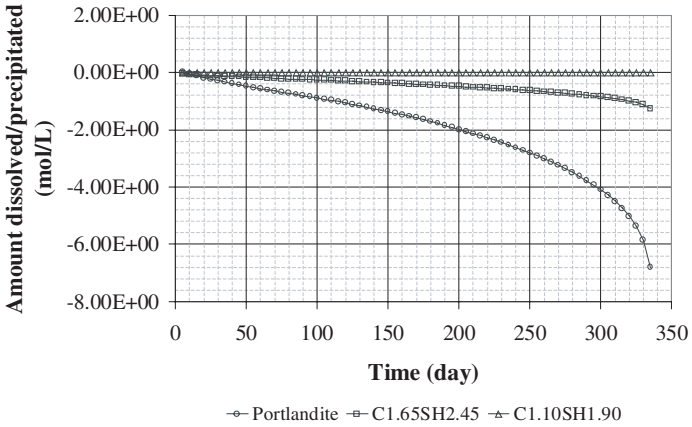

Figure 5. Evolution of the mineral phases of cement as simulated by the model, at the inlet surface of the specimen.

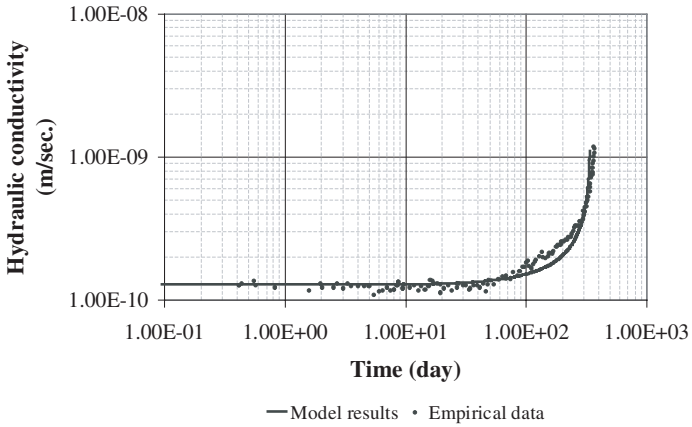

Figure 6. Evolution of hydraulic conductivity as computed by the reactive transport model against empirical evidence.

Therefore, the dissolution of portlandite is the main factor leading to the gradual increase of the volume of pores, which turns the material more permeable, as seen in Fig. 6.

As can be observed, the increase of hydraulic conductivity is excellently reproduced by the model. This does underline the reliability of reactive transport models, when coupled with the digital-image-based microstructure modeling. Indeed, it is worth pointing out that these results were obtained based upon knowledge of the mineralogical composition of clinker cement with almost no additional calibration.

5. CONCLUSIONS

A reactive transport model was built and applied to simulate concrete degradation. The analyzed approach accounts for the combined phenomena involving groundwater flow, solute transport and chemical processes. The mathematical foundations of reactive transport models were discussed and particular attention was paid to the analysis of the peculiar features of cement in relation to its mineralogical composition and thermodynamic behavior, as well as the constitutive relationships linking the variation of porosity and both the diffusivity and the hydraulic conductivity of cement-based materials.

A case study taken from scientific literature has brought the reference against which the performance of modeling procedures was tested. It was found that both the hydrochemical evolution of the system and the development of the hydraulic properties (e.g., hydraulic conductivity) of the hardened cement paste were simulated with reasonable accuracy on the basis of the knowledge of the mineralogical composition of clinker cement and no calibration. In general terms, it must be concluded that the model output is, above all, sound, which significantly adds to the practical power of these numerical tools.

As a consequence, it can be derived that reactive transport models provide a reliable theoretical framework for further study of the degradation of concrete for such facilities as nuclear waste repositories. The present work is but an attempt to test the current models with experimental data, as collected from scientific literature. It is expected that the performance of these models will improve as long as more empirical evidence becomes available.

Acknowledgments

This work has been carried out within the framework of a Research Project (DECON Project) funded by the Swedish Nuclear Fuel and Waste Management Company (SKB). Thanks are especially given to Ignasi Puigdomenech for their support, encouragement and suggestions.

References

[1] Faucon, P., Adenot, F., Jacquinot, J.F., Petit, J.C., Cabrillac, R., Jorda, M., Long-term behaviour of cement pastes used for nuclear waste disposal: review of physico-chemical mechanisms of water degradation, *Cem. Concr. Res.* **28** (1998) 847–857

[2] Matte, V., Moranville, M., Adenot, F., Richet, C., Torrenti, J.M., Simulated microstructure and transport properties of ultra-high performance cement-based materials, *Cem. Concr. Res.* **30** (2000) 1947-1954

[3] Pihlajavaara, S. E., Estimation of the service life of concrete under different conditions with special reference to radioactive waste repositories, *Nucl. Eng. Des.* **138(2)** (1992) 127-133

[4] Goñi, S. Guerrero, A., Hernández, M.S., Spanish LLW and MLW disposal: durability of cemented materials in (Na, K)Cl simulated radioactive liquid waste, *Waste Manage.* **21** (2001) 69-77

[5] Kamali, S., Gérard, B., Moranville, M., Modelling the leaching kinetics of cement-based materials—influence of materials and environment, *Cem. Concr. Compos.* **25** (2003) 451–458

[6] Barbarulo, R., Marchand, J., Snyder, K.A., Prene, S., Dimensional analysis of ionic transport problems in hydrated cement systems Part 1. Theoretical considerations, *Cem. Concr. Res.* **30** (2000) 1955-1960

[7] Richardson, I.G., The nature of C-S-H in hardened cements, *Cem. Concr. Res.* **29** (1999) 1131–1147

[8] Taylor, H.F.W., Cement chemistry, 2nd ed. Thomas Telford, London, 1997

[9] Chen, J.J., Thomas, J.J., Taylor, H.F.W., Jennings, H.M., Solubility and structure of calcium silicate hydrate, *Cem. Concr. Res.* **34** (2004) 1499–1519

[10] Richardson, I.G., Tobermorite/jennite- and tobermorite/calcium hydroxide-based models for the structure of C-S-H: applicability to hardened pastes of tricalcium silicate, β-dicalcium silicate, Portland cement, and blends of Portland cement with blast-furnace slag, metakaolin, or silica fume, *Cem. Concr. Res.* **34** (2004) 1733–1777

[11] Berner, U.R., Modelling the incongruent dissolution of hydrated cement minerals, *Radiochim. Acta* **44/45** (1988) 387-393

[12] Nonat, A., The structure and stoichiometry of C-S-H, *Cem. Concr. Res.* **34** (2004) 1521–1528

[13] Moranville, M., Kamali, S., Guillon, E., Physicochemical equilibria of cement-based materials in aggressive environments—experiment and modeling, *Cem. Concr. Res.* **34** (2004) 1569–1578

[14] Bentz, D.P., Garboczi, E.J., Percolation of phases in a three-dimensional cement paste microstructural model, *Cem. Concr. Res.* **21(2)** (1991) 325-344

[15] Garboczi, E.J., and Bentz, D.P., Computer simulation of the diffusivity of cement-based materials, *J. Mater. Sci.* **27** (1992) 2083-2092

[16] Pfingsten, W., Shiotsuki, M., Modeling a cement degradation experiment by a hydraulic transport and chemical equilibrium coupled code, 21st International Symposium on the Scientific Basis for Nuclear Waste Management, Davos, Switzerland, 1997, (I.G. McKinley and C. McCombie Eds., 1998) *Mat. Res. Soc. Symp. Proc.* **506** pp. 805-812

[17] Huang, W.-H., Improving the properties of cement–fly ash grout using fiber and superplasticizer, *Cem. Concr. Res.* **31** (2001) 1033–1041

[18] Bear, J., Bachmat, Y., Introduction to modeling of transport phenomena in porous media, Kluwer Academic Publishing, Netherlands, 1991

[19] Samper, J., Juncosa, R., Delgado, J., Montenegro, L., CORE^{2D}. A code for non-isothermal water flow and reactive solute transport. Users' manual version 2, ENRESA Technical report 6, 2000

[20] Molinero, J., Samper, J., Juanes, R., Numerical modeling of the transient hydrogeological response produced by tunnel construction in fractured bedrocks, *Eng. Geol.* **64** (2002) 369–386

[21] Molinero, J., Samper, J., Zhang, G., Yang, C., Biogeochemical reactive transport model of the redox zone experiment of the Äspö hard rock laboratory in Sweden, *Nucl. Tech.* **148** (2004) 151-165

[22] Molinero, J., Samper, J., Groundwater flow and solute transport in fracture zones: an improved model for a large-scale field experiment at Äspö (Sweden), *J. Hydraul. Res.* **42** (2004) 157-172
[23] Molinero, J., Samper, J., Large-scale modeling of reactive solute transport in fracture zones of granitic bedrocks, *J. Contam. Hydrol.* **82** (2006) 293-318
[24] Samper, J., Yang, C., Naves, A., Yllera, A., Hernández, A., Molinero, J., Soler, J.M., Hernán, P., Mayor, J.C., Astudillo, J., A fully 3-D anisotropic numerical model of the DI-B in situ diffusion experiment in the Opalinus clay formation, *Phys. Chem. Earth* **31** (2006a) 531-540
[25] Samper, J., Dai, Z., Molinero, J., García-Gutiérrez, M., Missana, T., Mingarro, M., Inverse modeling of tracer experiments in FEBEX compacted Ca-bentonite, *Phys. Chem. Earth* **31** (2006b) 640-648
[26] Xu, T., Samper, J., Ayora, C., Manzano, M., Custodio, E., Modeling of non-isothermal multicomponent reactive transport in field scale porous media flow systems, *J. Hydrol.* **214** (1999) 144–164
[27] Pfingsten, W., personal communication, 2006
[28] Bentz, D.P., CEMHYD3D: a three-dimensional cement hydration and microstructure development modelling package. Version 2.0, NISTIR 6485, U.S. Department of Commerce, 2000
[29] Bentz, D.P., Three-dimensional computer simulation of cement hydration and microstructure development, *J. Am. Ceram. Soc.* **80(1)** (1997) 3-21
[30] Bentz, D.P., Haecker, C.J., An argument for using coarse cements in high performance concretes, *Cem. Concr. Res.* **29** (1999) 615–618
[31] Bentz, D.P., Garboczi, E.J., Haecker, C.J., Jensen, O.M., Effects of cement particle size distribution on performance properties of cement-based materials, *Cem. Concr. Res.* **29** (1999) 1663–1671
[32] Bentz, D.P., Jensen, O.M., Hansen, K.K., Olesen, J.F., Stang, H., Haecker, C.J., Influence of cement particle size distribution on early age autogenous strains and stresses in cement-based materials, *J. Am. Ceram. Soc.* **84(1)** (2000a) 129–135
[33] Bentz, D.P., Feng, X., Haecker, C.J., Stutzman, P.E., Analysis of CCRL proficiency cements 135 and 136 using CEMHYD3D, NISTIR 6545, U.S. Department of Commerce, 2000b
[34] Bentz, D.P., Conway, J.T., Computer modeling of the replacement of 'coarse' cement particles by inert fillers in low w/c ratio concretes: Hydration and strength, *Cem. Concr. Res.* **31** (2001) 503–506
[35] Carde, C., François, R., Torrenti, J.M., Leaching of both calcium hydroxide and C-S-H from the cement paste: modeling the mechanical behavior, *Cem. Concr. Res.* **26** (1996) 1257-1268

Appendix II

Paper II

Assessment of the long-term stability of cementitious barriers of radioactive waste repositories by using digital-image-based microstructure generation and reactive transport modelling

Galíndez, Juan Manuel; Molinero, Jorge

Submitted to Cement and Concrete Research
(in press)

Cement and Concrete Research xxx (2009) xxx–xxx

Contents lists available at ScienceDirect

Cement and Concrete Research

journal homepage: http://ees.elsevier.com/CEMCON/default.asp

Assessment of the long-term stability of cementitious barriers of radioactive waste repositories by using digital-image-based microstructure generation and reactive transport modelling

Juan Manuel Galíndez [a,*], Jorge Molinero [b,1]

[a] Department of Agroforestal Engineering, University of Santiago de Compostela, Campus Universitario, 27002 Lugo, Spain
[b] Amphos XXI Consulting S.L., Passeig de García i Faria, 49-51, E08019 Barcelona, Spain

ARTICLE INFO

Article history:
Received 25 February 2009
Accepted 17 November 2009
Available online xxxx

Keywords:
Hydration (A)
Microstructure (B)
Durability (C)
Silica Fume (D)
Modeling (E)

ABSTRACT

Cement-based grout plays a significant role in the design and performance of nuclear waste repositories: used correctly, it can enhance their safety. However, the high water-to-binder ratios, which are required to meet the desired workability and injection ability at early age, lead to high porosity that may affect the durability of this material and undermine its long-term geochemical performance.

In this paper, a new methodology is presented in order to help the process of mix design which best meets the compromise between these two conflicting requirements. It involves the combined use of the computer programs CEMHYD3D for the generation of digital-image-based microstructures and CrunchFlow, for the reactive transport calculations affecting the materials so simulated. This approach is exemplified with two grout types, namely, the so-called Standard mix 5/5, used in the upper parts of the structure, and the "low-pH" P308B, to be injected at higher depths.

The results of the digital reconstruction of the mineralogical composition of the hardened paste are entirely logical, as the microstructures display high degrees of hydration, large porosities and low or nil contents of aluminium compounds.

Diffusion of solutes in the pore solution was considered to be the dominant transport process. A single scenario was studied for both mix designs and their performances were compared. The reactive transport model adequately reproduces the process of decalcification of the C–S–H and the precipitation of calcite, which is corroborated by empirical observations. It was found that the evolution of the deterioration process is sensitive to the chemical composition of groundwater, its effects being more severe when grout is set under continuous exposure to poorly mineralized groundwater. Results obtained appear to indicate that a correct conceptualization of the problem was accomplished and support the assumption that, in absence of more reliable empirical data, it might constitute a useful tool to estimate the durability of cement-based structures.

1. Introduction

Sealing of fractured bedrocks by means of the injection of cement-based grout is a standard procedure to enhance the compactness of the medium and reduce its permeability, thus precluding the spread of pollutants and minimizing groundwater inflow into tunnels. Under prolonged contact with groundwater, however, cement-based grout undergoes a slow, yet continuous degradation process which may undermine its integrity in the long-term. It is therefore apparent that the evaluation of the durability of cement-based grout is a relevant issue to be considered in the safety assessment of nuclear waste repositories.

The problem just set is complex as the selection of the grout mix design should also take into account the requirements of workability and injection ability. For the sake of illustration, an excerpt of a recent report on the subject [1] reads:

> 'The development of low-pH cementitious grout consisted of several tasks. First the potential systems were selected, based on the outcome of the earlier studies and on expert judgement, and the technical properties of some **two hundred recipes** (emphasis added) were tested. The most promising recipes were then selected for pH and leaching tests. Based on these results, the most promising recipes were tested in two small pilot field-tests in Finland.'

In fact, the question as to which mix is best regarding the objectives pursued remains nevertheless open, in spite of several mix designs

* Corresponding author.
E-mail address: juanmanuel.galindez@usc.es (J.M. Galíndez).
[1] Tel.: +34 93 583 05 00; fax: +34 93 307 59 28.

0008-8846/$ – see front matter © 2009 Elsevier Ltd. All rights reserved.
doi:10.1016/j.cemconres.2009.11.006

having been tested over recent years. Furthermore, as pointed out by Trotignon et al. [2], previous modelling works have not addressed the comparative evaluation of the performance of different types of concrete, or have only focused on Portland cement-based concrete.

In this paper, a methodological approach is presented to tackle this issue, which is expected to help narrow the range of the "ideal" mix design by evaluating in a simple and effective manner the long-term geochemical performance of digitally-generated cement-based grout microstructures. The digital simulation of the microstructure of the hardened cement paste represents a critical juncture of the analysis since, despite entailing a number of non-trivial assumptions, it provides a rational method to obtain the likely constitution of a grout wherever the conditions of hydration (and actually any data other than the volume fractions involved in the un-hydrated mixture) are uncertain. In other words, the present work is not intended to dissipate the incertitude connected to the actual evolution of the process of hydration under field conditions but, rather, to define reasonable starting points for subsequent modelling of degradation.

The results of the simulation of the microstructure of hardened cement paste are then linked to the evaluation of its long-term degradation under aggressive conditions. The estimated mineralogical and physical properties of the microstructure of cement-based grout are input into a reactive transport model set up in order to match the characteristics of the structure under analysis. In this case, a model was developed in an attempt to reproduce the degree of alteration undergone by a cylindrical grout specimen. Even though precedents of this approach exist in previous works [3–5], this field of research remains relatively unexplored, and it will serve well to illustrate some of the major concerns involved in the numerical simulation of concrete deterioration.

2. Materials

Two different mixtures have been analyzed in this work. As stated in [6], the mix design labelled as Standard grout mix 5/5 is an example of an injection grout for use in the upper sections of a tunnel under construction at Olkiluoto, Finland, whereas the P308B grout is a so-called "low-pH" grout which was developed to be injected at greater depths and was found to be one of the most promising ones for that purpose [7]. Mixes are listed in Table 1. Both include the sulphate-resistant low alkaline microcement Ultrafin 16 (a product manufactured by Cementa AB), which, thanks to its extremely finely ground especially selected clinker, has excellent penetration characteristics. Ultrafin 16 also complies with the low C_3A requirement for sulphate-resistant cement, in accordance with SS 13 42 04. C_3A content is normally restricted to 2% by weight.

Even though Ultrafin 16 is the cement positively used in the mixtures analyzed hereafter, in this work, an additional sensitivity analysis was carried out with respect to the particle size distribution of cement clinker, in order to evaluate its effect on the resulting microstructure of the hardened grout. To that aim, two additional microcements (namely Ultrafin 12 and Injektering 30) were studied. Ultrafin 16, Ultrafin 12 and Injektering 30 share the same chemical composition but have different

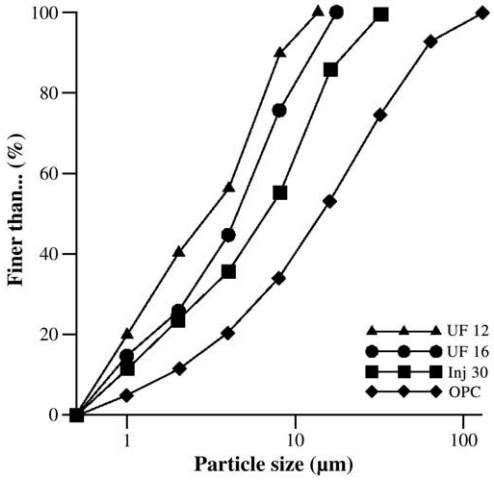

Fig. 1. Particle size distribution curves of different types of cement (product information provided by Cementa AB).

particle size distributions. Their characteristic PSD curves were provided by manufacturers and are shown in Fig. 1. The chemical composition of Ultrafin 16 is, according to [8], the one given in Table 2, where all components are expressed in weight percentages.

The lowering of pH of the pore solution is accomplished, in the case of P308B grout, by the larger addition of silica fume and has beneficial effects on the long-term safety because the pore water of the material is much less reactive towards the bentonite clay that surrounds the metal canisters of the waste repository. Silica fume was used as GroutAid, a silica-fume-based additive developed by Elkem Materials. The main feature of GroutAid is that its particles are extremely fine: a typical particle size distribution is shown in Fig. 2, where it is seen that more than 90% by weight is less than 1 μm. The microscopic particle size and pozzolanic reactivity of the so-called microsilica act to reduce bleeding and segregation, develop stronger and less permeable grout and increase durability and resistance to chemical attack.

In order to reduce the requirements of water, superplasticizer Mighty 150 (naphthalene sulphonate-based superplasticizer by Degussa, now BASF Construction Chemicals) was also added to the mixture. Its addition results in water reductions which amount to up to 30%.

3. Simulation of the microstructure of the cement-based materials

The tools provided by the Virtual Cement and Concrete Testing Laboratory (VCCTL; http://ciks.cbt.nist.gov) have been used in order to set up the initial state of cement grout. The main program of the VCCTL, namely CEMHYD3D, has been described previously [9] and was intensively tested in numerous applications [10–15].

The process of numerical generation of the final microstructure of the hardened grout proceeds in a series of steps consisting of: 1) the creation of the particle size distribution for both cement clinker and silica fume (when used); 2) the generation of the initial microstructure; 3) the distribution of cement phases; and 4) the simulation of hydration.

Table 1
Grout mixes to be used at ONKALO (After Holt, 2006 [6]).

Component	Standard grout mix 5/5 (kg)	P308B (kg)	Specific gravity	Standard grout mix 5/5 (dm^3)	P308B (dm^3)
Water	781.00	882.00	1.00	781.00	882.00
Ultrafin 16	664.00	372.00	3.20	207.50	116.25
Silica fume	117.00	256.00	2.20	53.18	116.36
Superplasticizer	21.90	25.30	–	–	–
Water/cement ratio	1.18	2.37			
Total	1583.90	1535.30	–	1041.68	1114.61

Table 2
Chemical composition of Ultrafin 16, main component of the low alkali grout.

Component	Weight percentage
CaO	64.80
SiO_2	22.30
Al_2O_3	3.40
Fe_2O_3	4.30
SO_3	2.40
Na_2O	–
Others	2.80

Please cite this article as: J.M. Galíndez, J. Molinero, Assessment of the long-term stability of cementitious barriers of radioactive waste repositories by using digital-image-based microstructure generation..., Cem. Concr. Res. (2009), doi:10.1016/j.cemconres.2009.11.006

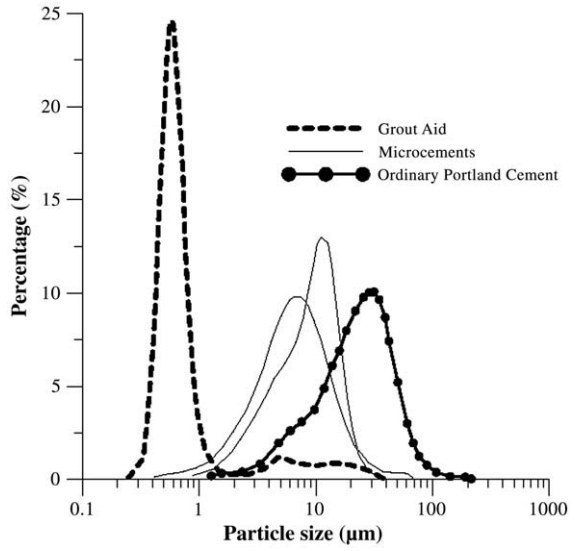

Fig. 2. Particle size distribution of silica fume compared to typical microcements and ordinary Portland cement (product information provided by Elkem Materials).

3.1. Creation of the particle size distribution

By creating a particle size distribution (i.e., the mass fraction expressed as a function of particle diameter) the number of cement particles of each diameter to be placed in a starting three-dimensional microstructure is specified. Two different input (PSD) files were generated, one corresponding to the anhydrous cement itself, and the other to the silica fume added, on the basis of data shown in Figs. 1 and 2, respectively. As said earlier, the process was repeated three times (one each for Ultrafin 16, Ultrafin 12 and Injektering 30) for each grout recipe (either Standard 5/5 or P308B), resulting in a total of six different microstructures of hardened grout.

3.2. Generation of the initial microstructure

The number of pixels of a three-dimensional image of the mixture which is assigned to each of its solid compounds was calculated from the volumes of each component shown in Table 1, and corrected in order to match the prescribed water-to-cement ratio for each mix design.

A three-dimensional cement-based grout mixture microstructure is then generated, consisting of the sum of the selected compounds in water, namely cement clinker and silica fume, with their respective particle size distribution. The influence of the superplasticizer can also be modelled in a two-fold way: by enabling the flocculation into several flocs; and by "dispersing" the particles into the initial microstructure. Details of the process can be found in the User's Guide of CEMHYD3D [16].

3.3. Distribution of the cement phases

Since the microstructure image created by the preceding steps is composed of single-phase particles only, once the initial arrangement of generic anhydrous particles in water has been created, the four major phases of cement clinker (i.e., C_3S, C_2S, C_3A and C_4AF) should be distributed amongst the cement particles.

Based on the data shown in Table 2, a Bogue calculation was used to determine the major phases present in the clinker (Table 3).

Ideally, the three-dimensional microstructure image is filtered using two-point correlation functions measured on the actual two-dimensional SEM (Scanning Electron Microscopy) images of the cement used. This is not possible in this case, for no SEM images of Ultrafin 16 clinker are available. Instead, the assumption was made that similar results would be obtained by distributing the major anhydrous cement phases according to the two-dimensional pattern described by a cement clinker whose composition matched closely that of Ultrafin 16, as listed in Table 3. That cement is found in the VCCTL database under the label "cementhoc", attributed to Danish white (low aluminate) cement. A detailed description on the process to obtain the digital images such as the one on the picture can be found in [17].

3.4. Simulation of the hydration

Once the anhydrous mixture was determined, the simulation of the hydration process was performed by means of CEMHYD3D. A non-trivial assumption was made in this respect, for the conditions to which cement-based grout is subjected after injection differ considerably from the controlled conditions the program was intended to reproduce. In fact, whereas the latter can be set to be either saturated or sealed, and either adiabatic, isothermal or temperature-programmed for a given period of time (for the present case, hydration was assumed to progress under saturated conditions and a constant temperature of 25 °C), in-situ temperature and humidity may change during construction periods, thus altering the rate of hydration and increasing the risks of drying shrinkage, and the potential for cracking, due to a higher rate of evaporation from the fresh grout. Furthermore, grout is very sensitive and somewhat weak during its early ages and vibrations during excavation and construction can upset the quality of grouting and of bond in fissures; this

Table 3
Mineralogical composition of the cement clinker for Ultrafin 16.

Anhydrous compound*	Volume percentage
C_3S	70.46
C_2S	15.42
C_3A	1.98
C_4AF	12.14

* C_3S = tricalcium silicate; C_2S = dicalcium silicate; C_3A = tricalcium aluminate; C_4AF = tetracalcium ferrite aluminate.

Table 4
Calculated volume fractions (%) by the CEMHYD3D software for every mix design and cement particle size distribution.

Component[1]	Standard grout mix 5/5			P308B		
	UF 12	UF 16	Inj 30	UF 12	UF 16	Inj 30
Porosity	45.456	45.757	45.996	57.026	55.647	57.659
C_3S	0.000	0.001	0.008	0.000	0.011	0.005
C_2S	0.011	0.170	0.311	0.227	0.000	0.493
C_3A	0.000	0.000	0.000	0.000	0.000	4.742
C_4AF	0.000	0.000	0.000	0.000	0.000	0.038
Silica fume	0.458	0.607	0.639	4.547	3.622	0.029
$Ca(OH)_2$	3.637	3.836	3.903	0.001	0.031	0.614
C–S–H	29.402	29.164	28.347	0.021	0.003	0.003
C_3AH_6	1.173	1.177	1.177	0.611	0.000	0.000
FH_3	0.005	0.006	0.005	0.002	0.000	0.000
PozzC–S–H	19.856	19.282	19.615	37.566	40.686	36.417

[1] C–S–H = calcium silicate hydrates ($C_{1.7}SH_4$); FH_3 = iron hydroxide; PozzC–S–H = Pozzolanic calcium silicate hydrates ($C_{1.1}SH_{3.9}$).

Table 5
Volume fractions as input into the reactive transport model. The cases studied are highlighted.

Component	Standard grout mix 5/5	P308B
Porosity	45.757	55.647
SiO_2(am)	0.607	3.622
$Ca(OH)_2$	3.836	0.031
$C_{1.8}$–S–H	29.335	0.014
$C_{1.1}$–S–H	19.282	40.686
$C_{0.8}$–S–H	0.000	0.000

Please cite this article as: J.M. Galíndez, J. Molinero, Assessment of the long-term stability of cementitious barriers of radioactive waste repositories by using digital-image-based microstructure generation..., Cem. Concr. Res. (2009), doi:10.1016/j.cemconres.2009.11.006

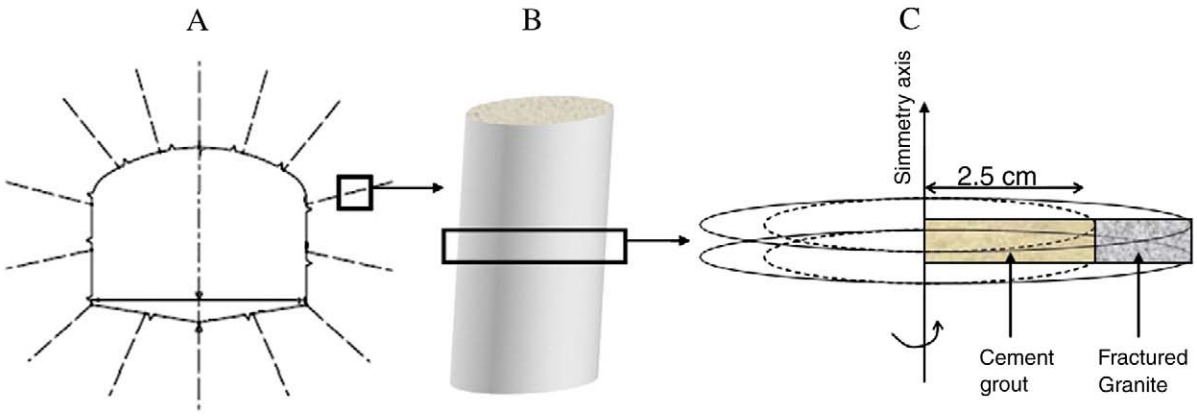

Fig. 3. Scheme of the model.

could result in additional pathways for future leaching or deterioration. As a consequence, the hypothesis was made that the microstructural characteristics of the hydrated paste would be roughly the same regardless of the conditions of curing if the degree of hydration was high. Further research might be needed on this topic.

3.5. Results

Table 4 shows the obtained outputs of CEMHYD3D after a period of hydration of more than 100 days, displaying the volume fraction distribution of the components of the hydrated microstructure of cement-based grout for the simulations carried out for the 6 cases resulting from the combinations between 2 cement–grout recipes and 3 particle size distributions. The extremely low volume fractions obtained for the anhydrous components of cement denote that the degree of hydration reached is close to 100% for all cases. It is also apparent that the addition of silica fume results in a large decrease of the volume fraction of portlandite ($Ca(OH)_2$), absent for mix P308B.

The higher water-to-binder ratio (see Table 1) is reflected in the higher porosity of the mix design P308B. Even though volume fractions assigned to each mineral (and, therefore, also to porosity) vary considerably as a function of the mix design considered, the influence of the particle size distribution of cement clinker is of lesser relevance. Yet, simulations are consistent, as finer clinker particles are associated with higher degrees of hydration and, therefore, to smaller porosities. It is also worth pointing out the low content of aluminium compounds remaining, to which both the use of sulphate-resistant cement and the addition of silica fume have contributed.

The volume fractions obtained were regrouped in order to meet the requirements of the future reactive transport model that will be used to simulate the cement degradation process. Some hypotheses were made in the process: firstly, the anhydrous calcium compounds remaining were grouped together with calcium silicate hydrates. This entails the assumption that anhydrous compounds, initially preserved from the contact with water by surrounding hydrated cement, will be exposed as soon as outer layers dissolve, thus turning into hydrated products themselves.

Furthermore, katoite ($Ca_3Al_2(SiO_4)_{3-x}(OH^-)_{4x}$, with $x = 1.5$ to 3) and FH_3 were not considered in the initial microstructures. In fact, aluminium system is not simulated in the current version of the reactive transport model for grout degradation since the amount of aluminium phases in the hydrated cement grouts considered in this work is very small. These considerations notwithstanding, neglecting aluminium and iron compounds responds to an attempt to simplify the reactive transport model rather than to the acknowledgment of their actual relevance.

Table 6
Chemical composition of boundary water: Borehole KLX02 at a depth of −452.5 m.a.s.l. [24].

Component	Concentration (mol/L)	Concentration (mol/L) (see Section 4)
pH	7.8	7.8
$SiO_{2(aq)}$	1.43E-04	1.43E-04
Na^+	1.70E-02	1.70E-02
K^+	9.64E-05	9.64E-05
Ca^{2+}	3.30E-03	3.30E-03
Mg^{2+}	4.19E-04	4.19E-04
HCO_3^-	2.14E-03	2.14E-04
SO_4^{2-}	1.51E-03	1.51E-03

Table 7
Hydrogeochemical reactions considered in the reactive transport model.

Homogeneous hydrogeochemical reactions	Log K	
$H^+ + OH^- \leftrightarrow H_2O$	+13.9951	
$CaHCO_3^+ \leftrightarrow Ca^{2+} + HCO_3^-$	−1.0467	
$CaSO_{4(aq)} \leftrightarrow Ca^{2+} + SO4^{2-}$	−2.1111	
$NaHCO_{3(aq)} \leftrightarrow HCO_3^- + Na^+$	−0.1541	
$NaSO_4^- \leftrightarrow Na^+ + SO_4^{2-}$	−0.8200	
$NaCO_3^- \leftrightarrow CO_3^{2-} + Na^+$	−0.5144	
$NaOH_{(aq)} + H^+ \leftrightarrow H_2O + Na^+$	+14.1800	
$NaHSiO_{3(aq)} + H^+ \leftrightarrow H_2O + Na^+ + SiO_{2(aq)}$	+8.3040	
$KOH_{(aq)} + H^+ \leftrightarrow H_2O + K^+$	+14.4600	
$KSO_4^- \leftrightarrow K^+ + SO_4^{2-}$	−0.8796	
$CO_{2(aq)} + H_2O \leftrightarrow H^+ + HCO_3^-$	−6.3447	
$CO_3^{2-} + H^+ \leftrightarrow HCO_3^-$	+10.3288	
$CaCO_{3(aq)} + H^+ \leftrightarrow Ca^{2+} + HCO_3^-$	+7.0017	
$CaOH^+ + H^+ \leftrightarrow Ca^{2+} + H_2O$	+12.8500	
$H_2SO_{4(aq)} \leftrightarrow SO_4^{2-} + 2H^+$	+1.0200	
$HSO_4^- \leftrightarrow H^+ + SO_4^{2-}$	−1.9791	
$H_2SiO_4^{2-} + 2H^+ \leftrightarrow SiO_{2(aq)} + 2H_2O$	+22.9116	
$H_4(H_2SiO_4)_4^{4-} + 4H^+ \leftrightarrow 4SiO_{2(aq)} + 8H_2O$	+35.9400	
$H_6(H_2SiO_4)_2^{2-} + 2H^+ \leftrightarrow 4SiO_{2(aq)} + 8H_2O$	+13.6400	
$HSiO_3^- + H^+ \leftrightarrow SiO_{2(aq)} + H_2O$	+9.9525	
$KHSO_{4(aq)} + H^+ \leftrightarrow H^+ + K^+ + SO_4^{2-} +$	−0.8136	
Mineral processes	**Log K**	**Molar volume (cm^3/mol)**
$Ca(OH)_2 + 2H^+ \leftrightarrow Ca^{2+} + 2H_2O$	+22.5552	33.056
$C_{0.8}$–S–H + $1.6H^+ \leftrightarrow 1.8H_2O + SiO_{2(aq)} + 0.8Ca^{2+}$	+10.8614*	101.800
$C_{1.1}$–S–H + $2.2H^+ \leftrightarrow 2.1H_2O + SiO_{2(aq)} + 1.1Ca^{2+}$	+16.5014*	101.800
$C_{1.8}$–S–H + $3.6H^+ \leftrightarrow 2.8H_2O + SiO_{2(aq)} + 1.8Ca^{2+}$	+32.4814*	108.000
$SiO_{2(s)} \leftrightarrow SiO_{2(aq)}$	−2.7136	29.000
$CaCO_{3(s)} + H^+ \leftrightarrow Ca^{2+} + HCO_3^-$	+1.8487	36.934

* The solubility product was deduced from data reported by Stronach and Glasser [25] and Westall et al. [26].

Please cite this article as: J.M. Galíndez, J. Molinero, Assessment of the long-term stability of cementitious barriers of radioactive waste repositories by using digital-image-based microstructure generation..., Cem. Concr. Res. (2009), doi:10.1016/j.cemconres.2009.11.006

At this point, it is also worth noting that, because of C–S–H comprising a wide variety of phases, ranging from cryptocrystalline to nearly amorphous and variable solid solution compositions of different Ca/Si ratios, their thermodynamic behaviour is extremely complex. A remarkably large amount of effort has been devoted in recent years to the characterization of C–S–H. Nevertheless, as was opportunely pointed out in [18], a phenomenological framework is lacking which is able to synthesize the current knowledge of C–S–H in terms of the variations of significant parameters such as the calcium-to-silica ratio, the silicate structure and the contents of Si–OH and Ca–OH. Moreover, such factors as the composition of cement, the water-to-cement ratio, the curing temperature, the degree of hydration, and the presence of chemical and mineral admixtures add to the inherent complexity of the task in question.

A plethora of modelling techniques was developed as a consequence, the description of which is beyond the scope of this work and can be found elsewhere [19]. One of them consists of considering C–S–H to be an assemblage of different mineral phases, characterized by diverse calcium-to-silica ratios and solubility products. This approach has already been taken in previous investigations [5,20] and it involves a simplified representation of the actual thermodynamic behaviour of C–S–H.

In Table 5, the volume fractions considered for every case, arranged according to the assumptions made above concerning the use of either cement (Ultrafin 12, Ultrafin 16 or Injektering 30), are listed. In view that the composition of the hydrated paste is not remarkably sensitive to the size distribution curves of cement clinker, only one microstructure of each recipe (the one corresponding to Ultrafin 16 particle size distribution) has been considered for subsequent reactive transport modelling of grout degradation.

4. Reactive transport modelling

4.1. Conceptual model for the degradation of cement-based grout

Under the assumption of local chemical equilibrium, which has proved to hold for most practical cases involving diffusion of ions in cementitious materials [21], the reactive transport problem may be formulated in terms of a mixed set of equations, comprising both algebraic and partial differential equations. In view of the intrinsic microstructural complexity of the hardened cement paste, the scale over which the integration of differential equations is performed becomes a matter of concern. In this respect, paths have diverged. On the one hand, the problem might indeed be solved at a microscopic scale, which implies the digital simulation of the pore structure of cement systems based, for instance, on microstructural information obtained by means of experimental procedures (e.g., mercury intrusion porosimetry). On the other hand, a Representative Elementary Volume (REV) might be defined, such that its properties can properly describe the heterogeneous material which is composed of. Using this method the most relevant variables are averaged over such volume, thus relaxing the need for detailed knowledge of the microstructure of the material. Such average properties can easily be measured in practice. The validity of this approach, often referred to as the homogenization technique, lies on the adequacy of the definition of the REV for the problem of interest. This is attained when, regardless of its location within the domain, the REV always contains persistent volumes of solid and voids [22]. This latter approach was the one taken in this work for the resolution of the reactive transport problem. Indeed, in this case, the size of the REV is given by the three-

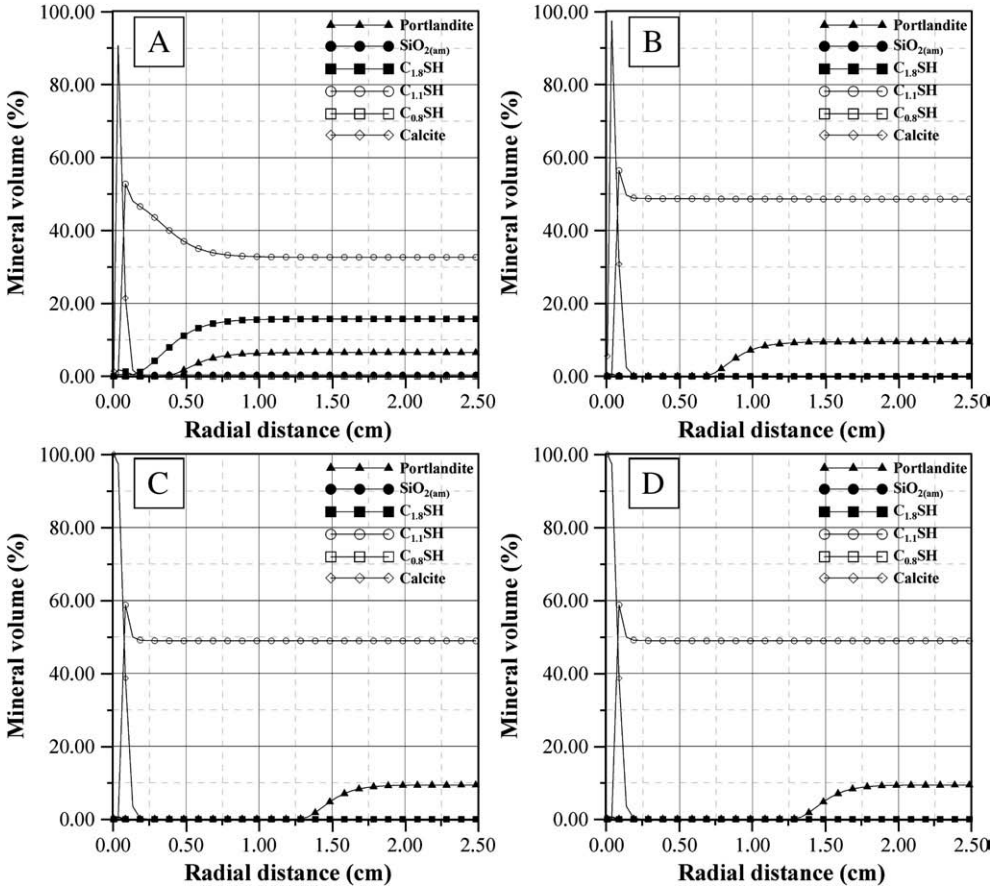

Fig. 4. Mineral constitution of Standard 5/5 injection grout after (A) 0.25 year, (B) 1 year, (C) 50 years and (D) 1000 years.

Please cite this article as: J.M. Galíndez, J. Molinero, Assessment of the long-term stability of cementitious barriers of radioactive waste repositories by using digital-image-based microstructure generation..., Cem. Concr. Res. (2009), doi:10.1016/j.cemconres.2009.11.006

dimensional picture obtained by the digital-image-based cement hydration modelling software, i.e., 100 μm × 100 μm × 100 μm [23].

4.2. Description of the scenario under study

A model was developed which is intended to simulate the degradation of a long drill hole for grout injection in fractured granite, as the one depicted in Fig. 3, for a typical cross-section of a tunnel (Fig. 3A). If the hole is long enough, the degradation induced by leaching would progress in a radial direction from the surface towards its centre, i.e., the assumption of axisymmetry would hold, and a one-dimensional axisymmetric model would be sufficient. Fig. 3B shows a slice of the cylindrical drill hole (filled with cement-based grout up to 2.50 cm from the central axis) surrounded by a thick granite layer. The scheme considered for the simulations on which degradation will be analyzed, is depicted in Fig. 3C.

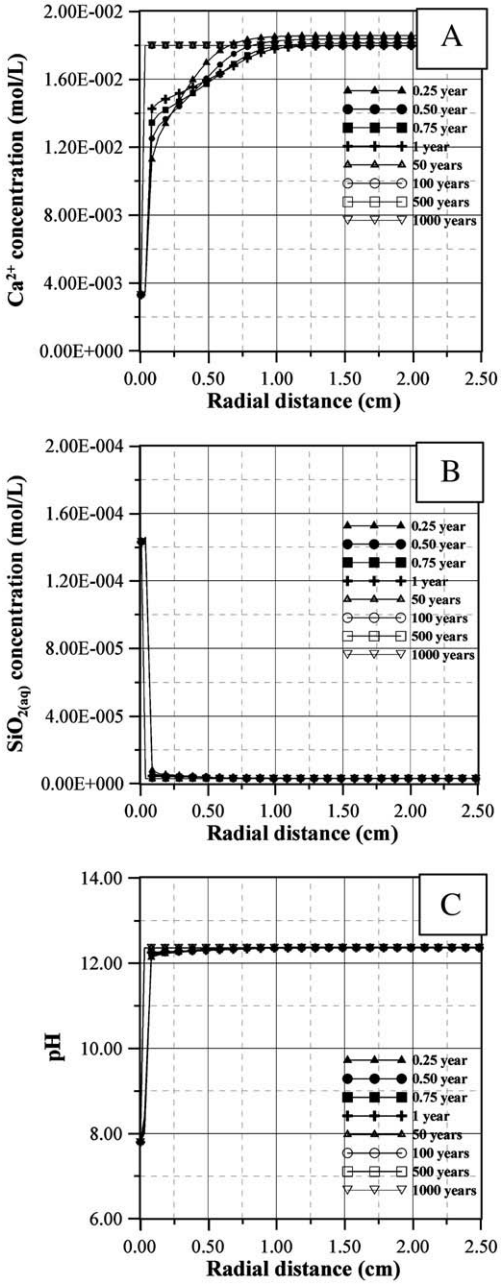

Fig. 5. Concentration of (A) calcium and (B) silica, and (C) pH in the pore water of the Standard 5/5 injection grout specimen.

The numerical resolution of the problem was based on a finite-element scheme. Grout was discretized into a one-dimensional mesh consisting of 50 elements with a uniform length of 0.05 cm.

In a worst case scenario, interstitial granite water might be constantly renewed through the fractures of the bedrock and, as a consequence, the hyperalkaline front spreading away from the grout specimen will dilute into the large volume of groundwater. Such scenario can be represented by fixing the chemical composition of water at the outer surface of grout to equal the chemical composition of the surrounding rock (i.e., imposing a boundary condition of the Dirichlet type). Some aspects of the simulation must then be acknowledged:

1) The model entails the assumption that the volume of grout is not relevant to induce a significant hyperalkaline plume in the surroundings.
2) The conditions are aggressive for grout (similar boundary conditions were applied in an analogous problem presented in [2]) but hardly critical for its surroundings, since their likely sphere of influence is constrained.

Granite was assumed to be unreactive. The chemical composition of the boundary water was assumed to match a water sample of the Laxemar area (Sweden) at a depth of 500 m, a characteristic depth often considered for a nuclear waste repository (see Table 6).

A total of 21 homogeneous hydrogeochemical reactions and 6 mineral processes were considered in the modelling and are listed in Table 7.

Molar volumes of C–S–H species are taken from [23].

4.3. Numerical tools

The numerical modelling tool CrunchFlow is a computer program for multicomponent reactive transport in porous media. CrunchFlow is an enhanced version of the GIMRT/OS3D package [27,28] which can be used for reactive transport problems of arbitrary complexity and size (i.e., there is no a priori restriction on the number of species or reactions considered). Some of its main features include the simulation of advective, dispersive, and diffusive transport in up to two dimension using the global implicit (GIMRT) option; non-isothermal transport and reaction; multicomponent aqueous complexation; kinetically-controlled mineral precipitation and dissolution; and reaction-induced porosity and permeability feedback to both diffusion and flow. The reader is referred to the User's Guide of CrunchFlow [29] for a more comprehensive discussion of the conceptual and mathematical foundations of reactive transport models.

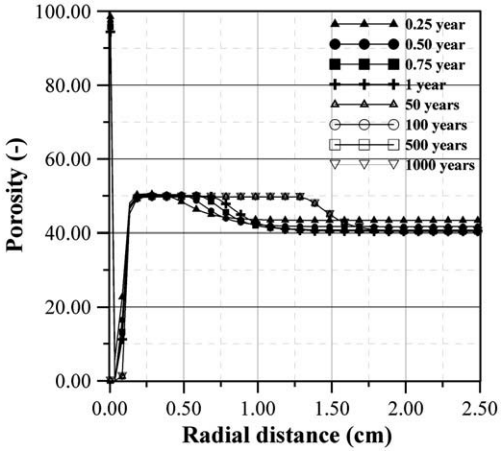

Fig. 6. Evolution of porosity with time for the Standard 5/5 injection grout specimen.

Please cite this article as: J.M. Galíndez, J. Molinero, Assessment of the long-term stability of cementitious barriers of radioactive waste repositories by using digital-image-based microstructure generation..., Cem. Concr. Res. (2009), doi:10.1016/j.cemconres.2009.11.006

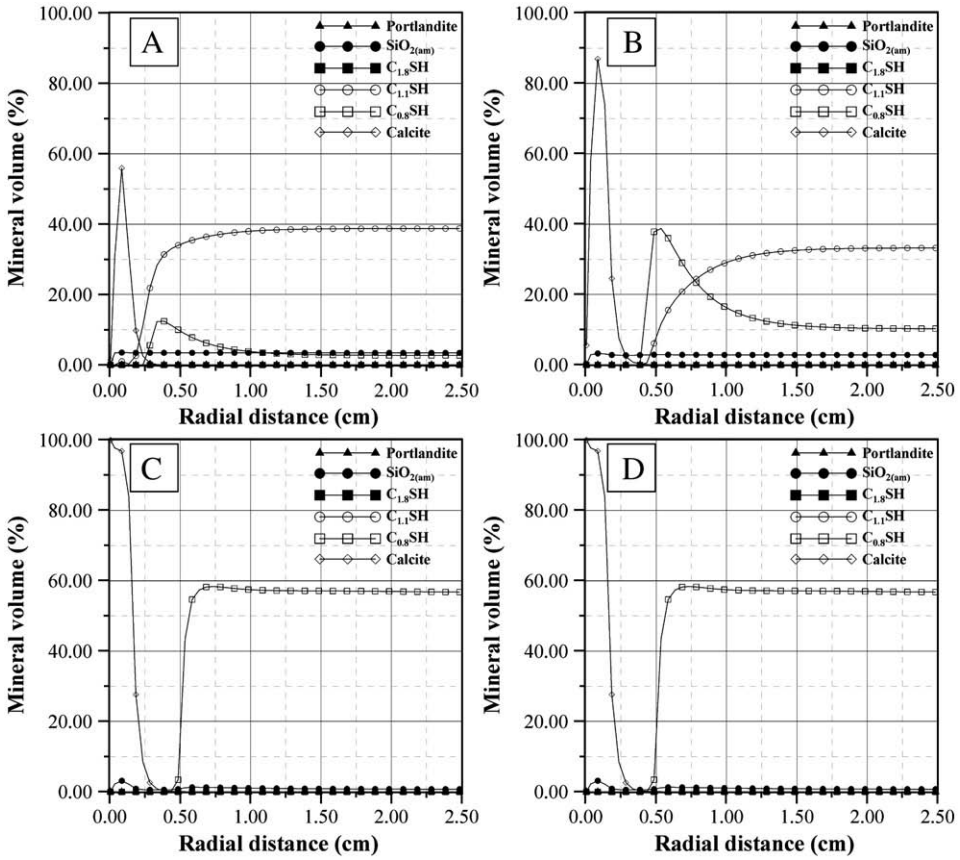

Fig. 7. Mineral constitution of P308B injection grout after (A) 0.25 year, (B) 1 year, (C) 50 years and (D) 1000 years.

For the sake of simplification, physical adsorption of ionic species at the mineral phases and electrostatic effects were neglected.

CrunchFlow makes use of the relationship given in Eq. (1) [30]:

$$D_{\text{eff}} = \frac{\phi^m}{F} D_0 \tag{1}$$

Where D_{eff} denotes the effective diffusion coefficient; $D_0 = 2.20\text{E-}09$ m^2/s, the diffusion coefficient in pure water; and the parameters F and m are respectively the formation factor and the cementation exponent.

Research on computer-simulated microstructures of cement-based materials, though, has shown that a more precise expression for the diffusion coefficient would be [31]:

$$D_{\text{eff}} = [0.001 + 0.07\phi^2 + 1.8H(\phi - \phi_c)(\phi - \phi_c)^2]D_0 \tag{2}$$

Where $\phi_c = 0.18$ represents the critical capillary porosity of the material; and $H(\phi_f - \phi_c)$ is the Heavyside function.

The parameters F and m were therefore estimated by fitting the curve ϕ vs. D_{eff} obtained with Eq. (1) to the one described by Eq. (2), for the range of porosities of the grout under study. The values calculated in this manner were $m = 2.55$ and $F = 0.78$.

4.4. Results

4.4.1. Case I: Standard grout mix 5/5

One feature of the evolution of the degradation front for the grout specimen made up of Standard grout mix 5/5 (Fig. 4) is the complete depletion of portlandite from a 1.25-cm-thick superficial layer at approximately 50 years of simulation. This is consistent with the widely accepted observation that portlandite is the first solid species to totally dissolve [5,32,33].

On the other hand, the process of decalcification of C–S–H (which is denoted by the gradual shift of their calcium-to-silica ratio from high values towards lower ones) is reproduced by the increase of the relative proportion of $C_{1.1}$–S–H in detriment of $C_{1.8}$–S–H, induced by the simultaneous dissolution of $C_{1.8}$–S–H and the precipitation of $C_{1.1}$–S–H. This phenomenon is particularly evident in the proximity of the exposed surface, but it also takes place in inner regions of the grout specimen. The process of decalcification of C–S–H is, however, not entirely detrimental for the integrity of the grout specimen, since the emerging $C_{1.1}$–S–H appears to be significantly more stable than $C_{1.8}$–S–H under the new geochemical conditions of the pore solution.

The progress of deterioration is therefore not entirely related to the advance of a sharp front but, rather, to the gradual alteration of the governing equilibrium between a changing pore solution and the reacting solid phase, which undergoes the dissolution of the richer calcium-containing mineral phases of grout. Another noteworthy feature of degradation is the precipitation of calcite on the exposed surface of the specimen (arising from the presence of bicarbonates in the surrounding groundwater, in combination with the calcium ions which are released outwards from the core of the specimen), which tends to fill the capillary pores. This is corroborated by empirical observations reported in previous works [34,35]. The clogging of the pore network also has a beneficial effect on the lowering of the diffusion rate and, as a consequence, on the decrease of the rate of advance of the front of dissolution of portlandite. This holds true to such extent that after less than 50 years, the surface of the specimen is completely sealed, hindering the further advance of deterioration. The snapshots at simulation times of 50 years and later suggest that a new equilibrium stage was reached where dissolution of portlandite has halted its progress, and no further decalcification of C–S–H is seen.

In strong agreement with observations made by [5] for ordinary Portland cements, calcium concentration rises sharply up to 1.80E-

Please cite this article as: J.M. Galíndez, J. Molinero, Assessment of the long-term stability of cementitious barriers of radioactive waste repositories by using digital-image-based microstructure generation..., Cem. Concr. Res. (2009), doi:10.1016/j.cemconres.2009.11.006

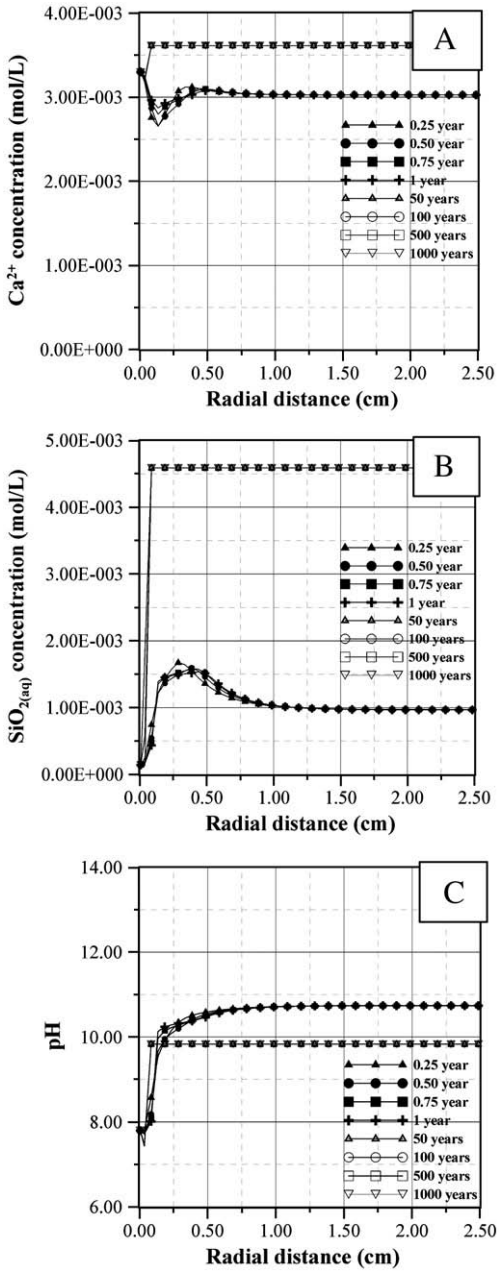

Fig. 8. Concentration of (A) calcium and (B) silica, and (C) pH in the pore water of the P308B injection grout specimen.

02 mol/L after less than a year of exposure (Fig. 5A). In that work, this process is attributed to the depletion of alkali ions from the pore solution, due to diffusive fluxes, and the subsequent replacement by calcium ions, released from the cement paste through portlandite dissolution. The decalcification of C–S–H adds to this effect. Whereas pH stays relatively stable at 12.35 (Fig. 5C), at later stages of deterioration, calcium ions are leached outwards due to the concentration gradient which is established between the pore solution and the boundary groundwater. This phenomenon continues as long as there is some pore space remaining connecting the pore solution to the environment, i.e., until the "barrier" of calcite which forms on the surface of the specimen does not hinder the transport of species. By sealing the pores, calcite isolates the pore solution from its environment, and therefore enables calcium to increase uniformly along the entire depth of the specimen.

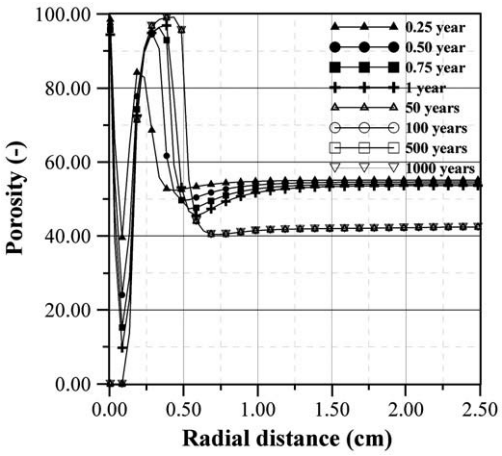

Fig. 9. Evolution of porosity with time for the P308B injection grout specimen.

Fig. 6 shows the evolution of the porosity in successive profiles obtained after different times of simulation. It is apparent that the increase of the porosity is related to a great extent to the dissolution of portlandite, which progresses towards the centre of the grout specimen, and the precipitation of a large amount of calcite on the exposed surface, which tends to seal the pore network. After 1000 years of simulation, however, it is seen that the most dramatic effects of deterioration are confined to 1.5 cm from the exposed surface. The core of the specimen remains virtually unaltered.

4.4.2. Case II: P308B grout mix

The results of the simulation of the deterioration of P308B grout are shown in Fig. 7, in terms of the evolution of the mineral phases. As can be observed, in absence of portlandite, the process of deterioration is reflected mainly on the decalcification of C–S–H. It is apparent that the behaviour of the solid phase in response to the changes that the entry of external groundwater induces on the geochemical properties of the pore solution is two-fold. On the one hand, the process of decalcification (i.e., the dissolution of $C_{1.1}$–S–H and the precipitation of $C_{0.8}$–S–H) leads to almost the complete disintegration of the material in the vicinity of the exposed surface. On the other hand, the process of decalcification involves the evolution of the C–S–H from calcium-richer, more soluble phases towards more stable compounds under low-pH conditions. As a consequence, the front of deterioration advances at a low rate and the most dramatic effects of degradation are confined to less than 0.5 cm after 1000 years. Moreover, the higher amount of $C_{0.8}$–S–H precipitated induces the decrease of the porosity, thus further hindering the progress of degradation. As can be seen, calcite tends to fill the space of the original position of the surface of the specimen and stays isolated from the core of the specimen. Whether this is mechanically possible remains an open question to which it is not possible to give a definite answer with the results obtained at hand. However, a rational analysis based upon physical, rather than numerical, considerations would enable to hypothesize that calcite should precipitate around the actual surface of the solid, wherever its position, around which the initial crystals may nucleate. In that scenario, the trend observed in the sequence shown in Fig. 7 allows one to envisage a final less porous material made up of a large amount of C–S–H with a calcium-to-silica ratio of Ca/Si = 0.8, protected by a relatively thick layer of calcite.

The properties of the P308B cement and, in general, of low-pH cement grouts become apparent from Fig. 8. The pore solution in contact with such grout is characterized by lower contents of calcium and higher concentrations of silica with respect to Ordinary Portland cements. The numerical simulations also reproduce the significantly lower value of pH (Fig. 8C) obtained as a consequence of the addition of silica fume into the dry mixture. As in the previous case, the barrier

Please cite this article as: J.M. Galíndez, J. Molinero, Assessment of the long-term stability of cementitious barriers of radioactive waste repositories by using digital-image-based microstructure generation..., Cem. Concr. Res. (2009), doi:10.1016/j.cemconres.2009.11.006

of calcite formed on the surface of the specimen shields the pore solution from the environment. The pH of the pore solution drops then down to approximately 9.8 once the equilibrium stage is attained.

The porosity of the grout specimen undergoes a dramatic increase near the surface, which virtually leads to the disintegration of the material (Fig. 9). As discussed above, the transformation of $C_{1.1}$–S–H into larger quantities $C_{0.8}$–S–H induces the decrease of the porosity in inner regions of the specimen, thus preventing the disintegration from advancing inwards. The associated decrease of the diffusion rate, along with the formation of a protective layer of calcite on the surface and the lower solubility of $C_{0.8}$–S–H, eventually settle into a state of pseudo-equilibrium at a certain distance from the exposed surface safeguarding the integrity of the core of the specimen.

5. Testing the hydrochemical boundary condition

After the construction of the tunnel, the composition of groundwater at high depths (which, under undisturbed conditions is well known and might remain essentially constant) may undergo substantial variations as a consequence of different types of water flowing towards the tunnel as if towards a sink and mixing with deep groundwater. Given that the most suitable locations for deposit tunnels that are currently under consideration are generally to be found in coastal areas, different mixings between fresh waters of meteoric origin, marine waters and deep brines are possible at the depth of the tunnel. In turn, the actual composition of the boundary water determines the rate of advance of the front of degradation. In view of this, additional simulations were performed in order to get a notion of the sensitivity of the results with respect to the chemical composition of groundwater and, in particular, with respect to the content of bicarbonate, which was found to dampen the rate of degradation by contributing to the formation of calcite. Such sensitivity analyses might prove fruitful in estimating the range over which the actual rate of degradation can vary and, in particular, the maximum values that can occur. The additional simulations were carried out for both Standard 5/5 cement and P308B cement grout specimens exposed to a boundary water whose chemical composition is described in the third column of Table 6. Its main feature, with respect to the one of the reference cases, is that the content of HCO_3^- is one order of magnitude lower, which may be due to a greater contribution of meteoric water.

5.1. Case I: Standard 5/5 cement

As can be observed (Fig. 10), the effects of the relative lack of bicarbonate in groundwater has deleterious effects on grout since, by preventing the formation of a calcite "barrier" (although calcite does precipitate, it does not seal the pores tightly), it accelerates the processes of dissolution of portlandite and the decalcification of C–S–H. Indeed, after less than 50 years of exposure, portlandite is completely exhausted and the remaining fraction of C–S–H recedes approximately 1 cm from the initial position of the surface. Towards the inner regions of the specimen, the effects of degradation are seen as a larger proportion of $C_{0.8}$–S–H in the solid phase, which reflects a higher degree of decalcification. The process appears to be of an unstable nature since, apart from the precipitation of calcite, the lower solubility of $C_{0.8}$–S–H, and their dampening effect on the rate of degradation, there are no signs of a new equilibrium state. In other words, the deterioration would progress, though at lower rates, indefinitely.

Fig. 11 shows the gradual decrease that affects the concentration of calcium at earlier simulation times, due to the diffusive fluxes induced by the concentration gradient between the boundary and the pore waters. After 50 years of simulation, a concentration of approximately 4E-03 mol/L is reached, which is comparable to that observed in Fig. 8,

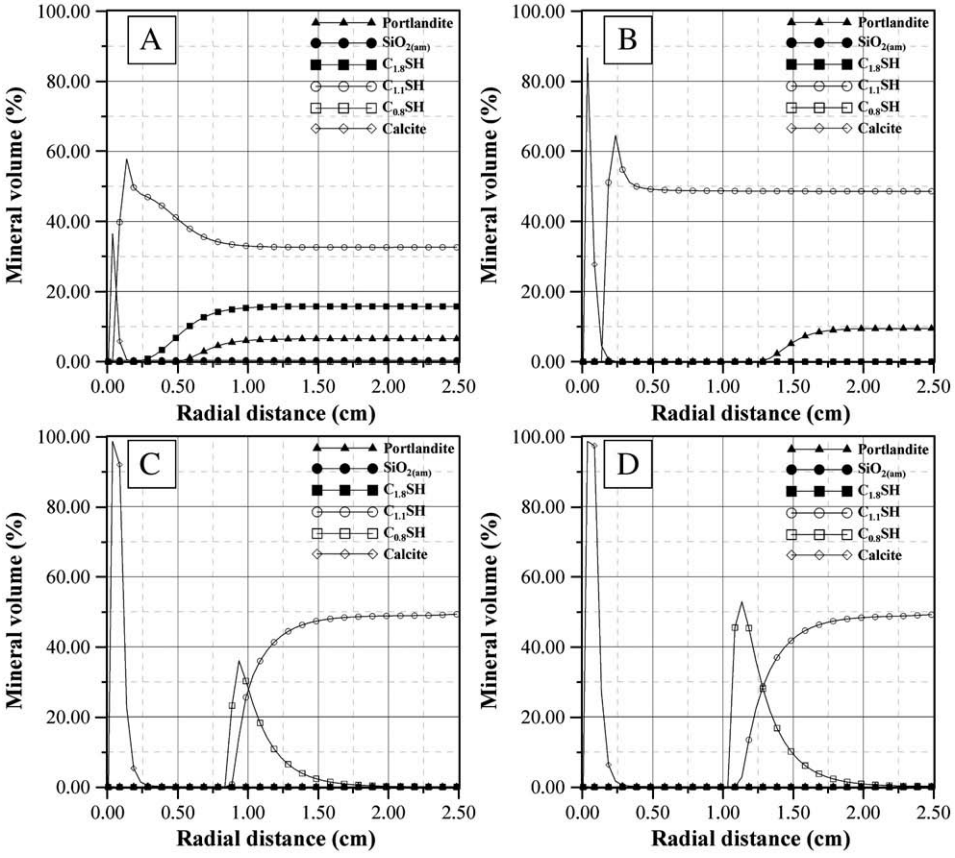

Fig. 10. Mineral constitution of Standard 5/5 injection grout after (A) 0.25 year, (B) 1 year, (C) 50 years and (D) 1000 years.

Please cite this article as: J.M. Galíndez, J. Molinero, Assessment of the long-term stability of cementitious barriers of radioactive waste repositories by using digital-image-based microstructure generation..., Cem. Concr. Res. (2009), doi:10.1016/j.cemconres.2009.11.006

and in accordance with the prominence of C–S–H phases with lower Ca/Si ratios that remain. The evolution of pH (Fig. 11) follows a similar pattern: the typically high value of 12.35 drops down to 10.7 after 50 years of exposure.

As said above, in the present case, degradation progresses as a sharp front, due to the dissolution of C–S–H and the steep increase of the porosity, up to nearly 100% (Fig. 12). Distinct from the reference case (Case I), as well as the changes in the microstructure of grout, the most noteworthy effect of deterioration is the reduction of the effective diameter of the grout specimen, by disintegration of the outer solid layers.

5.2. Case II: P308B cement

As Fig. 13 shows, the durability of grout might be dramatically damaged by the lower bicarbonate in groundwater. Indeed, the process of degradation is accelerated to such extent that the grout specimen is completely disintegrated after a few years (less than 50) of exposure.

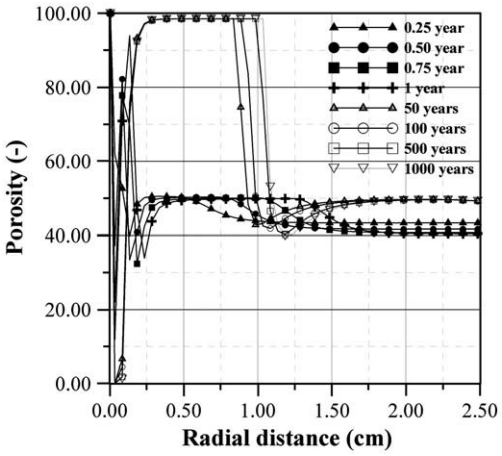

Fig. 12. Evolution of porosity with time for the Standard 5/5 injection grout specimen.

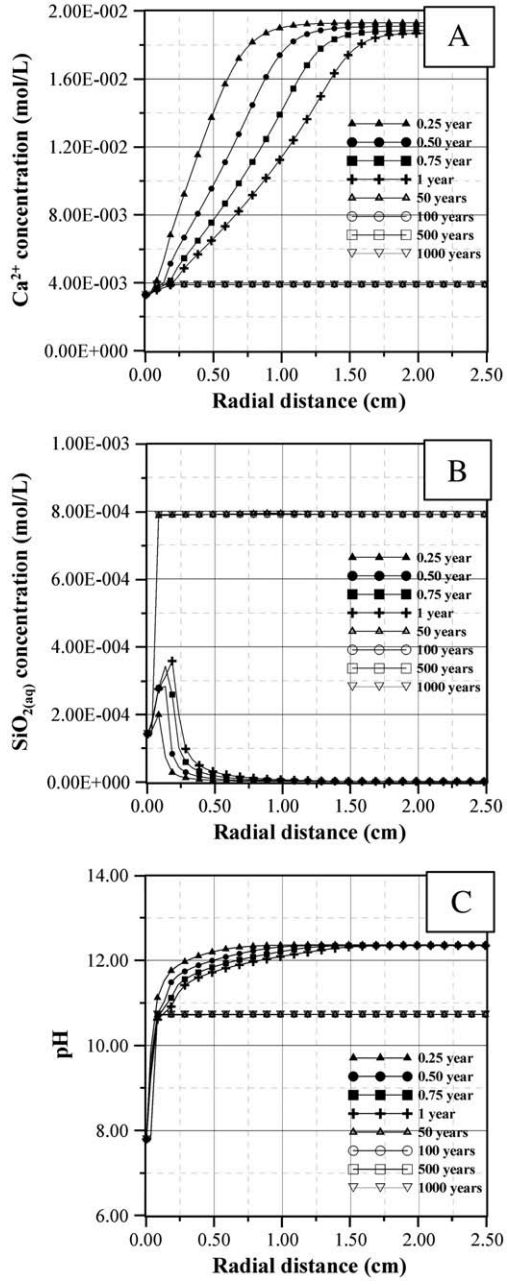

Fig. 11. Concentration of (A) calcium and (B) silica, and (C) pH in the pore water of the Standard 5/5 injection grout specimen.

Given that the availability of bicarbonates precludes the formation of a calcite layer, the core of the grout specimen cannot be preserved from the exposure to groundwater, and calcium-containing mineral phases are steadily degraded. In this manner, it can be concluded that the service life of grout is intimately linked to the precipitation of calcite on the surface.

6. Conclusions

A new methodological approach to a rational study of the optimum mix design for injection grout was presented. Although not intended to dissipate the uncertainties connected to the actual evolution of the process of hydration under field conditions, the method is, in fact, useful with views to define reasonable starting points for modelling of degradation. In turn, reactive transport models would provide insight into the performance of the mixtures analyzed in the long-term and guide the pursuit in a practical and effective manner.

The microstructure of the hardened paste was simulated by digital-image-based algorithms, on the basis of typical mix designs. Simulated microstructures have been linked to reactive solute transport models to evaluate the durability of two different types of cement-based grout in contact with granitic groundwater.

Results of the microstructure simulations match the characteristic properties expected from injection grout. Computed microstructures display a high degree of hydration, high porosity (i.e., between 40% and 60%), low contents of aluminium compounds, (including nil amounts of ettringite and hydrogarnet) and, for the P308B grout, low contents of portlandite due to the addition of silica fume. Furthermore, the pH of the pore solution in equilibrium with the solid phases in that case (P308B grout), obtained by means of geochemical speciation, is in the range of typical low-pH cements.

The reactive transport model was aimed at evaluating the degradation of a long drill hole for grout injection surrounded by a relatively thick layer of highly porous granite, and immersed in seawater.

Simulations were carried out for the two mix designs considered and for a boundary water with a chemical composition typical of the Laxemar area (Sweden) at the projected depth of a repository for nuclear spent fuel. They were repeated for a different water in which the content of bicarbonates was reduced by one order of magnitude.

The results obtained show that the process of deterioration is related to two main phenomena, namely, the decalcification of mineral phases (which involves the depletion of portlandite, when

Please cite this article as: J.M. Galíndez, J. Molinero, Assessment of the long-term stability of cementitious barriers of radioactive waste repositories by using digital-image-based microstructure generation..., Cem. Concr. Res. (2009), doi:10.1016/j.cemconres.2009.11.006

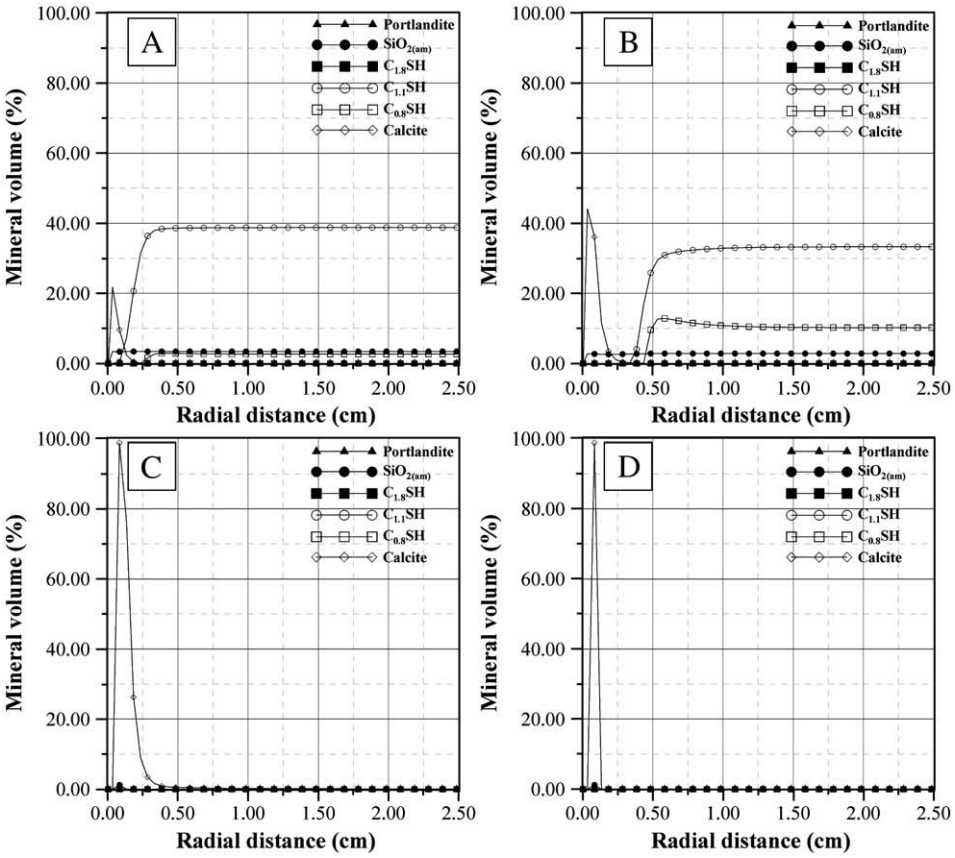

Fig. 13. Mineral constitution of P308B injection grout after (A) 0.25 year, (B) 1 year, (C) 50 years and (D) 100 years.

available) and the precipitation of calcite. It is seen that, under the exposure of typical Laxemar groundwater, the durability of both grout mixes will be guaranteed for thousands of years. However, the sensitivity analysis shows that groundwaters with low bicarbonate concentrations could accelerate dramatically the degradation process, this effect being related to the absence of calcite precipitation.

Acknowledgments

This work has been carried out within the framework of a Research Project (DECON Project) funded by the Swedish Nuclear Fuel and Waste Management Company (SKB). Thanks are especially given to Ignasi Puigdomenech for his support, encouragement and suggestions. The authors would also like to acknowledge the constructive comments of two anonymous reviewers which have contributed significantly to improve the original manuscript.

References

[1] A. Bodén, U. Sievänen, Low-pH injection grout for deep repositories, Summary Report from a Co-operation Project between NUMO (Japan), Posiva (Finland) and SKB (Sweden), R-05-40, 2005.
[2] L. Trotignon, H. Peycelon, X. Bourbon, Comparison of performance of concrete barriers in a clayey geological medium, Phys. Chem. Earth 31 (2006) 610–617.
[3] V. Matte, M. Moranville, F. Adenot, C. Richet, J.M. Torrenti, Simulated microstructure and transport properties of ultra-high performance cement-based materials, Cem. Concr. Res. 30 (2000) 1947–1954.
[4] J. Marchand, D.P. Bentz, E. Samson, Y. Maltais, Influence of Calcium Hydroxide Dissolution on the Transport Properties of Hydrated Cement Systems, Reactions of Calcium Hydroxide in Concrete, American Ceramic Society, Westerville, USA, 2001.
[5] M. Moranville, S. Kamali, E. Guillon, Physicochemical equilibria of cement-based materials in aggressive environments—experiment and modeling, Cem. Concr. Res. 34 (2004) 1569–1578.
[6] E. Holt, Durability of Low-pH Injection Grout — A Literature Survey, Posiva Oy working report 2006-XX, , 2006.
[7] A. Kronlöf, Injection grout for deep repositories — low-pH cementitious grout for large fractures: Testing technical performance of materials. VTT Building and Transport, Posiva working report 2004–45, 2004.
[8] U. Sievänen, P. Syrjänen, S. Ranta-aho, Injection grout for deep repositories — low-pH cementitious grout for larger fractures: field testing in Finland, pilot tests. Posiva working report 2004–47, 2005.
[9] D.P. Bentz, P.V. Coveney, E.J. Garboczi, M.F. Kleyn, P.E. Stutzman, Cellular automaton simulations of cement hydration and microstructure development, Model. Simul. Mat. Sci. Eng. 2 (1994) 783–808.
[10] D.P. Bentz, Three-dimensional computer simulation of cement hydration and microstructure development, J. Am. Ceram. Soc. 80 (1) (1997) 3–21.
[11] D.P. Bentz, C.J. Haecker, An argument for using coarse cements in high performance concretes, Cem. Concr. Res. 29 (1999) 615–618.
[12] D.P. Bentz, E.J. Garboczi, C.J. Haecker, O.M. Jensen, Effects of cement particle size distribution on performance properties of cement-based materials, Cem. Concr. Res. 29 (1999) 1663–1671.
[13] D.P. Bentz, O.M. Jensen, K.K. Hansen, J.F. Olesen, H. Stang, C.J. Haecker, Influence of cement particle size distribution on early age autogenous strains and stresses in cement-based materials, J. Am. Ceram. Soc. 84 (1) (2000) 129–135.
[14] D.P. Bentz, X. Feng, C.J. Haecker, P.E. Stutzman, Analysis of CCRL Proficiency Cements 135 and 136 Using CEMHYD3D, NISTIR 6545, U.S. Department of Commerce, 2000.
[15] D.P. Bentz, J.T. Conway, Computer modeling of the replacement of "coarse" cement particles by inert fillers in low w/c ratio concretes: Hydration and strength, Cem. Concr. Res. 31 (2001) 503–506.
[16] J.W. Bullard, User's Guide to the Virtual Cement and Concrete Testing Laboratory Version 1.1 (2000). Available online at http://vcctl.cbt.nist.gov/vcctl/vcctl11/master.html.
[17] D.P. Bentz, P.E. Stutzman, SEM/X-ray imaging of cement-based materials, in: H.S. Pietersen, J.A. Larbi, H.H.A. Janssen (Eds.), Proceedings of the 7th Euroseminar on Microscopy Applied to Building Materials, 1999, pp. 457–466.
[18] J.J. Chen, J.J. Thomas, H.F.W. Taylor, H.M. Jennings, Solubility and structure of calcium silicate hydrate, Cem. Concr. Res. 34 (2004) 1499–1519.
[19] J.M. Galíndez, Coupled water flow and reactive transport modeling and its application to the simulation of cement degradation processes, Master thesis, Universidade de Santiago de Compostela, Spain, 2006.
[20] E. Guillon, Durabilité des matériaux cimentaires. Modélisation de l'influence des équilibres physico-chimiques sur la microstructure et les propriétés mécaniques résiduelles, PhD Thesis, École Normale Supériere de Cachan, France, 2004.
[21] R. Barbarulo, J. Marchand, K.A. Snyder, S. Prene, Dimensional analysis of ionic transport problems in hydrated cement systems Part 1. Theoretical considerations, Cem. Concr. Res. 30 (2000) 1955–1960.
[22] J. Bear, Y. Bachmat, Introduction to Modeling of Transport Phenomena in Porous Media, Kluwer Academic Publishing, Dordrecht, The Netherlands, 1991.

Please cite this article as: J.M. Galíndez, J. Molinero, Assessment of the long-term stability of cementitious barriers of radioactive waste repositories by using digital-image-based microstructure generation..., Cem. Concr. Res. (2009), doi:10.1016/j.cemconres.2009.11.006

[23] D.P. Bentz, CEMHYD3D: A Three-Dimensional Cement Hydration and Microstructure Development Modeling Package. Version 2.0, NISTIR 6485, U.S. Department of Commerce, 2000.
[24] M. Laaksoharju, Hydrogeochemical evaluation. Preliminary site description Laxemar subarea — version 2.1, SKB Report R-06-70, 2006. Available online at http://www.skb.se/upload/publications/pdf/R-06-70webbNY.pdf.
[25] S.A. Stronach, F.P. Glasser, Modelling the impact of abundant geochemical components on phase stability and solubility of the CaO–SiO2–H2O system at 25 °C: Na+, K+, SO42−, Cl− and CO32−, Adv. Cem. Res. 9 (1997) 167–181.
[26] J.C. Westall, J.L. Zachary, F.M. Morel, MINEQL — A Computer Program for the Calculation of Chemical Equilibrium Composition of Aqueous Systems, Massachusetts Institute of Technology, Cambridge, USA, 1976.
[27] C.I. Steefel, S.B. Yabusaki, OS3D/GIMRT, Software for Multicomponent–Multidimensional Reactive Transport: User's Manual and Programmer's Guide, PNL–11166, Pacific Northwest National Laboratory, Richland, Washington, USA, 1996.
[28] C.I. Steefel, GIMRT, Version 1.2: Software for Modeling Multicomponent, Multidimensional Reactive Transport. User's Guide, UCRL-MA-143182, Lawrence Livermore National Laboratory, Livermore, USA, 2001.
[29] C.I. Steefel, CrunchFlow - Software for Modeling multicomponent reactive flow and transport, Lawrence Berkeley National Laboratory, 2008. Available online at http://www.csteefel.com/CrunchPublic/CrunchFlowManual.pdf.
[30] G.E. Archie, The electrical resistivity log as an aid to determining some reservoir characteristics, Trans. Am. Inst. Min. Eng. 146 (1942) 54–61.
[31] E.J. Garboczi, D.P. Bentz, Computer simulation of the diffusivity of cement-based materials, J. Mater. Sci. 27 (1992) 2083–2092.
[32] C. Carde, R. François, J.M. Torrenti, Leaching of both calcium hydroxide and C–S–H from the cement paste: modeling the mechanical behavior, Cem. Concr. Res. 26 (1996) 1257–1268.
[33] P. Faucon, F. Adenot, J.F. Jacquinot, J.C. Petit, R. Cabrillac, M. Jorda, Long-term behaviour of cement pastes used for nuclear waste disposal: review of physico-chemical mechanisms of water degradation, Cem. Concr. Res. 28 (1998) 847–857.
[34] B. Lagerblad, Leaching Performance of Concrete Based on Studies of Samples from Old Concrete Constructions, SKB Technical Report TR-01-27, 2001.
[35] T. Van Gerven, D. Van Baelen, V. Dutré, C. Vandecasteele, Influence of carbonation and carbonation methods on leaching of metals from mortars, Cem. Concr. Res. 34 (1) (2004) 149–156.

Please cite this article as: J.M. Galíndez, J. Molinero, Assessment of the long-term stability of cementitious barriers of radioactive waste repositories by using digital-image-based microstructure generation..., Cem. Concr. Res. (2009), doi:10.1016/j.cemconres.2009.11.006

Appendix III

Paper III

On the relevance of electrochemical diffusion for the modeling of degradation of cementitious materials

Galíndez, Juan Manuel; Molinero, Jorge

Submitted to Cement and Concrete Composites
(in press)

Cement & Concrete Composites 32 (2010) 351–359

Contents lists available at ScienceDirect

Cement & Concrete Composites

journal homepage: www.elsevier.com/locate/cemconcomp

On the relevance of electrochemical diffusion for the modeling of degradation of cementitious materials

Juan Manuel Galíndez [a,*], Jorge Molinero [b]

[a] University of Santiago de Compostela, Dept. of Agroforestal Engineering, Campus Universitario, 27002 Lugo, Spain
[b] Amphos XXI Consulting S.L., Passeig de García i Faria, 49-51, E08019 Barcelona, Spain

ARTICLE INFO

Article history:
Received 3 December 2009
Received in revised form 17 February 2010
Accepted 22 February 2010
Available online 1 March 2010

Keywords:
Cement degradation modeling
Fick's law
Poisson–Nernst–Planck equations
Sulfate attack

ABSTRACT

Reactive solute transport models have been broadly used over the last years to evaluate the durability of cementitious materials because they provide a mechanistic approach to cope with the complex diffusion–reaction phenomena involved in cement and concrete degradation processes. However, most of the numerical models published in the scientific literature use Fick's law as the constitutive equation for the diffusive transport of dissolved ions, neglecting the electrochemical constraints imposed by the various ionic fluxes, which conspire against the local electroneutrality of the system.

In this work, the relevance of electrochemical diffusion and its impact on the nonlinear coupled phenomena concerned by cement degradation were evaluated, on the basis of its influence on the simulation of deterioration of concrete exposed to weak sulfate solutions.

Results obtained show that diffusive approaches based on Fick's law may not be accurate enough for modeling the degradation of cementitious materials since, for the case considered, when ignored, electrochemical interactions in the diffusion process may lead to the inability of reactive transport models to reproduce key phenomena such as gypsum precipitation near the exposed cement surface.

1. Introduction

Over the last years, the study of concrete degradation has increasingly gathered the interest of the scientific community, in a certain measure due to the more stringent requirements of durability which are associated with the development of new materials (e.g., low-pH cements, sulfate-resisting cements, etc.) and relevant civil structures, such as nuclear waste repositories. In that context, the use of reactive transport models, capable of simulating the behavior of concrete under diverse boundary conditions has transcended the role of a mere complement of experimental studies and has become of paramount relevance in itself. Proof of this can be found in [1]. Through the use in very disparate hydrogeochemical systems, reactive transport models have gained in reliability over the years. Yet, cement being a very idiosyncratic material, there are things that are not quite settled. The debate that has been opened on the subject matter of the simulation of the transport of ionic species is evidence of the dynamic development of reactive transport modeling in this field of research.

Gradually, modelers have arrived to the realization that the problem cannot be formulated entirely in terms of molecular diffusion, for then the influence of forces arising from the generation of an electrical potential due to the movement of charged particles is neglected. As a consequence of the building up of an electrical potential, ions tend to move at different speeds from what could be expected on account of concentration gradients taken in isolation. Such divergences might or might not be of importance and thus the problem acquires shades of a practical nature, which can be reduced essentially to the following terms: Are actual results so different to justify the use of more demanding, complex, models? Is it worth the effort they entail when, as pointed out in [2], even the most sophisticated macroscopic models are unable to reproduce a number of non-standard phenomena when cement-based materials are dealt with? This dilemma has already been reckoned with [3], yet a conclusive answer remains to be given, and that is probably one of the main reasons that have prevented the Poisson–Nernst–Planck equations from achieving more widespread use, in comparison to the mathematically simpler, more straightforward, Fick's law. Thanks to the work of several researchers [3–11], however, a trend may be envisaged towards the reversal of the current state of affairs.

The objective of this paper is to contribute to this discussion by analyzing a problem which was already published in the scientific literature, although focused from an altogether different standpoint. Indeed, the paper which is being referred to [4], which deals with the effect of weak sulfate solutions on the durability of concrete, was originally oriented towards the verification of a reactive

* Corresponding author.
E-mail address: juanmanuel.galindez@usc.es (J.M. Galíndez).

0958-9465/$ - see front matter © 2010 Elsevier Ltd. All rights reserved.
doi:10.1016/j.cemconcomp.2010.02.006

transport model developed by the authors, by means of the numerical simulation of the degradation of concrete under such aggressive conditions. On the other hand, the same example will be used herein to analyze the divergence of two different conceptual models of diffusive transport of electrically charged particles in aqueous solutions, with special attention to the coupled dissolution/precipitation processes evolving in the solid matrix.

2. Description of the two models for diffusion of ionic species

2.1. Fick's law

The contact of two different kinds of water is crucial for the process of degradation to unfold as it alters the reigning equilibrium of the concrete pore solution and gives rise to the transport of aqueous species at expense of the gradient of concentration between them. The application of the mass conservation equation for a given ionic species diffusing in the liquid phase yields:

$$\frac{\partial c_i}{\partial t} + \nabla \cdot (j_i) = 0 \tag{1}$$

where c_i is the concentration of the considered species in solution and j_i is the flux of the same species in the liquid phase. If the flux is taken to be proportional to the gradient of concentration of the species considered, as:

$$j_i = -D_i \nabla c_i \tag{2}$$

where D_i is the diffusion coefficient of the species, then Eq. (1) turns into the well-known Fick's second law

$$\frac{\partial c_i}{\partial t} = \nabla \cdot (D_i \nabla c_i) \tag{3}$$

As is well known, Fick's law applies when dealing with molecular diffusion, providing the exact solution of the problem. The conceptual model that Fick's law entails is, however, not entirely reliable when the movement of ionic species is involved, for it neglects the particular features of ionic diffusion mechanisms in liquids. Indeed, unlike neutral molecules, ions are electrically charged particles and they are subjected to various electrical forces. The charged nature of the ionic particles is at the origin of various interactions between the drifting particles (ion/ion and ion/solvent interactions). These so-called activity effects become important as the concentration of the various ions in solution increase. The electrical charge of the particles may also contribute to generate specific ion/solid interactions.

2.2. The Poisson–Nernst–Planck equations

Despite the relative importance of activity effects and ion/solid interaction phenomena, the most relevant feature which distinguishes ion diffusion from molecular diffusion involves the electrical coupling of the various ionic fluxes. Indeed, during the diffusion process, the different ionic species tend to drift at divergent speeds (in response to their respective concentration gradients and diffusion coefficients in the medium where the movement takes place) thus inducing electrical unbalances which conspire against the local electroneutrality of the system. Nevertheless, any local excess charge transferred by the ions movement generates an electrical field (referred to as diffusion potential) which tends to restore the electroneutrality by harmonically altering the diffusion rate of all the species involved.

Diffusion transport of ionic species is therefore constrained by the electroneutrality requirement, which should hold at any point of the liquid phase. Electroneutrality is evaluated by lumping the electric contribution of all the species present in solution. This requirement is taken into account by the Poisson–Nernst–Planck equations, according to which j_i can be defined as follows [7]:

$$j_i = -D_i^{\mu} \operatorname{grad}(c_i) - \frac{D_i^{\mu} z_i F}{RT} c_i \operatorname{grad}(\psi) - D_i^{\mu} c_i \operatorname{grad}(\ln \gamma_i) \tag{4}$$

where R is the ideal gas constant; F is the Faraday constant; T is the absolute temperature; z_i is the valence of the ionic species; γ_i is the chemical activity coefficient of the chemical species; and D_i^{μ} is the diffusion coefficient in the liquid phase, assumed to be an ideal solution. Finally ψ stands for the diffusion potential set up by the drifting ions, according to the Poisson equation [12]:

$$\nabla^2 \psi - \frac{\rho}{\varepsilon} = 0 \tag{5}$$

where ε is the permittivity of the medium and ρ represents the electrical charge density, which is defined as:

$$\rho = F \sum_{i=1}^{N} z_i c_i \tag{6}$$

N being the number of ionic species in solution.

The calculation of the chemical activity coefficient in Eq. (4), might be carried out by means of, for instance, the expression of Debye–Hückel (Eq. (7)), which was found to give accurate results [13]:

$$\ln \gamma_i = -\frac{A z_i^2 \sqrt{I}}{1 + a_i B \sqrt{I}} + bI \tag{7}$$

where A and B and b are temperature-dependent parameters; a_i is a constant characteristic of a given species; and I is the ionic strength of the solution, defined as:

$$I = \frac{1}{2} \sum_{i=1}^{N} z_i^2 m_i \tag{8}$$

where m_i represents the molality of the i-th ionic species.

Thus, two different approaches were outlined, namely, those provided by Fick's and the Poisson–Nernst–Planck laws. One of the obvious advantages of Fick's law lies on its extremely simple mathematical formulation, which has favored its use in a wide range of practical problems. In fact, Fick's law provides accurate results for diffusive transport problems of neutral species. Its applicability could, nevertheless, be subjected to question when dealing with multi-solute diffusion problems, for the effects of electrical gradients might no longer be negligible. Both the Poisson–Nernst–Planck equations and Fick's law will be tested in the next section in relation to the water–concrete interaction problem which was previously set up.

3. Description of the experiment

The subject matter of the simulation is the case of a concrete slab resting on a sulfate contaminated soil. The scheme of the experiment under simulation is seen in Fig. 1. As can be seen, the thickness of the slab was fixed at 15 cm and the bottom part of it was considered to be directly in contact with the soil (containing Na^+ and SO_4^{2-} ions).

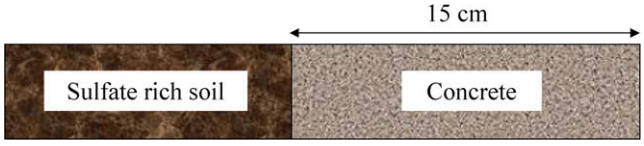

Fig. 1. Schematic representation of the modeled problem.

On the other hand, the interstitial solution contained in the porous structure of the cement paste is highly charged with alkaline Na^+, K^+, OH^- and Ca^{2+} ions.

It is worth pointing out here that, since the original intention of the cited research [4] was to evaluate the performance of different kinds of concrete – in particular, that of sulfate-resisting cement in relation to ordinary Portland cement – several scenarios were set up, under both saturated and unsaturated conditions, involving a wide range of water-to-cement ratios and of the concentration of sodium sulfate in the aggressive solution.

The scope of the present work is, nonetheless, narrower, as it is focused only on a single case, where the saturated hardened paste is made of CSA type 50 cement, with a water-to-cement ratio of 0.65, and the concentration of sodium sulfate in the boundary water is fixed at 10 mmol/L. The initial composition of the pore solution, the mineralogical distribution of the unaltered cement paste and the porosity of the mixture for that particular concrete are given in Table 1. For more details, the reader is referred to [4].

Calcite, gypsum, quartz and amorphous silicon, although initially absent, were also taken into account in case precipitation could take place. As shown in Table 1, the influence of coarse and fine aggregates was also considered by means of a fictitious mineral, capable of dissolving into calcium and bicarbonate ions, and which occupies 71.90% of the total volume.

As reported in [4], the computer code STADIUM, which takes into consideration the coupled transport of ions and liquid and the chemical equilibrium of solid phases within the saturated system, was used in order to investigate the process of concrete degradation. The numerical model has proven reliable at simulating the deterioration of hydrated cement systems subjected to sulfate attack and calcium leaching [6,10]. The numerical modeling tool applied herein, CrunchFlow [14], is a computer program for multicomponent reactive transport in porous media. CrunchFlow is an enhanced version of the GIMRT/OS3D package [15,16] which can be used for reactive transport problems of arbitrary complexity and size (i.e., there is no a priori restriction on the number of species or reactions considered). Some of its main features include the simulation of advective, dispersive, and diffusive transport in up to two dimension using the global implicit (GIMRT) option; non-isothermal transport and reaction; multicomponent aqueous complexation; kinetically-controlled mineral precipitation and dissolution; and reaction-induced porosity and permeability feedback to both diffusion and flow.

In the following, advantage will be taken of the capability of CrunchFlow of simulating transport by either molecular or ionic diffusion, i.e., by either Fick's law or the Poisson–Nernst–Planck equations, respectively. As said above, the application of the latter requires the determination of the specific diffusion coefficient of each ionic species. These were provided by means of migration tests carried out by Samson et al. [17] on cylindrical samples of 25 mm thickness.

Results are reproduced from [4] and shown in Table 2.

A total of 31 homogeneous hydrogeochemical reactions and 8 precipitation/dissolution mineral processes were considered in the modeling and are listed in Table 3.

A numerical simulation was carried out over a period of 20 years, in order to test the performance of CrunchFlow in contrast to that of STADIUM.

Numerical simulations were then carried out over a period of 2500 days. The conditions of the problem were in all cases designed to properly reproduce those of the original model, in relation to the chemical composition of both the interstitial solution and the boundary water as well as the mineralogical composition of concrete. The thickness of the slab was discretized into 150 constant-size elements of 0.1 cm each.

Table 1
Physicochemical characteristics of the hardened cement paste.

Aqueous species		Concentration (mmol/L)
Initial pore solution		
OH^-		183.42
Na^+		71.40
K^+		108.90
SO_4^{2-}		1.17
Ca^{2+}		2.74
$Al(OH)_4^-$		0.03
Mineral phase	**Weight (g/kg)**	**Volume fraction (%)**
Initial solid phase		
Portlandite	38.10	4.00
C–S–H	76.10	8.77
Ettringite	12.40	1.33
Hydrogarnet	4.30	0.40
Aggregates		71.90
Porosity		13.60

4. Results of the numerical simulations

4.1. Verification of the numerical model

Before proceeding to set forth in further detail the subject matter of this work, it is worth corroborating whether or not the results obtained with CrunchFlow match those reported in [4] whenever they are indeed comparable. The problem was solved using the Poisson–Nernst–Planck formulation for the description of ionic transport which was, as said above, also the choice made in [4].

Fig. 2 shows the results obtained in [4] and in the present work. Whereas the overall picture exhibits an analogous pattern for the distribution of the mineral phases, divergences are instantly apparent from the extent of the penetration reached by the degradation fronts. These discrepancies might be attributed to the fact that the effective diffusion coefficients, as calculated by either STADIUM or CrunchFlow, obey two different constitutive relationships. In fact, the numerical model STADIUM follows [18]:

$$\frac{D_{\text{eff}}}{D_0} = [0.001 + 0.07\phi^2 + 1.8H(\phi - \phi_c)(\phi - \phi_c)^2] \tag{9}$$

where D_{eff} and D_0 denote the effective diffusion coefficients and diffusion coefficients in water, respectively; ϕ represents the capillary porosity of concrete and $\phi_c = 0.18$ is a critical constant dependent on the material; and $H(\phi - \phi_c)$ is the Heavyside function.

On the other hand, CrunchFlow assumes that the variation of the effective diffusion coefficients in the porous medium as a function of the capillary porosity is reasonably well approached by [5]:

$$D_{\text{eff}} = \frac{D_0}{\phi^m F} \tag{10}$$

where the parameters $F = 140.533$ and $m = 1.0$ are respectively the formation factor and the cementation exponent.

Table 2
Specific effective diffusion coefficients, as reported by Marchand et al. [4].

Species	Effective diffusion coefficient (m^2/s)
OH^-	25.8E–11
Na^+	6.50E–11
K^+	9.60E–11
SO_4^{2-}	5.20E–11
Ca^{2+}	3.90E–11
SO_4^{2-}	2.70E–11

Table 3
Hydrogeochemical reactions considered in the reactive transport model.

Homogeneous hydrogeochemical reactions	log *K*
$H^+ + OH^- \leftrightarrow H_2O$	+13.9951
$Al^{3+} + 2H_2O \leftrightarrow AlO_2^- + 4H^+$	−22.8833
$Al(OH)_2^+ + 2H^+ \leftrightarrow Al^{3+} + 2H_2O$	+10.5945
$AlOH^{2+} + H^+ \leftrightarrow Al^{3+} + H_2O$	+4.9571
$Al(SO_4)_2^- \leftrightarrow Al^{3+} + 2SO_4^{2-}$	−4.9000
$AlSO_4^+ \leftrightarrow Al^{3+} + SO_4^{2-}$	−3.0100
$CaCO_{3(aq)} + H^+ \leftrightarrow Ca^{2+} + HCO_3^-$	+7.0017
$CaCl^+ \leftrightarrow Ca^{2+} + Cl^-$	+0.6956
$CaCl_{2(aq)} \leftrightarrow Ca^{2+} + 2Cl^-$	+0.6436
$CaHCO_3^+ \leftrightarrow Ca^{2+} + HCO_3^-$	−1.0467
$CaOH^+ + H+ \leftrightarrow Ca^{2+} + H_2O$	+12.8500
$CaSO_{4(aq)} \leftrightarrow Ca^{2+} + SO_4^{2-}$	−2.1111
$CO_{2(aq)} + H_2O \leftrightarrow H^+ + HCO_3^-$	−6.3447
$CO_3^{2-} + H^+ \leftrightarrow HCO_3^-$	+10.3288
$HAlO_{2(aq)} + 3H^+ \leftrightarrow Al^{3+} + 2H_2O$	+16.4329
$HCl_{(}aq) \leftrightarrow Cl^- + H^+$	−0.6700
$H_2SiO_4^{2-} + 2H^+ \leftrightarrow SiO_{2(aq)} + 2H_2O$	+22.9600
$HSiO_3^- + H^+ \leftrightarrow SiO_{2(aq)} + H_2O$	+9.9525
$H_2SO_{4(aq)} \leftrightarrow SO_4^{2-} + 2H^+$	+1.0209
$HSO_4^- \leftrightarrow H^+ + SO_4^{2-}$	−1.9791
$KCl_{(aq)} \leftrightarrow Cl^- + K^+$	+1.4946
$KHSO_{4(aq)} + H^+ \leftrightarrow H^+ + K^+ + SO_4^{2-} +$	−0.8136
$KOH_{(aq)} + H^+ \leftrightarrow H_2O + K^+$	+14.4600
$KSO_4^- \leftrightarrow K^+ + SO_4^{2-}$	−0.8796
$NaAlO_{2(aq)} + 4H^+ \leftrightarrow Al^{3+} + Na^+ + 2H_2O$	+23.6266
$NaCl_{(aq)} \leftrightarrow Cl^- + Na^+$	+0.7770
$NaHCO_{3(aq)} \leftrightarrow HCO_3^- + Na^+$	−0.1541
$NaHSiO_{3(aq)} + H^+ \leftrightarrow H_2O + Na^+ + SiO_{2(aq)}$	+8.3040
$NaCO_3^- + H^+ \leftrightarrow HCO_3^- + Na^+$	+9.8144
$NaOH_{(aq)} + H^+ \leftrightarrow H_2O + Na^+$	+14.7948
$NaSO_4^- \leftrightarrow Na^+ + SO_4^{2-}$	−0.8200

Mineral processes	log *K*	Molar volume (cm^3/mole)
Portlandite $\leftrightarrow Ca^{2+} + 2OH^-$	−5.2000	33.056
C−S−H $\leftrightarrow Ca^{2+} + 2OH^-$	−5.6000	95.100
Gypsum $\leftrightarrow Ca^{2+} + SO_4^{2-} + 2H_2O$	−4.6000	74.690
Ettringite $\leftrightarrow 4OH^- + 2AlO_2^- + 3SO_4^{2-} + 6Ca^{2+}$	−44.0000	569.890
Hydrogarnet $\leftrightarrow 4OH^- + 2AlO_2^- + 6Ca^{2+}$	−23.0000	149.520
Quartz $\leftrightarrow SiO_{2(aq)}$	−3.9993	22.688
$SiO_{2(s)} \leftrightarrow SiO_{2(aq)}$	−2.7136	29.000
Calcite $+ H^+ \leftrightarrow Ca^{2+} + HCO_3^-$	+1.8487	36.934

Another source of disagreement lies in the formulation of the activity coefficients chosen in [4] which, in contrast to the Debye–Hückel equation used in this work, consists of a modification of the Davies equation

$$\ln \gamma_i = -\frac{Az_i^2\sqrt{I}}{1 + a_iB\sqrt{I}} + \frac{(0.2 - 4.17E - 05I)Az_i^2 I}{\sqrt{1000}} \quad (11)$$

The mentioned differences notwithstanding, in view of the output of CrunchFlow as shown in Fig. 2, it can be assumed that the phenomenology of the process is reliably reproduced. This will emerge even more patently in the following, as further evidence will be provided.

4.2. Results assuming diffusion transport is ruled by the Poisson–Nernst–Planck equations

The evolution of the concentration of aqueous species in the pore solution, as simulated by CrunchFlow, is shown in Fig. 3. It is clearly seen that one of the earliest effects of degradation is

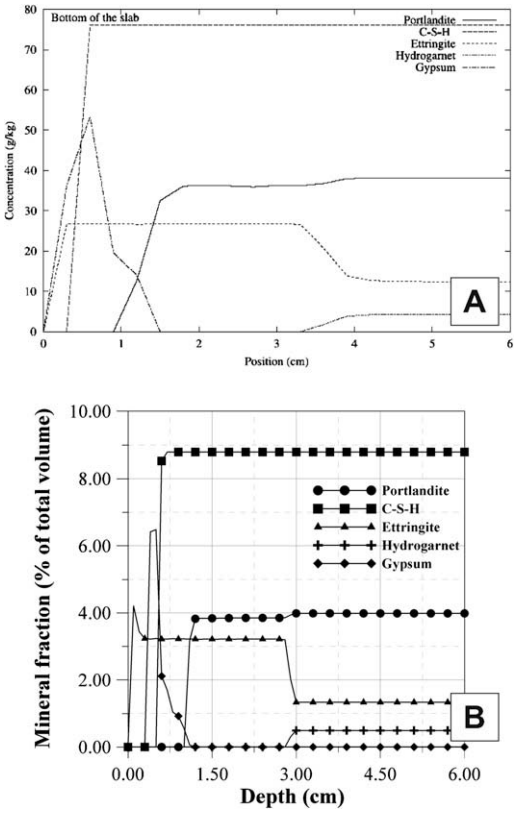

Fig. 2. Distribution of the solid phases after 20 years for the concrete under analysis. A. Results reported in Marchand et al. [4] and B. Results obtained in the present work.

the depletion of alkali ions, which is followed by an increase in calcium concentration, at the expense of the dissolution of portlandite and the decalcification of C–S–H. The concentration of calcium after 2500 days displays a gently sloped profile behind the first front, as calcium ions are released to provide a source for ettringite to precipitate. A peak is reached of about 26 mmol/L, and then an abrupt decline, which rules the leaching of calcium ions out of interstitial solution towards the boundary water. Sulfate ions reach also a relatively high concentration near the surface. It is remarkable that the highest peak is located some millimeters inside the concrete slab and not on its surface, where it would be expected to be had only molecular diffusion been considered, as the boundary water is the main source of sulfate ions. This particular feature is related to the influence of electrical forces on the movement of charged particles.

The statement made by Marchand et al. [4], as to that the 'internal reorganization' of the geochemical composition of the concrete slab is affected by the advance of degradation fronts that steadily penetrate from its external surface towards its center is clearly illustrated in Fig. 4, where the evolution of the solid phases during the prescribed time of simulation is shown. Alongside the formation of ettringite, which is the most well known and worrisome consequence of the sulfate attack, also the precipitation of gypsum near the exposed surface is predicted by the model. As noted in [4], these results are in good correlation with most investigations on this subject. Additional evidence can be found in [6].

The precipitation of ettringite is mostly explained by the presence of aluminum in excess in the pore solution, as a result of the dissolution of hydrogarnet. Yet, once all the hydrogarnet is dissolved, the source of aluminum vanishes, which impedes the further precipitation of ettringite. On the other hand, the dissolution

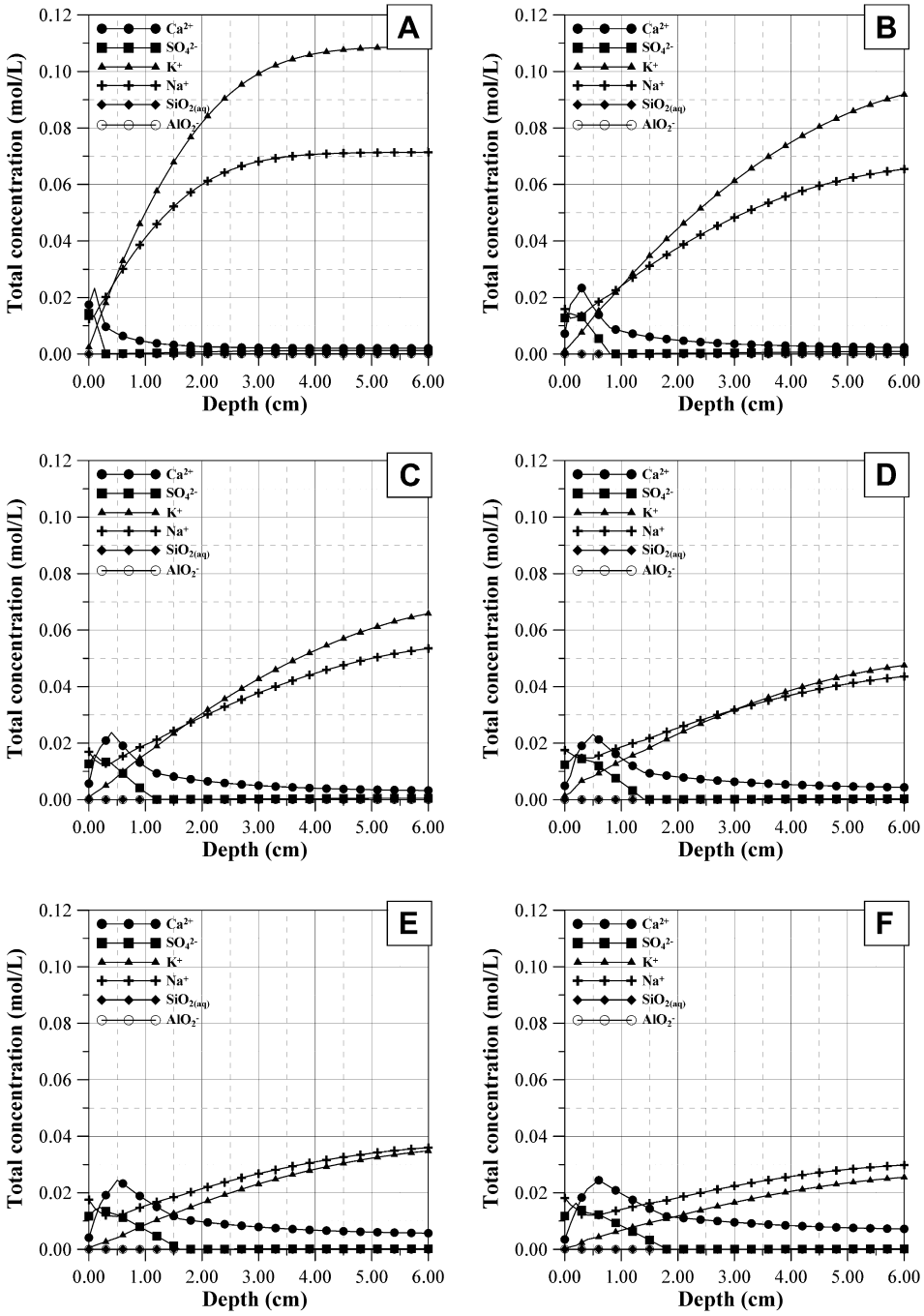

Fig. 3. Aqueous species concentration after 100 (A), 500 (B), 1000 (C), 1500 (D), 2000 (E) and 2500 days (F), assuming diffusion is ruled by the Poisson–Nernst–Planck equations.

of portlandite and decalcification of C–S–H, for which there is also experimental evidence, induces the rise of concentration of calcium. The rise of concentration of calcium in the interstitial solution, in conjunction with that of sulfate, causes the saturation index to turn critical.

4.3. Results assuming diffusion transport is ruled by Fick's law

A second series of simulations was performed with CrunchFlow, this time employing Fick's law to describe diffusion phenomena. Accordingly, all species were assumed to have the same diffusion coefficient. That unique diffusion coefficient was equal to the average of the specific diffusion coefficients assigned to each of them when using the Poisson–Nernst–Planck equations.

Fig. 5 shows the evolution of the chemical composition of the pore solution with depth at different times. Three divergent aspects are particularly noticeable with respect to the results obtained with the Poisson–Nernst–Planck equations. First, the sodium profile after 2500 days exhibits a much milder slope when the diffusion gradient reverses, thus preserving somewhat the alkaline conditions in the pore solution and buffering the leaching of calcium ions. Second, as a consequence, the peak of calcium concentration decreases down to approximately 1.85 mmol/L. Finally, unlike the previous case, the sulfate concentration profile displays

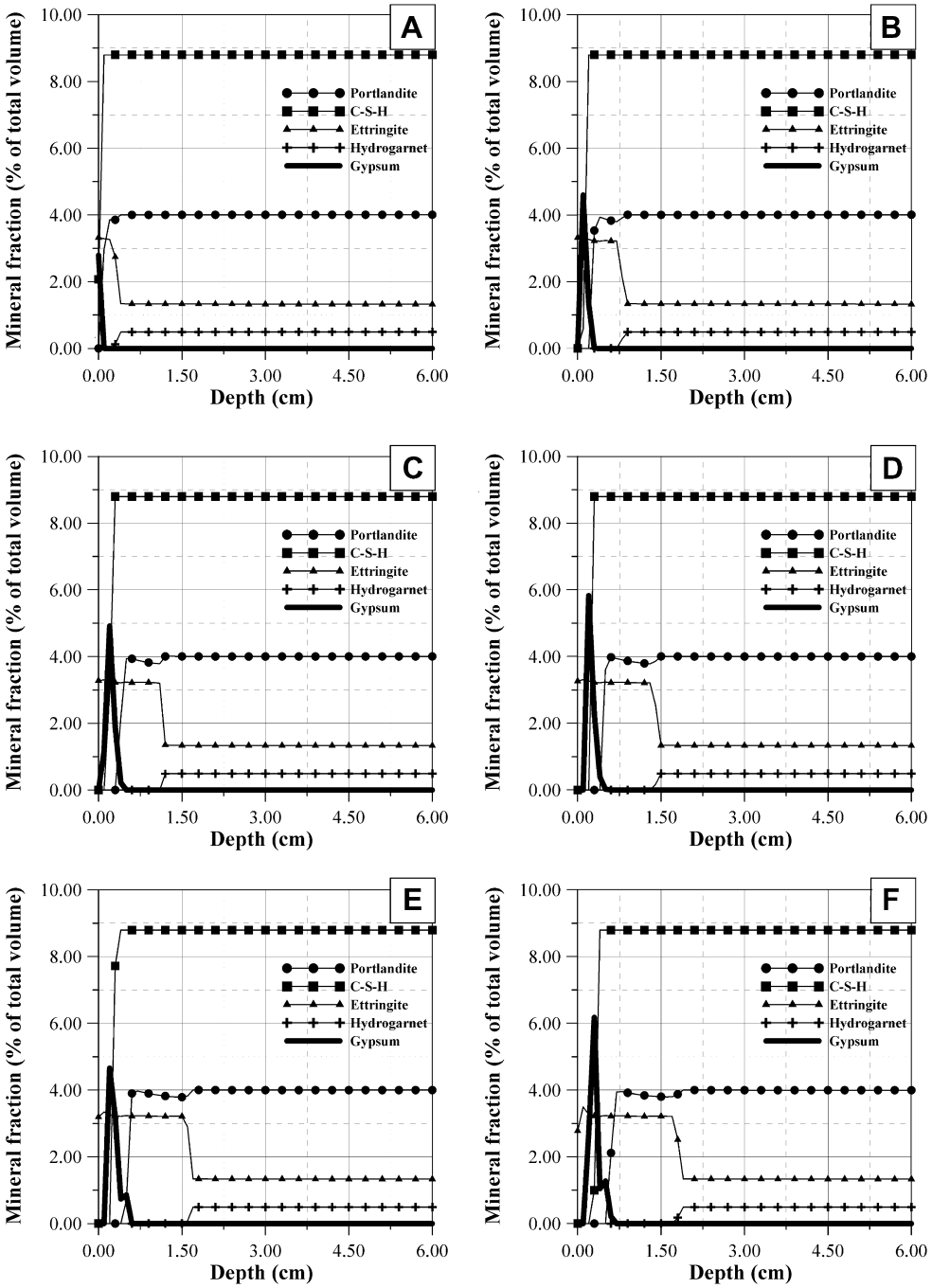

Fig. 4. Distribution of the solid phases after 100 (A), 500 (B), 1000 (C), 1500 (D), 2000 (E) and 2500 days (F), assuming diffusion is ruled by the Poisson–Nernst–Planck equations (gypsum precipitation was highlighted with a thick solid line).

a gradual decline from the exposed surface towards the center of the slab.

The mineral evolution of the solid phase is shown in Fig. 6.

As can be observed, results computed by assuming that ionic diffusion can be described by Fick's law (Fig. 6) show a similar pattern with respect to those obtained when using the Poisson–Nernst–Planck approach (Fig. 4). Mainly two fronts evolve from the surface towards the center of the slab – the first one denoted by the dissolution of hydrogarnet and precipitation of ettringite, and the second one by dissolution of portlandite and C–S–H. All mineral components develop roughly in an analogous manner to that predicted by the Poisson–Nernst–Planck equations, except for gypsum, which does not precipitate at all, since calcium and sulfate are present in smaller amounts in the interstitial solution, and the system is below the saturation threshold.

This point is more explicitly illustrated in Fig. 7. Given that the solubility constant of gypsum is, by definition:

$$K_{\text{gypsum}} = \left[Ca^{2+}\right]\left[SO_4^{2-}\right] = \left(\gamma_{Ca^{2+}} m_{Ca^{2+}}\right)\left(\gamma_{SO_4^{2-}} m_{SO_4^{2-}}\right) \tag{12}$$

where $[Ca^{2+}]$ and $[SO_4^{2-}]$, and $m_{Ca^{2+}}$ and $m_{SO_4^{2-}}$ are the activities and the molal concentration of calcium and sulfate, respectively.

Then, operating and rearranging, the following formula is obtained:

$$\log\left(\gamma_{SO_4^{2-}} m_{SO_4^{2-}}\right) = \log K_{\text{gypsum}} - \log\left(\gamma_{Ca^{2+}} m_{Ca^{2+}}\right) \tag{13}$$

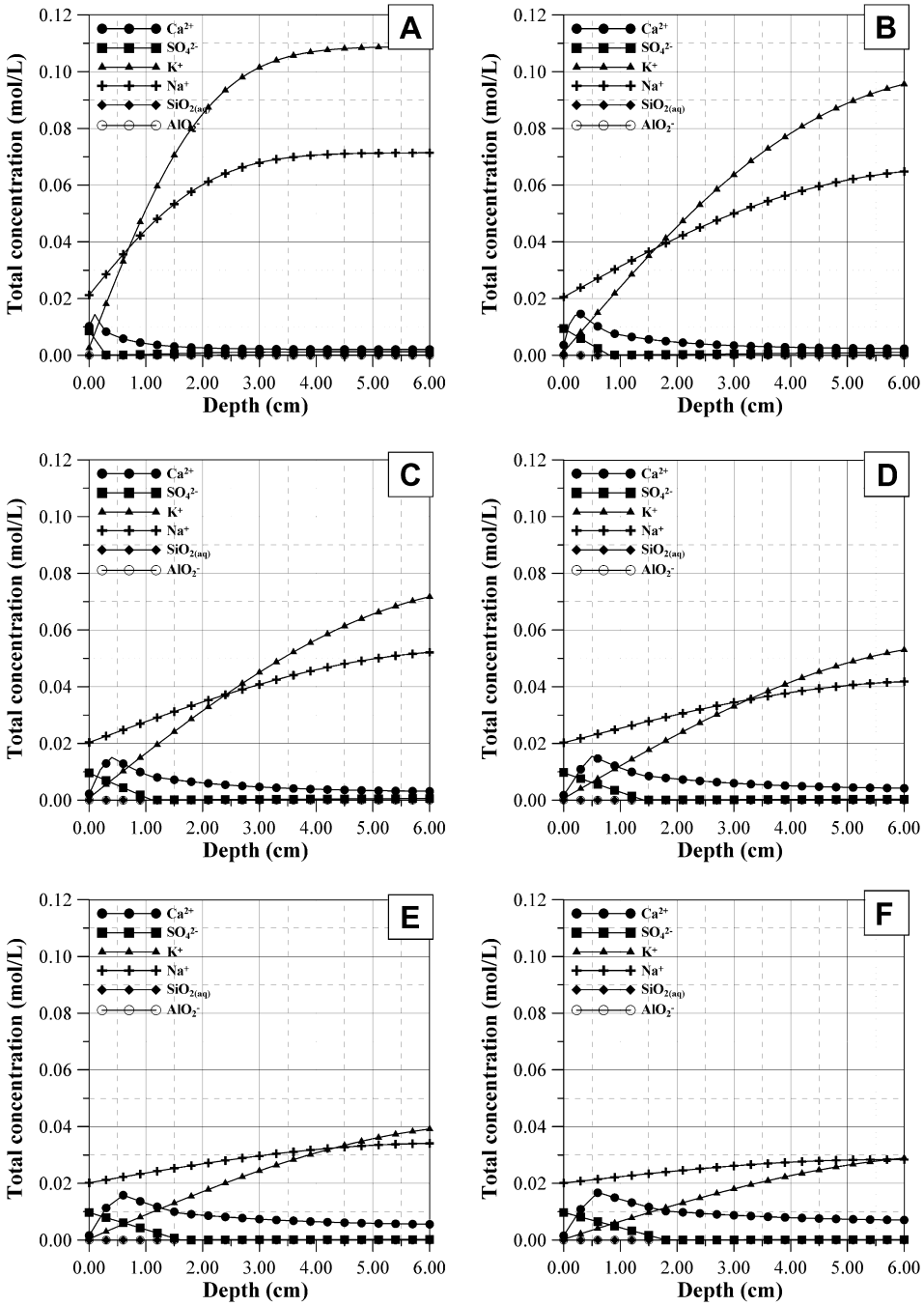

Fig. 5. Aqueous species concentration after 100 (A), 500 (B), 1000 (C), 1500 (D), 2000 (E) and 2500 days (F), assuming diffusion is ruled by Fick's law.

which is the equation of the solid line shown in Fig. 7. The space above that line denotes an oversaturation state with respect to gypsum. Dotted lines each represent the state of the pore solution over a depth of 6 cm (measured from the exposed surface of the slab) at a particular time step. As can be seen, given that Fick's law underestimates the peak concentration of both calcium and sulfate in the pore solution, all points sampled appear to remain slightly, but consistently, undersaturated with respect to gypsum.

Simulations made contemplating the Poisson–Nernst–Planck equations, on the other hand, result in a global shift towards saturation. At any time step considered, points exist that are lying on the equilibrium curve, which is in correspondence with the actual precipitation of gypsum shown in Fig. 4 and validated by experimental evidence [6].

5. Conclusions

A numerical simulation of the deterioration of concrete exposed to a weak sulfate solution was carried out and analyzed under the framework of two different formulations for the diffusive ionic transport in the aqueous phase, namely Fick's law and the Poisson–Nernst–Planck equations. It was found that, in spite of some minor divergences (presumably arising from both the different constitutive relationships porosity–diffusivity and the definition of the activity coefficients used in either the original paper or the present work), the results obtained in this work are coherent and entirely comparable with those reported previously, thus providing support and confidence on both independent models.

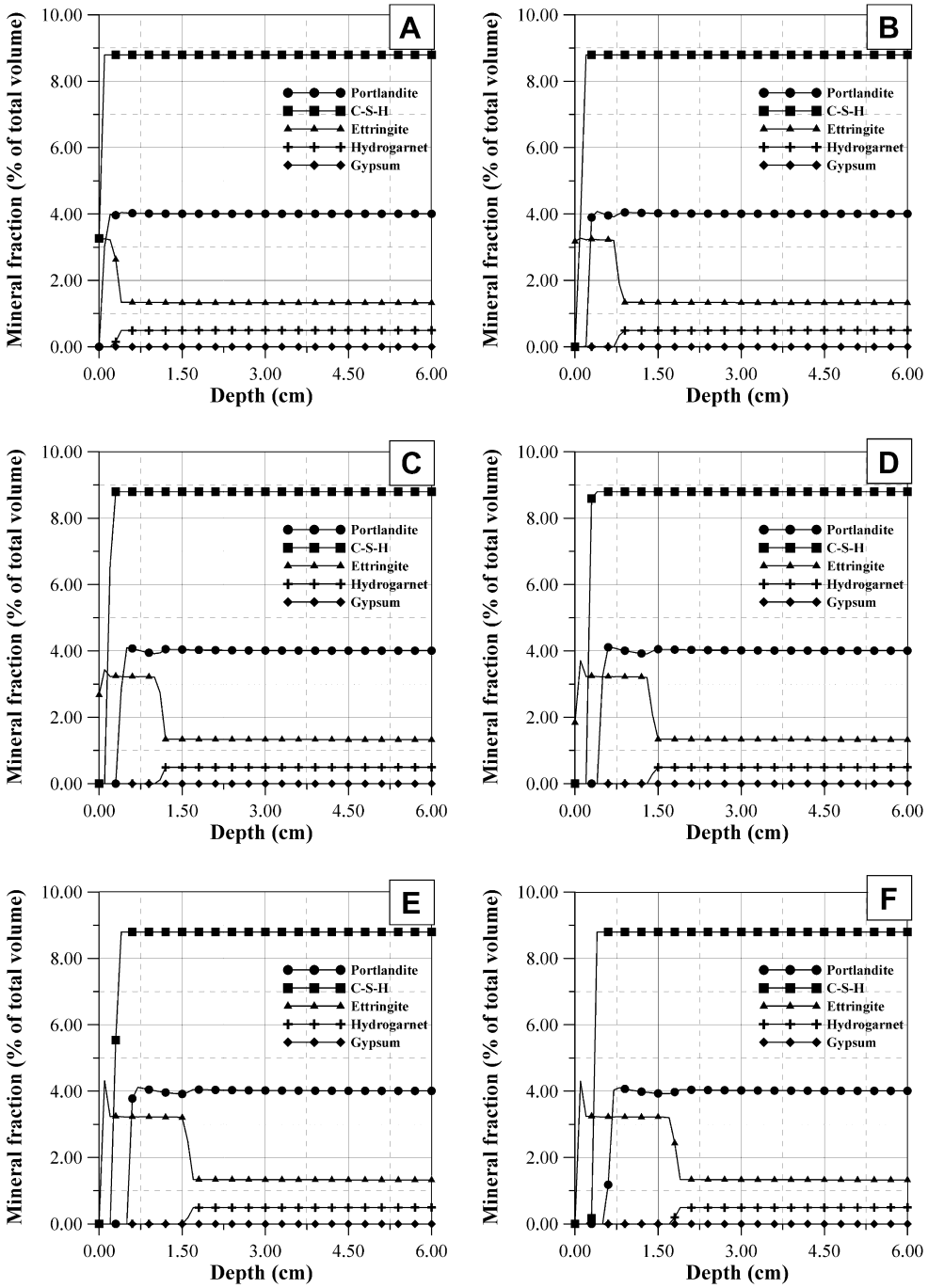

Fig. 6. Distribution of the solid phases after 100 (A), 500 (B), 1000 (C), 1500 (D), 2000 (E) and 2500 days (F), assuming diffusion is ruled by Fick's law.

The model set-up was used to compare the performance of the two theoretical conceptualizations of diffusion transport. On comparing the performance of Fick's law and the Poisson–Nernst–Planck equations, results show that the former fails to reproduce the precipitation of a thin layer of gypsum close to the exposed surface of concrete. The reasons behind this anomaly lie in the fact that Fick's law tends to underestimate the actual concentration of calcium and sulfate in the pore solution (which, on the other hand, is better predicted by the Poisson–Nernst–Planck equations), thus preventing it from reaching the saturation threshold with respect to gypsum.

Given that the precipitation of gypsum was corroborated by experimental studies, the preceding analysis raises the question as to which extent purely diffusive approaches are appropriate in modeling transport processes of electrically charged species in porous media in general and in cement-based materials in particular.

As was proved for the case analyzed, neglecting electrochemical interactions in the diffusion process may lead to the inability of the reactive transport models to reproduce such key phenomena as gypsum precipitation for sulfate attack scenarios, because of which it can be concluded that purely diffusive approaches based on Fick's law may not be accurate enough for modeling the degradation of cementitious materials. To that aim, in light of the results obtained, the Poisson–Nernst–Planck equations may provide a more suitable alternative framework.

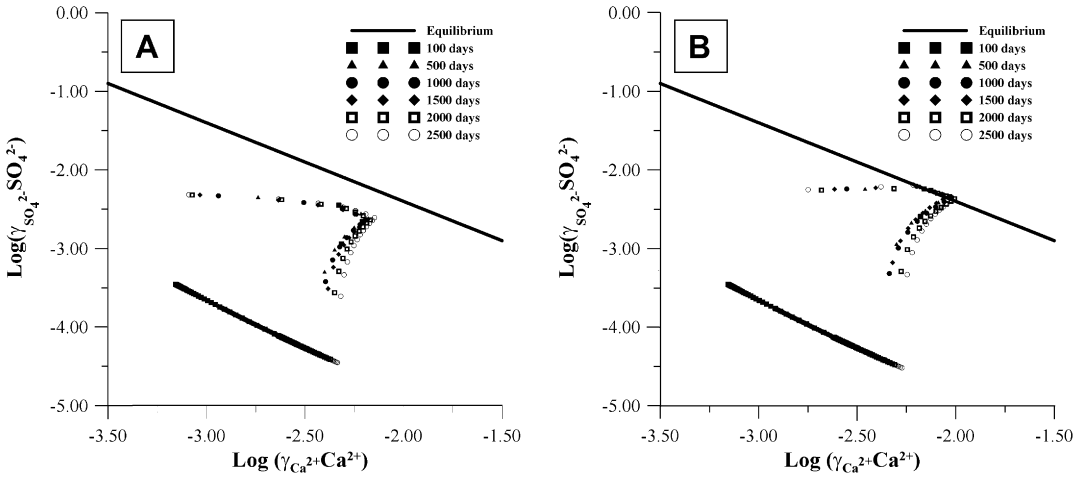

Fig. 7. Saturation state of the pore solution with respect to gypsum. (A) Simulation results obtained using Fick's law and (B) Simulation results obtained using the Poisson–Nernst–Planck equations.

Acknowledgments

This work has been carried out with the financial support of the Swedish Nuclear Fuel and Waste Management Company (SKB). The authors are particularly indebted to Dr. Javier Samper and Dr. Ignasi Puigdomenech for their encouragement and suggestions. Thanks are also given to the two anonymous reviewers of this paper, whose pertinent comments have significantly contributed to improve the original manuscript.

References

[1] Steefel CI, DePaolo DJ, Lichtner PC. Reactive transport modeling: an essential tool and a new research approach for the Earth sciences. Earth Planet Sci Lett 2005;240:539–58.
[2] Krabbenhøft K, Krabbenhøft J. Application of the Poisson–Nernst–Planck equations to the migration test. Cem Concr Res 2008;38:77–88.
[3] Steefel CI. Geochemical kinetics and transport. In: Brantley SL, Kubicki JD, White AF, editors. Kinetics of water–rock interaction. New York: Springer; 2007. p. 545–89.
[4] Marchand J, Samson E, Maltais Y, Beaudoin JJ. Theoretical analysis of the effect of weak sodium sulfate solutions on the durability of concrete. Cem Concr Compos 2002;24(3–4):317–29.
[5] Giambalvo ER, Steefel CI, Fisher AT, Rosenberg ND, Wheat CG. Effect of fluid-sediment reaction on hydrothermal fluxes of major elements, eastern flank of the Juan de Fuca Ridge. Geochim Cosmochim Acta 2002;66:1739–57.
[6] Maltais Y, Samson E, Marchand J. Predicting the durability of Portland cement systems in aggressive environments – laboratory validation. Cem Concr Res 2004;34(9):1579–89.
[7] Samson E, Marchand J, Snyder KA, Beaudoin JJ. Modeling ion and fluid transport in unsaturated cement systems in isothermal conditions. Cem Concr Res 2005;35(1):141–53.
[8] Samson E, Marchand J. Modeling the effect of temperature on ionic transport in cementitious materials. Cem Concr Res 2007;37(3):455–68.
[9] Glasser FP, Marchand J, Samson E. Durability of concrete – degradation phenomena involving detrimental chemical reactions. Cem Concr Res 2008;38(2):226–46.
[10] Marchand J, Bentz DP, Samson E, Maltais Y. Influence of calcium hydroxide dissolution on the transport properties of hydrated cement systems. In: Skalny J, Gebauer J, Odler I, editors. Materials science of concrete special volume: calcium hydroxide in concrete; 2001. p. 113–29.
[11] Steefel CI, Maher K. Fluid–rock interaction: a reactive transport approach. Rev Miner Geochem 2009;70:485–532.
[12] Helfferich F. Ion exchange. New York: McGraw-Hill; 1961.
[13] Lewis GN, Randall M. Thermodynamics. New York: McGraw-Hill; 1961.
[14] Steefel CI. CrunchFlow – software for modeling multicomponent reactive flow and transport, Lawrence Berkeley National Laboratory; 2008. <http://www.csteefel.com/CrunchPublic/CrunchFlowManual.pdf.>
[15] Steefel CI, Yabusaki SB. OS3D/GIMRT, software for multicomponent-multidimensional reactive transport: user's manual and programmer's guide, PNL-11166. Richland (WA, USA): Pacific Northwest National Laboratory; 1996.
[16] Steefel CI. GIMRT, version 1.2: software for modeling multicomponent, multidimensional reactive transport. User's guide, UCRL-MA-143182. Livermore (USA): Lawrence Livermore National Laboratory; 2001.
[17] Samson E, Marchand J, Snyder KA. Calculation of ionic diffusion coefficients on the basis of migration test results. Mater Struct 2003;36(257):156–65.
[18] Garboczi EJ, Bentz DP. Computer simulation of the diffusivity of cement-based materials. J Mater Sci 1992;27:2083–92.